THREE-DIMENSIONAL NUMERICAL SIMULATIONS OF AIR QUALITY MODELS IN THE BTS SKYTRAIN STATIONS

KEWALEE SUEBYAT

A THESIS SUBMITTED IN PARTIAL FULFILLMENT OF THE REQUIREMENT FOR THE DEGREE OF DOCTOR OF PHILOSOPHY IN APPLIED MATHEMATICS

DEPARTMENT OF MATHEMATICS
FACULTY OF SCIENCE
KING MONGKUT'S INSTITUTE OF TECHNOLOGY LADKRABANG

2018
KMITL-2018-SC-D-001-006

THREE-DIMENSIONAL NUMERICAL SIMULATIONS OF AIR QUALITY MODELS IN THE BTS SKYTRAIN STATIONS

KEWALEE SUEBYAT

A THESIS SUBMITTED IN PARTIAL FULFILLMENT OF THE REQUIREMENT FOR THE DEGREE OF DOCTOR OF PHILOSOPHY IN APPLIED MATHEMATICS

DEPARTMENT OF MATHEMATICS
FACULTY OF SCIENCE
KING MONGKUT'S INSTITUTE OF TECHNOLOGY LADKRABANG

2018
KMITL-2018-SC-D-001-006

COPYRIGHT 2018
FACULTY OF SCIENCE
KING MONGKUT'S INSTITUTE OF TECHNOLOGY LADKRABANG

Thesis Title	Three-Dimensional Numerical Simulations of Air Quality Models in the BTS Skytrain Stations
Student Name	Miss Kewalee Suebyat
Student ID	58605002
Degree	Doctor of Philosophy (Applied Mathematics)
Department	Mathematics
Year	2018
Thesis Advisor	Asst. Prof. Dr. Nopparat Pochai

Abstract

Air pollution in Bangkok mostly occurs in street tunnels near Bangkok skytrain station areas, due to heavy traffic. These areas do not have air quality measurement stations installed, either in the station areas or the residential areas around them. We are interested in the air pollution problems around skytrain stations. We propose the numerical modeling of air pollutant concentration around a skytrain station with airflow obstacles on a heavy traffic road. A three-dimensional advection-diffusion equation with finite difference methods is used for approximating the air pollutant concentration. In our research, we indicate that the air pollution modeling depends on airflows and wind directions. Therefore, we considered two cases: a wind inflow in only the x-direction, and wind inflows in the x- and y-directions. The domain was distinguished into 3 zones, and the station is separated into three floors: street, ticket, and platform floors. We applied the model of air pollutant concentration assessment and air quality control to the aforementioned domain. Moreover, the development of mathematical models can be used to improve effective solutions, and it can also be applied to real-world problems.

Keywords : air pollutant concentration, air quality, finite difference techniques, heavy traffic, skytrain station, tunnel

Acknowledgements

I would like to thank my advisor, Asst.Prof.Dr.Nopparat Pochai for his many suggestions, support, and encouragement which help conducting of my thesis successfully.

I am thankful to all of committee, Assoc.Prof.Dr.Chartchai Leenawong, Asst.Prof.Dr.Kanchana Kumnungkit and Asst.Prof.Jaipong Kasemsuwan, for many useful recommendation and valuable advices. Next, I also thanks to my external committee, Assoc.Prof.Dr.Suwon Tangmanee from the Centre of Excellence in Mathematics Program of the Commission on Higher Education (CHE) for helpful advices and suggests. Moreover, I would like to thank the other professors as well.

I am greatly appreciated to the Department of Mathematics, Faculty of Science and Research Administration Division scholarship of King Mongkut's Institute of Technology Ladkrabang and the Centre of Excellence in Mathematics Program of the Commission on Higher Education (CHE) for providing me the necessary facilities and giving partial financial support during the preparation of the thesis.

I also wish to thank, Ms. Pravitra Oyjinda for attentiveness, encouragement, and providing suggestions about the mathematical program. I appreciate Ms. Piyada Phosri for help, encouragement and friendship. Moreover, I would like to thank all graduate students. This thesis wouldn't be finished without these people.

Finally, I am grateful to my parents for their encouragement and heartfelt love, which is the most important to my success to this day.

Kewalee Suebyat

Table of Contents

Page

Table of Contents (Continue)

Table of Contents (Continue)

List of Tables

List of Figures

List of Figures (Continue)

List of Figures (Continue)

List of Figures (Continue)

Chapter 1
Introduction

1.1 The air pollution problem

Nowadays, we face the problems of pollution, which have a big effect on society and the environment. “Air Pollution” is a problem that everyone all over the world should realize the gravity of, as it does not only affect one society and environment, but also creates problems for human life. Air pollution is harmful to human health because of the released pollutants and dirt in the air, which causes asthma, lung diseases, and cancer. Moreover, human-made structures and facilities are major factors which affect environmental resources and contribute to climate change.

Sources of air pollution can be classified into two types: natural sources and artificial sources. These can occur in many forms. Natural sources of pollution come from natural phenomena, such as volcanic eruptions, forest fires, biological decay, pollen grains, marshes, and radioactive materials. On the other hand, artificial sources are those created by human beings, such as thermal power plants, vehicular emissions, fossil fuel burning, agricultural activities, etc. In general, air pollution occurs in the formation of gas and particulate contaminants which are in our atmosphere. This includes carbon monoxide (CO), nitrogen dioxide (NO_2), nitrogen oxides (NO_x), sulfur dioxide (SO_2), ozone (O_3), volatile organic compounds (VOC_s), particulate matter (PM_{10} and $PM_{2.5}$), and various other gases.

According to the studies of scientists on the problem of whether indoors or outdoors has the most pollution, it was found that indoor air pollution is often more harmful than outdoor air pollution. The air inside our homes and offices can sometimes be much more polluted compared to outdoor air and thus, presents a major health threat, especially as we spend most of the time per day indoors and inside our home or office. In recent studies, British scientists measured air quality inside and outside three residential buildings with different types of energy use. They found that one of the most common air pollutants are nitrogen dioxide from kitchens in city center apartments with gas cookers, which had the levels as much as three times higher than those measured outdoors, and which were well above clean air quality standards.

Thailand is making rapid strides in agriculture, industry, commerce, science, and technology. This increases comfort by utilizing natural resources and leads to rapid industrialization, with big cities consequently witnessing excessive air pollution. Transportation development in Bangkok, Thailand, is experiencing an exponential

growth in vehicular usage, which increases air pollution. On the other hand, the existing weather patterns of Bangkok is not favorable for the dispersion of air pollutants. Therefore, we should control air pollution in traffic jams, such as those found under Bangkok skytrain platform area.

Currently, Bangkok has rapid growth in both agriculture and industry, resulting in it being the center of prosperity in all aspects, it has had a rapid population increase, followed by a high demand for travel and transportation. The cumulative effects of these aspects have intensified traffic congestion and has seen an increase of cars, vehicles, and automobile emission levels. Bangkok's air pollution is one of its biggest problems. It has reached a critical level, with hazardous substances in some areas, as pollution is created by human beings and natural phenomena, damaging the environment and human well-being. Not only is air pollution hazardous locally, but it is one of the world's biggest killers and issues, because people face health problems, such as asthma, bronchitis, cancer, etc. Therefore, it can be said that air pollution from traffic is a tremendously serious issue, especially around Bangkok, which has more skytrain platform than any other area. This has made the volume of carbon monoxide and nitrogen oxides in this area be higher than the standard volume. Therefore, this issue should be realized for study interest and further research to find solutions to reduce pollution.

In Bangkok, Thailand, air pollution from car exhausts on the street contains particulates, especially from old cars or diesel cars, which are harmful to people's health. Scientists are concerned that particulates carrying toxic chemicals, such as nitrous oxide and carbon monoxide, when inhaled deeply, can be harmful to people's health. The Bangkok Transit System (BTS) provides an effective route of urban transportation for Bangkok people, as it facilitates speed and convenience. The major source of air pollution under Bangkok skytrain platform comes from vehicle exhaust, mobile sources, and other sources, including smoke from restaurants, construction, and building demolition. The air pollutants emitted from mobile source, which are carbon monoxide and nitrogen oxides, have concentration levels which cause injury to human health and are harmful for survival. The effects of air pollution are alarming. Several people are known to have died due to the direct or indirect effect of air pollution. It is known that air pollution contributes to cancer, among other threats to the body. Moreover, it also causes some environmental impact, especially that of air pollutants to the vicinity around platforms with high traffic and a large number of people.

These days, an increasing population causes heavy traffic and air pollution on the road. Air pollution around areas under BTS platforms has increased dramatically. Therefore, if we know the value of the concentration of pollution that is likely to

occur from existing pollution accumulation or from sources of emissions, such as from car smoke, we might be able to control the concentration of air pollution in that area, and prevent it from exceeding the standard. As has already been mentioned, we recognize the importance of air pollution, so it is interesting to study.

1.2 Literature reviews

Study and research on mathematical models to estimate air pollutant concentration is important and useful. We also use mathematical models to describe the dispersion of air pollution. In addition, we can use a numerical method to solve the air pollution problem. This leads to the control of air pollution. Therefore, many researchers have studied air pollution.

In [1], the Kriging method for regression analysis was used to analytically relate the mass emission rate of carbon monoxide and nitrogen dioxide around the Bangkok Mass Transit System (BTS). The results indicated that the concentration of carbon monoxide exceeded the Bangkok standard volume, and the concentration of nitrogen dioxide did not exceed the Bangkok standard volume. Undeniably, the air pollutant concentration was related to the traffic flow pattern, traffic characteristics, street geometries, and human activities. The traffic flow is the main pollution source in many urban areas. It causes more ambient air pollutants, such as carbon monoxide (CO), sulfur dioxide (SO_2), nitrogen dioxide (NO_2), nitrogen oxides (NO_x), volatile organic compounds (VOC_s), ozone (O_3), particulate matter (PM_{10}), benzene, heavy metals, and respirable particulate matter ($PM_{2.5}$ and PM_{10}) [2]. In 2002, [3] studied average air pollutant concentration during weekdays and found it to be higher than during the weekend. The test results showed that the average air pollutant concentrations for three urban sites were noticeably higher than for suburban sites. Our analysis revealed that an obvious way to reduce the build-up of pollutant concentration on Bangkok streets would be to speed up the flow of traffic and prevent long periods of idling in congested streets. In 2004, [4] studied the stability conditions for several different numerical techniques, which were developed and compared in order to solve a three-dimensional advection-diffusion equation with constant coefficient. The results of the numerical experiment were presented, and the accuracy and central processor time needed were discussed and compared. A three-dimensional advection-diffusion equation of air pollutant is applied to a street tunnel configuration by using the forward time and central space finite difference method, with air flow in the x- and y-directions in [5]. In [6], a one-dimensional advection-diffusion equation with variable coefficients in semi-infinite media was presented.

A study of vehicle exhaust dispersion within different street canyon models in urban areas ventilated by crosswinds was conducted by using the advanced computational and the mathematical models. The pollutant concentrations were estimated for the street canyon models, which included simplified photochemistry and particle deposition suspension algorithms. After application of a Box model to the street canyon, [7] calculations for CO, NO_x, SPM, and PM_{10} were made. In 2011, [8] studied a mathematical model of the smoke dispersion from two sources and one source with a structural obstacle. In 2016, [9] studied a mathematical model for describing the dispersion of the air pollutants released from a source into the atmosphere, which was examined by using the three-dimensional fractional step method. The results obtained indicated that the proposed experimental variations of the atmospheric stability classes and wind velocities affected the air quality around industrial areas. In 2016, [10] studied and presented the development of a next generation air sensor system and application in an ad hoc air monitoring network, in which the air sensors were placed and operated at the street level to monitor the air along the Marathon route in urban Hong Kong, providing near real-time calculation and communication of health-indexed findings of air quality to the public. In 2017, [11] studied a three-dimensional advection-diffusion equation by using the explicit forward difference method. The wind inflows were considered in two cases: wind inflow only in the x-direction, and wind inflow in the x-direction and y-direction. Moreover, obstacles were added along the middle into the tunnel. The results of the model were satisfactory.

As mentioned, it can be seen that many researchers have studied air pollution. Therefore, we are interested in studying air pollutant concentration. In this research, we are interested in the traffic density of the area around a Bangkok skytrain platform. We propose the numerical modeling of air pollutant concentration around a skytrain platform with airflow obstacles on a heavy traffic road. An estimated three-dimensional advection-diffusion equation is used with the finite difference method to approximate the air pollutant concentration. In our research, we indicate that the air pollution modeling depends on air pollution flows and wind directions. However, the wind inflow directions near the tunnel should be considered, because it affects the concentration of air pollutant. Therefore, the wind inflow directions are an important factor of the model. So, we distinguish two cases: wind inflow only in the x-direction, and wind inflow in the x- and y-directions. The major air pollutant selected for analysis is CO. We distinguish 3 zones in the considered domain: zone 1, zone 2, and zone 3. The study is carried out on 3 floors: street, ticket, and platform floors.

1.3 Objectives of the thesis

1) To apply a three-dimensional advection-diffusion equation to the wind inflow directions and obstacles in an area under a Bangkok skytrain platform.
2) To apply a three-dimensional advection-diffusion equation of a dispersion model to the dispersion of air pollutant concentration around a Bangkok skytrain platform over heavy traffic road.
3) To apply a three-dimensional advection-diffusion equation to variations of the boundary conditions around the entrance gate which affect the air pollutant concentration of each floor at Bangkok skytrain platform.
4) To simulate the numerical solution of air pollutant concentration to find an approximate solution by using the finite difference method (FDM).
5) To improve the models and to develop more realistic models.

1.4 Scopes of the thesis

1) To study the airflow and wind directions in street tunnel configuration focused on an area around a Bangkok skytrain platform.
2) To study the behavior of an air pollutant released from sources with obstacles (the columns) and multiple layers.
3 To consider flow in the x- and y-directions of an air pollutant released from the area sources with one layer and three layers.
4) To describe the dispersion of an air pollutant concentration, which is considered by a three-dimensional advection-diffusion equation.
5) To approximate the solution of air pollutant concentration calculated by using the finite difference method, and to illustrate the forward time, central space (FTCS) and forward time, backward space (FTBS) methods.
6) To propose numerical experiments and construct a computer program to support the numerical solution.

1.5 Plan of the thesis

1) To study the air pollution using a mathematical model and the finite difference techniques.
2) To study the research papers related to the numerical solution of air pollutant concentration and the control of air quality to apply them to this thesis.
3) To review related research on urban air pollution assessment models.
4) To analyze a Bangkok skytrain platform which stands over a heavy traffic road.

5) To propose a simple model for air pollution measurement under the platform.
6) To propose an air pollution measurement model when there are obstacles present.
7) To propose an air pollution measurement model when the amount of traffic is varied.
8) To propose a three-dimensional model for air pollution measurement over three-floors of the platform when the effect of heavy traffic on the ground floor is considered.
9) To analyze the simulation results.
10) To write a mathematical program to calculate the numerical results to support the problems raised in this thesis.
11) To compile and check the accuracy of data and to write the thesis.

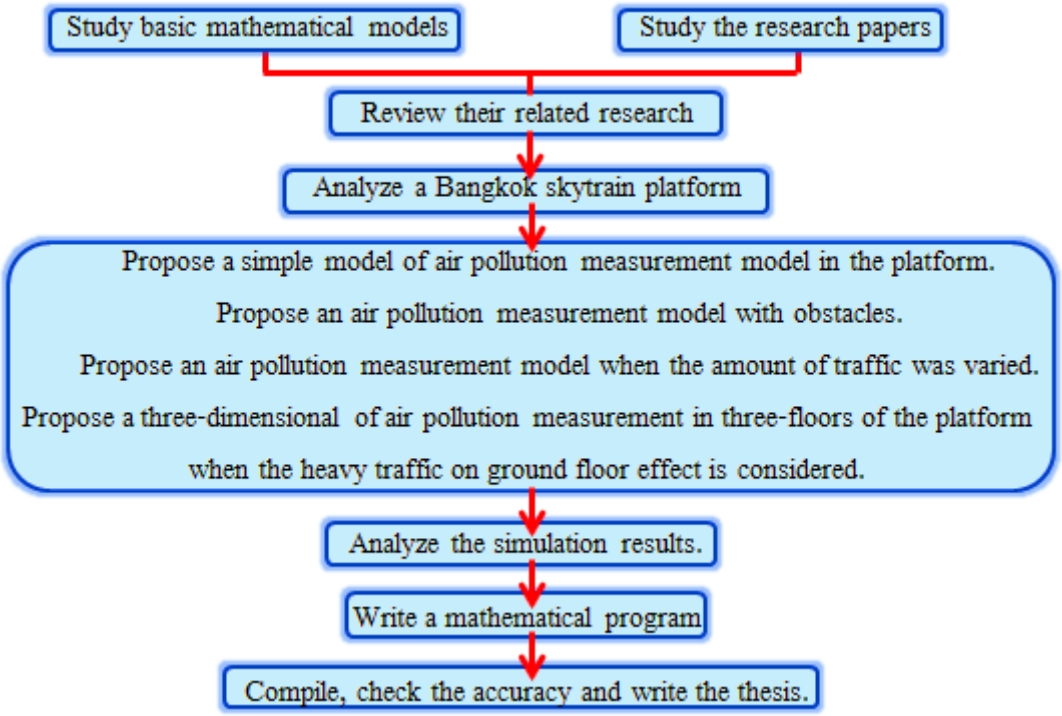

Figure 1.1 Plan of the thesis

1.6 Expected results

1) To apply the model of air pollutant concentration assessment and control of air quality to an area under a Bangkok skytrain platform.
2) To develop mathematical models created from real-world problems, such as the area under a Bangkok skytrain platform, an area over a heavy traffic road, and on each floor of a Bangkok skytrain platform.

3) To obtain dispersion of air pollutant concentration pollution models for a street tunnel, to improve the models for more effective solutions for the estimation of air pollutant concentration, and to continue developing them.

The contexts of the chapters of this thesis are as follows:

In chapter 2 (Basic concepts and preliminaries), the preliminary and the governing equations of air pollution concentration corresponding to the finite difference approximations and the model of a three-dimensional advection-diffusion equation are presented.

Chapter 3 (Three-dimensional air quality model in an area under a Bangkok skytrain platform) is divided into two sections. Firstly, a numerical simulation of a three-dimensional air quality model in an area under a Bangkok skytrain platform, using an explicit finite difference scheme to describe the wind inflow directions and obstacles in this area, is presented. Secondly, numerical simulation of a three-dimensional air pollution measurement model in a heavy traffic area under the Bangkok skytrain platform is done. We add sources or sinks of air pollutants; source or sink emissions are averaged, moving, and mixed.

In chapter 4 (Three-dimensional air quality assessment simulations inside skytrain platform with airflow obstacles on heavy traffic road), the finite difference techniques are introduced for three methods for calculating air pollutant concentration. The three-dimensional advection-diffusion equation is solved by using the forward time, centered space (FTCS) and forward time, backward space (FTBS) schemes. The two methods and the simulations around skytrain platforms are compared to propose variations of the initial and boundary conditions around the entrance gate, which affects the air pollutant concentration of each floor under a Bangkok skytrain platform. Moreover, the air pollution controls are used in order to illustrate the performance of the model in this section.

In chapter 5 (Discussion and conclusion), discussion of the numerical simulation of the three-dimensional air quality model of the area under a Bangkok skytrain station with airflow obstacles on a heavy traffic road detailed in chapter 3 and chapter 4 is presented.

Chapter 2

Basic Concepts and Preliminaries

2.1 Air pollution

2.1.1 Definition of air pollution

Some specific definitions of air pollution are given, as per the following:

The Bureau of Indian Standards (BIS) defines air pollution “the presence in ambient atmosphere of substances, generally resulting from the activity of man, in sufficient concentration, present for a sufficient time, and under circumstances such as to interfere with the comfort, health or welfare of persons or with reasonable use or enjoyment of property”.

The World Health Organization (WHO) defines air pollution as “the presence of material in air in such concentrations which are harmful to man and his environment”.

The Engineers Joint Council (EJC) defines air pollution as “the presence in the outdoor atmosphere of one or more contaminants, such as dust, fumes, gas, mist, odor, smoke, or vapor, in quantities, of characteristics, and of duration such as to be injurious to human, plant, or animal life, or to property, or which unreasonably interfere with the comfortable enjoyment of life and property”.

Figure 2.1 Air Pollution
(http://angsila.informatics.buu.ac.th/~55660167/design/website/images/422.jpg)

2.1.2 Types of air pollutants

2.1.2.1 Air pollutants can be classified by causes of air pollutants into two general groups: natural sources and artificial sources.

1 Natural sources are divided as follows:
   - Volcanic activity: active volcanoes release a huge amount of gases, such as sulfur dioxide and ash. Volcanic ash itself is gritty and corrosive in nature.
   - Swamps and marshes: fermentation is the genesis of methane, which is toxic and flammable. Moreover, it is also key in causing global warming in addition to carbon dioxide.
   - Forest fires: sulfur dioxide, nitrous oxide, and carbon monoxide are just some of the poisonous gases formed during forest fires, which are easily inhaled and cause respiratory diseases.

2 Artificial sources are divided as follows:
   - Agricultural activities, which are farming practices that result in contamination or degradation from pesticides, fertilizers, contaminated water, soil erosion, sedimentation, livestock, pests, and weeds.
   - Combustion processes, such as combustion in vehicles, smoke coming out of vehicles, combustion for thermal electrical energy, and the generation of electricity.
   - Industrial constructions, such as construction of residences, emissions through chimneys, indoor air pollutants, commercial activities, road construction activities, etc.

2.1.2.2 Air pollutants can also be broadly classified by the occurrence of air pollutants into two general groups: primary and secondary air pollutants**.**

1 Primary air pollutants are those emitted directly from identifiable sources; examples of primary air pollutants are carbon monoxide, oxides of nitrogen, sulfur compounds, halogen compounds, organic compounds, radioactive compounds, and particles.

2 Secondary air pollutants are those which are produced in the air by the interaction or reaction among two or more primary pollutants; examples of secondary air pollutants are ozone, formaldehyde, peroxyacetyl nitrate (PAN), sulfur trioxide, nitrogen dioxide, and the formation of acid mists (H_2SO_4).

2.1.3 Effects of air pollution

The important effects of air pollution consist of those on human health and the environment.

1 Effects of air pollution on the environment
   - Nitrogen oxides lead to occurrences of smog. This causes the formation of ozone pollution, which damages trees and forests.
   - Fertilizers and waste are the cause of aquatic animal death from the reduction of oxygen amount in water.

2 Effects of air pollution on human health
   - There are increases of respiratory diseases, such as asthma, allergies, chronic obstructive pulmonary disorder, pneumonia, tuberculosis, lung damage, etc.
   - There are deleterious effects on the nervous system, such as breathlessness, headaches, dizziness, vomiting, and neurobehavioral disorders.
   - There are increases of the cardiovascular issues, diseases, cancers, and lung, skin, and gastric system problems.

2.1.4 Emission sources of air pollution

Emission sources of air pollution are categorized into three groups: point sources, area sources, and mobile sources.

1 Point sources mainly include industrial facilities like chemical plants, steel mills, oil refineries, power plants, and hazardous waste incinerators. Examples of pollutants emitted from these sources are sulfur dioxide, nitrogen oxides, and volatile organic compounds. Examples of point sources are shown in Figure 2.2.

Figure 2.2 Air pollution from industrial smokestacks
(http://www.ac-control.net/private_folder/health_02f.jpg)

2 Area sources include gas stations, commercial buildings, residential buildings, and fireplaces. Examples of pollutants are carbon monoxide pollution, nitrogen oxide, and volatile organic compounds. Examples of area sources are shown in Figure 2.3.

Figure 2.3 Air pollution from forest fires
(http://hilight.kapook.com/img_cms2/user/ratthakorn/variety/fire01.jpg)

3 Mobile sources or line sources mainly include vehicles, such as cars, trucks, and buses. Examples of pollutants from exhausted mobile sources are carbon monoxide, oxides of nitrogen, hydrocarbons, and nitrogen oxide. Examples of mobile sources are shown in Figure 2.4.

Figure 2.4 Air pollution from car exhaust pipes
(http://static.naewna.com/uploads/news/source/107568.jpg?t=1461633507252)

2.2 Problem definition

2.2.1 The topography of a considered domain

2.2.1.1 Tunnels and street tunnels

A tunnel is a long passageway through or under the ground, mountains, the sea, rivers, canals, transit systems in big cities, or congested urban areas, and are enclosed, except for the entrance and exit. A tunnel may be for pedestrians, for vehicular road traffic, or for railcar traffic. The definition of a tunnel can vary widely; for example:

The United Kingdom defines a tunnel as “a subsurface highway structure enclosed for a length of 150 meters (490 ft.) or more”.

The NFPA, United States, defines a tunnel as “an underground structure with a design length greater than 23 m (75 ft.) and a diameter greater than 1,800 millimeters (5.9 ft.)”.

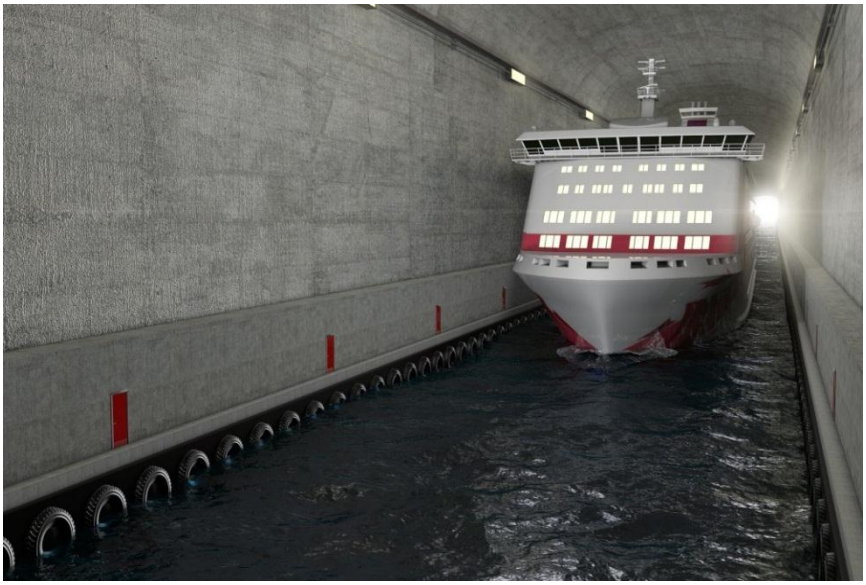

Figure 2.5 Norway to build world's first ship tunnel
(https://www.cnn.com/style/article/ship-tunnel-norway/index.html)

A street tunnel is a closed road on every side, opening only at the entrance and exit gates. It is mostly flanked by buildings on both sides.

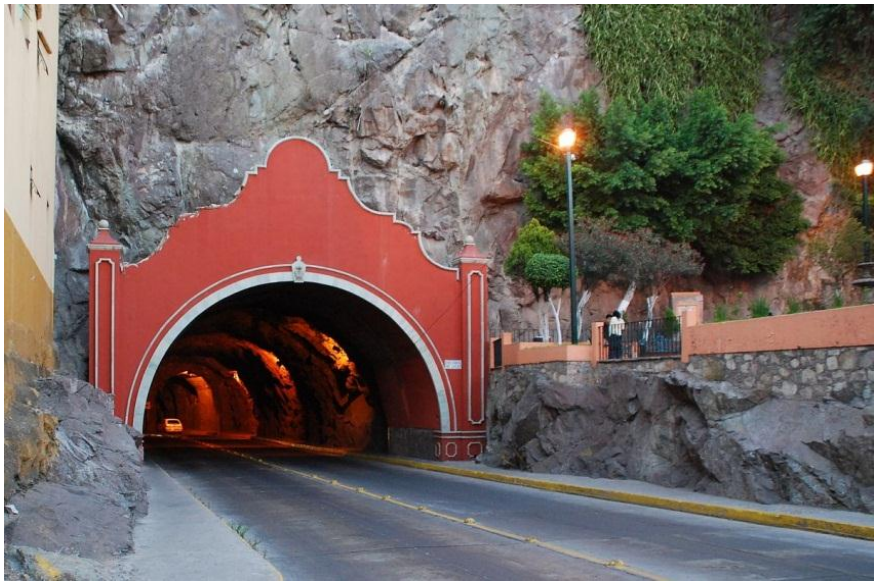

Figure 2.6 Decorated entrance to a road tunnel in Guanajuato, Mexico (https://upload.wikimedia.org/wikipedia/commons/6/64/Tunel_en_Guanajuato.jpg)

2.2.1.2 Canyons and street canyons

A canyon is a deep ravine between pairs of escarpments, cliffs, or are made by the erosion of a river. Canyons within cliffs or mountains or buildings have three open sides, such as an entrance, exit, and the top of the canyon. Similarly, a box canyon is a small canyon that is generally narrower than a canyon.

Figure 2.7 Grand canyon in the southwestern U.S. state of Arizona (http://3.bp.blogspot.com/-xgu2EA6UDao/VafmW9PkANI/AAAAAAAAAo4/2ng5om5It7M/s1600/grand-canyon-sunset.jpg)

A street canyon (or an urban canyon) is a relatively narrow street where the street is flanked by continuous buildings on both sides.

Figure 2.8 Crumlin road in the UK outside London
(http://www.southwalesargus.co.uk/resources/images/
5287092/?type=responsive-gallery)

2.2.1.3 Bangkok Mass Transit System (BTS)

The Bangkok Mass Transit System, commonly known as the BTS or the skytrain, is an elevated rapid transit system in Bangkok, Thailand. It is operated by the Bangkok Mass Transit System Public Company Limited (BTSC), under the control of the Bangkok Metropolitan Administration (BMA). The system consists of 35 stations along 2 lines: 1) the Sukhumvit line, running northwards and eastwards, terminating at Mo Chit and Samrong, respectively, and 2) the Silom line, which serves Silom and Sathon Roads, the central business district of Bangkok, terminating at National Stadium and Bang Wa.

A lot of train stations provide fast and convenient transport; therefore, it is popular. There is a higher number of passengers every year. The statistics of passengers on the BTS skytrain since 1999-2016 [12-13] show that the number of total ridership and average daily ridership has increased (Table 2.1). Figure 2.9 shows a graph of average daily ridership, using the data from Table 2.1.

Table 2.1 Ridership on the BTS Skytrain since 1999-2016

The number of the passengers		
Year	Total ridership	Average daily ridership
1999	4,585,743	169,842
2000	55,092,671	150,469
2001	74,025,652	202,685
2002	93,493,981	256,033
2003	102,348,697	280,379
2004	115,681,448	316,068
2005	127,350,084	348,795
2006	140,048,849	383,635
2007	132,070,502	361,977
2008	136,350,007	372,551
2009	140,957,969	386,145
2010	143,102,971	392,376
2011	167,348,070	458,275
2012	194,113,068	530,422
2013	208,764,971	571,855
2014	219,422,367	598,984
2015	229,853,593	629,218
2016	237,047,435	647,752

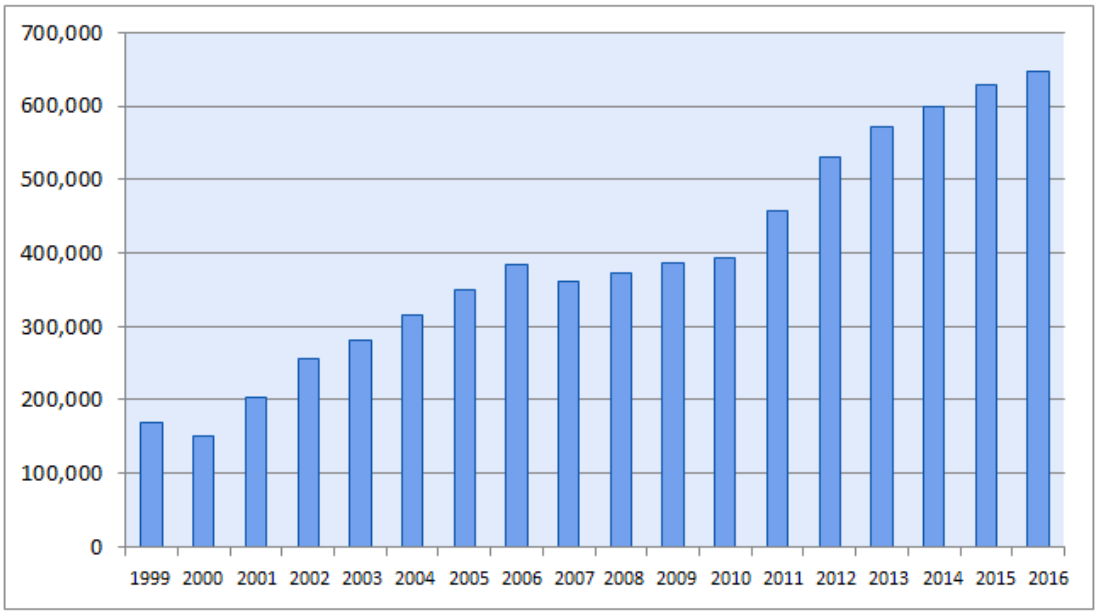

Figure 2.9 Average daily ridership on the BTS Skytrain since 1999-2016

Nowadays, the BTS is very popular for those who have to travel to the big city every day. The number of the passengers has increased as well. Currently, the average daily ridership is approximately 600,000-700,000 people/day. The most popular stations are located in the city center, near the shopping malls or connecting points. A list of the 10 most popular stations follows:

Table 2.2 The number of passengers from 10 most popular stations [14]

The number of the passengers		
No.	**Station**	**Number (people/day)**
1	Siam Station	112,600
2	Asok Station	85,100
3	Mo Chit Station	79,500
4	Victory Monument Station	79,000
5	Sala Daeng Station	52,900
6	On Nut Station	52,600
7	Chit Lom Station	47,300
8	Phaya Thai Station	42,800
9	Bearing Station	41,400
10	Phrom Phong Station	39,600

From Table 2.2, we conclude that the most popular stations is Siam Station. Accordingly, air pollution controls in this area are studied in this research.

2.2.2 Mass transfer

2.2.2.1 Advection

Advection is the transfer of heat or cold in the atmosphere by the flow in the horizontal movement of an air mass. Advection, in general, moves matter from one position in space to another. The transportation of matter by the advection shown in Figure 2.10.

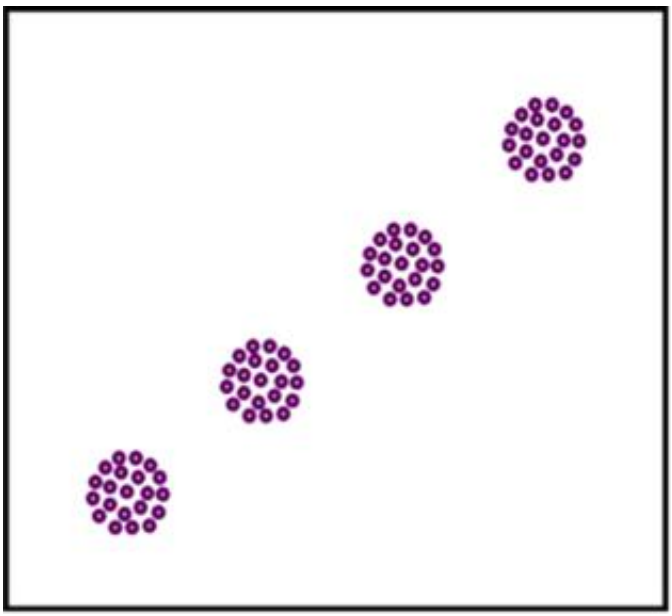

Figure 2.10 The transport by advection

2.2.2.2 Diffusion

Diffusion is the movement or the spread of mass in air or dissolved substances. Diffusion, in general, moves matter from regions of higher concentration to regions of lower concentration. The movement of mass will mix until they are evenly distributed in the concentration. The transportation of matter by diffusion shown in Figure 2.11.

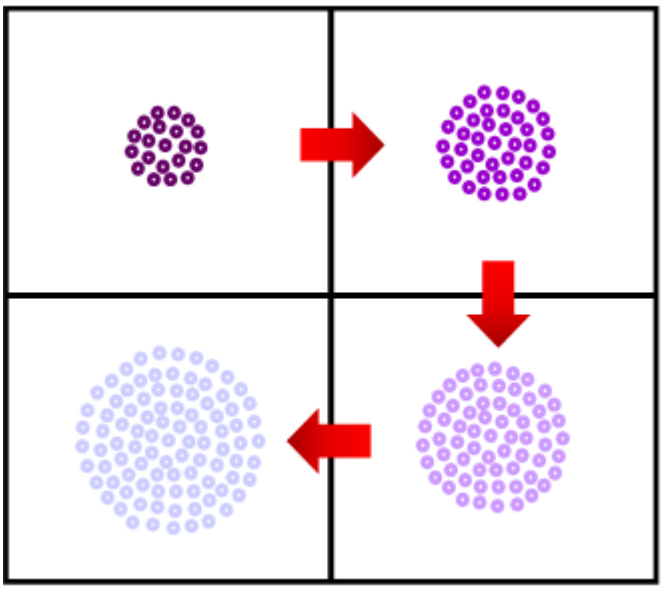

Figure 2.11 The transport by diffusion

2.2.2.3 Advection-diffusion

Advection-diffusion (Dispersion) is a system in which particles are dispersed continuously. It is the transfer of particles inside a system, due to two processes, the combination of the advection and diffusion, which is shown in Figure 2.12.

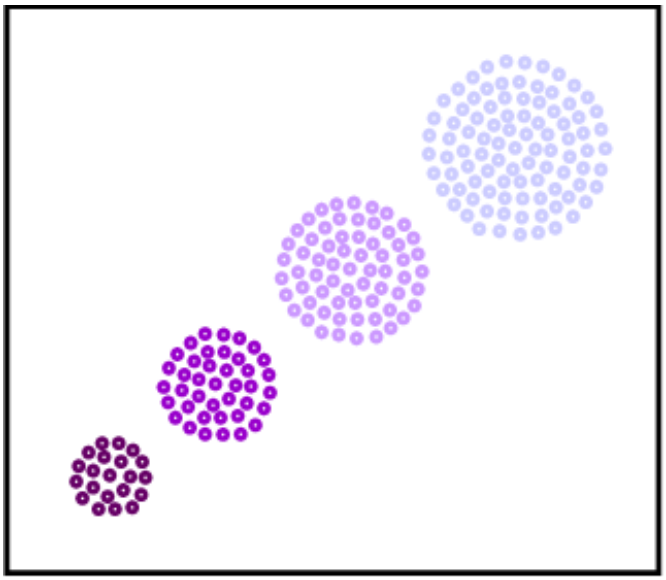

Figure 2.12 The transport by advection- diffusion

2.3 Finite difference approximations

We introduce the finite difference expression and describe the basic concepts and methods for approximating solutions. A typical grid point is given by $x = i\triangle x$, $y = j\triangle y$, $z = k\triangle z$, and $t = n\triangle t$, where $\triangle x, \triangle y, \triangle z$, and $\triangle t$ are the grid spacing or grid size or step size in the space and time coordinates, respectively, and i, j, k, and n are integers. Note that $h = \triangle x$ and define $C(x,y,z,t) = C^n_{i,j,k}$. The derivatives of the function are approximated using a Taylor series.

The finite difference time grid:

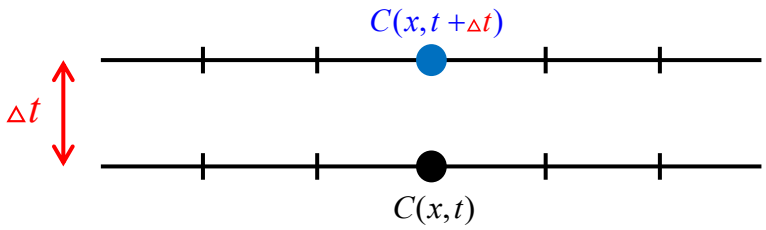

Figure 2.13 The time grid of finite difference

The finite difference space grid:

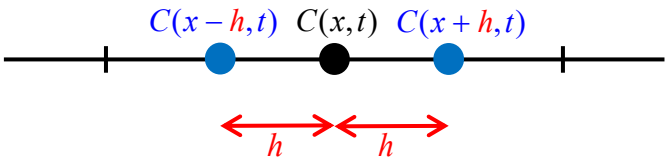

Figure 2.14 The space grid of finite difference

The Taylor series for a function $C(x,y,z,t)$:

$$C_{i+1,j,k} = C_{i,j,k} + h\frac{\partial C}{\partial x} + \frac{h^2}{2!}\frac{\partial^2 C}{\partial x^2} + \frac{h^3}{3!}\frac{\partial^3 C}{\partial x^3} + \frac{h^4}{4!}\frac{\partial^4 C}{\partial x^4} + \frac{h^5}{5!}\frac{\partial^5 C}{\partial x^5} + \ldots, \tag{2.1}$$

$$C_{i-1,j,k} = C_{i,j,k} - h\frac{\partial C}{\partial x} + \frac{h^2}{2!}\frac{\partial^2 C}{\partial x^2} - \frac{h^3}{3!}\frac{\partial^3 C}{\partial x^3} + \frac{h^4}{4!}\frac{\partial^4 C}{\partial x^4} - \frac{h^5}{5!}\frac{\partial^5 C}{\partial x^5} + \ldots, \tag{2.2}$$

2.3.1 Forward difference in space

From Eq. (2.1) and rearranging equation to isolate the first derivative,

$$\begin{aligned}
h\frac{\partial C}{\partial x} &= C_{i+1,j,k} - C_{i,j,k} - \frac{h^2}{2!}\frac{\partial^2 C}{\partial x^2} - \frac{h^3}{3!}\frac{\partial^3 C}{\partial x^3} - \frac{h^4}{4!}\frac{\partial^4 C}{\partial x^4} - \ldots, \\
\frac{\partial C}{\partial x} &= \frac{C_{i+1,j,k}}{h} - \frac{C_{i,j,k}}{h} + \left(-\frac{h}{2!}\frac{\partial^2 C}{\partial x^2} - \frac{h^2}{3!}\frac{\partial^3 C}{\partial x^3} - \frac{h^3}{4!}\frac{\partial^4 C}{\partial x^4} - \ldots\right), \\
\frac{\partial C}{\partial x} &= \frac{C_{i+1,j,k} - C_{i,j,k}}{h} + O(h), \\
\frac{\partial C}{\partial x} &\approx \frac{C^n_{i+1,j,k} - C^n_{i,j,k}}{\Delta x}.
\end{aligned} \tag{2.3}$$

2.3.2 Backward difference in space

From Eq. (2.2) and rearranging this equation to isolate the second derivative,

$$\begin{aligned}
h\frac{\partial C}{\partial x} &= C_{i,j,k} - C_{i-1,j,k} + \frac{h^2}{2!}\frac{\partial^2 C}{\partial x^2} - \frac{h^3}{3!}\frac{\partial^3 C}{\partial x^3} + \frac{h^4}{4!}\frac{\partial^4 C}{\partial x^4} - \ldots, \\
\frac{\partial C}{\partial x} &= \frac{C_{i,j,k}}{h} - \frac{C_{i-1,j,k}}{h} + \left(\frac{h}{2!}\frac{\partial^2 C}{\partial x^2} - \frac{h^2}{3!}\frac{\partial^3 C}{\partial x^3} + \frac{h^3}{4!}\frac{\partial^4 C}{\partial x^4} - \ldots\right), \\
\frac{\partial C}{\partial x} &= \frac{C_{i,j,k} - C_{i-1,j,k}}{h} + O(h), \\
\frac{\partial C}{\partial x} &\approx \frac{C^n_{i,j,k} - C^n_{i-1,j,k}}{\Delta x}.
\end{aligned} \tag{2.4}$$

2.3.3 Central difference in space for first derivative

Subtracting the second equation from the first equation [Eq. (2.1) - Eq. (2.2)],

$$
\begin{aligned}
&C_{i+1,j,k} - C_{i-1,j,k} = 2h\frac{\partial C}{\partial x} + \frac{2h^3}{3!}\frac{\partial^3 C}{\partial x^3} + \frac{2h^5}{5!}\frac{\partial^5 C}{\partial x^5} + ..., \\
&2h\frac{\partial C}{\partial x} = C_{i+1,j,k} - C_{i-1,j,k} - \frac{2h^3}{3!}\frac{\partial^3 C}{\partial x^3} - \frac{2h^5}{5!}\frac{\partial^5 C}{\partial x^5} - ..., \\
&\frac{\partial C}{\partial x} = \frac{C_{i+1,j,k}}{2h} - \frac{C_{i-1,j,k}}{2h} + \left(-\frac{h^2}{3!}\frac{\partial^3 C}{\partial x^3} - \frac{h^4}{5!}\frac{\partial^5 C}{\partial x^5} - ... \right), \\
&\frac{\partial C}{\partial x} = \frac{C_{i+1,j,k} - C_{i-1,j,k}}{2h} + O\left(h^2\right), \\
&\frac{\partial C}{\partial x} \approx \frac{C^n_{i+1,j,k} - C^n_{i-1,j,k}}{2\triangle x}.
\end{aligned}
\tag{2.5}
$$

2.3.4 Central difference in space for second derivative

Adding the second equation to the first equation [Eq. (2.1) + Eq. (2.2)],

$$
\begin{aligned}
&C_{i+1,j,k} + C_{i-1,j,k} = 2C_{i,j,k} + \frac{2h^2}{2!}\frac{\partial^2 C}{\partial x^2} + \frac{2h^4}{4!}\frac{\partial^4 C}{\partial x^4} + ..., \\
&\frac{2h^2}{2!}\frac{\partial^2 C}{\partial x^2} = C_{i+1,j,k} + C_{i-1,j,k} - 2C_{i,j,k} - \frac{2h^4}{4!}\frac{\partial^4 C}{\partial x^4} - ..., \\
&\frac{\partial^2 C}{\partial x^2} = \frac{C_{i+1,j,k}}{h^2} - \frac{2C_{i,j,k}}{h^2} + \frac{C_{i-1,j,k}}{h^2} + \left(-\frac{2h^2}{4!}\frac{\partial^4 C}{\partial x^4} - ... \right), \\
&\frac{\partial^2 C}{\partial x^2} = \frac{C_{i+1,j,k} - 2C_{i,j,k} + C_{i-1,j,k}}{h^2} + O\left(h^2\right), \\
&\frac{\partial^2 C}{\partial x^2} \approx \frac{C^n_{i+1,j,k} - 2C^n_{i,j,k} + C^n_{i-1,j,k}}{\left(\triangle x\right)^2}.
\end{aligned}
\tag{2.6}
$$

2.3.5 Forward difference in space for first derivative

From Eq. (2.1) and substituting forward difference in space,

$$
\begin{aligned}
&h\frac{\partial C}{\partial x} = C_{i+1,j,k} - C_{i,j,k} - \frac{h^2}{2!}\frac{\partial^2 C}{\partial x^2} - \frac{h^3}{3!}\frac{\partial^3 C}{\partial x^3} - \frac{h^4}{4!}\frac{\partial^4 C}{\partial x^4} - ..., \\
&\frac{\partial C}{\partial x} = \frac{C_{i+1,j,k}}{h} - \frac{C_{i,j,k}}{h} - \frac{h}{2!}\frac{\partial^2 C}{\partial x^2} + \left(-\frac{h^2}{3!}\frac{\partial^3 C}{\partial x^3} - \frac{h^3}{4!}\frac{\partial^4 C}{\partial x^4} - ... \right), \\
&\frac{\partial C}{\partial x} = \frac{C_{i+1,j,k} - C_{i,j,k}}{h} - \frac{h}{2!}\frac{\partial^2 C}{\partial x^2} + O\left(h^2\right), \\
&\frac{\partial C}{\partial x} \approx \frac{C_{i+1,j,k} - C_{i,j,k}}{h} - \frac{h}{2!}\frac{\partial}{\partial x}\left(\frac{C_{i+1,j,k} - C_{i,j,k}}{h} \right) + O\left(h^2\right), \\
&\frac{\partial C}{\partial x} \approx \frac{C_{i+1,j,k} - C_{i,j,k}}{h} - \frac{1}{2}\frac{\partial}{\partial x}\left(C_{i+1,j,k} - C_{i,j,k} \right) + O\left(h^2\right),
\end{aligned}
$$

$$\frac{\partial C}{\partial x} \approx \frac{C_{i+1,j,k} - C_{i,j,k}}{h} - \frac{1}{2}\left(\frac{C_{i+2,j,k} - C_{i+1,j,k}}{h} - \frac{C_{i+1,j,k} - C_{i,j,k}}{h} \right) + O\left(h^2\right),$$
$$\frac{\partial C}{\partial x} \approx \frac{C_{i+1,j,k} - C_{i,j,k}}{h} - \left(\frac{C_{i+2,j,k} - C_{i+1,j,k} - C_{i+1,j,k} - C_{i,j,k}}{2h} \right) + O\left(h^2\right),$$
$$\frac{\partial C}{\partial x} \approx \frac{C_{i+1,j,k} - C_{i,j,k}}{h} - \left(\frac{C_{i+2,j,k} - 2C_{i+1,j,k} - C_{i,j,k}}{2h} \right) + O\left(h^2\right),$$
$$\frac{\partial C}{\partial x} \approx \frac{2C_{i+1,j,k} - 2C_{i,j,k} - C_{i+2,j,k} + 2C_{i+1,j,k} - C_{i,j,k}}{2h} + O\left(h^2\right),$$
$$\frac{\partial C}{\partial x} \approx \frac{-3C_{i,j,k} + 4C_{i+1,j,k} - C_{i+2,j,k}}{2h} + O\left(h^2\right),$$
$$\frac{\partial C}{\partial x} \approx \frac{-3C^{n}_{i,j,k} + 4C^{n}_{i+1,j,k} - C^{n}_{i+2,j,k}}{2\triangle x}, \tag{2.7}$$

2.3.6 Backward difference in space for first derivative

From Eq. (2.2) and substituting backward difference in space,

$$h\frac{\partial C}{\partial x} = C_{i,j,k} - C_{i-1,j,k} + \frac{h^2}{2!}\frac{\partial^2 C}{\partial x^2} - \frac{h^3}{3!}\frac{\partial^3 C}{\partial x^3} + \frac{h^4}{4!}\frac{\partial^4 C}{\partial x^4} - \ldots,$$
$$\frac{\partial C}{\partial x} = \frac{C_{i,j,k}}{h} - \frac{C_{i-1,j,k}}{h} + \frac{h}{2!}\frac{\partial^2 C}{\partial x^2} + \left(-\frac{h^2}{3!}\frac{\partial^3 C}{\partial x^3} + \frac{h^3}{4!}\frac{\partial^4 C}{\partial x^4} - \ldots \right),$$
$$\frac{\partial C}{\partial x} = \frac{C_{i,j,k} - C_{i-1,j,k}}{h} + \frac{h}{2!}\frac{\partial^2 C}{\partial x^2} + O\left(h^2\right),$$
$$\frac{\partial C}{\partial x} \approx \frac{C_{i,j,k} - C_{i-1,j,k}}{h} + \frac{h}{2!}\frac{\partial}{\partial x}\left(\frac{C_{i,j,k} - C_{i-1,j,k}}{h} \right) + O\left(h^2\right),$$
$$\frac{\partial C}{\partial x} \approx \frac{C_{i,j,k} - C_{i-1,j,k}}{h} + \frac{1}{2}\frac{\partial}{\partial x}\left(C_{i,j,k} - C_{i-1,j,k} \right) + O\left(h^2\right),$$
$$\frac{\partial C}{\partial x} \approx \frac{C_{i,j,k} - C_{i-1,j,k}}{h} + \frac{1}{2}\left(\frac{C_{i,j,k} - C_{i-1,j,k}}{h} - \frac{C_{i-1,j,k} - C_{i-2,j,k}}{h} \right) + O\left(h^2\right),$$
$$\frac{\partial C}{\partial x} \approx \frac{C_{i,j,k} - C_{i-1,j,k}}{h} + \left(\frac{C_{i,j,k} - C_{i-1,j,k} - C_{i-1,j,k} + C_{i-2,j,k}}{2h} \right) + O\left(h^2\right),$$
$$\frac{\partial C}{\partial x} \approx \frac{C_{i,j,k} - C_{i-1,j,k}}{h} + \left(\frac{C_{i,j,k} - 2C_{i-1,j,k} + C_{i-2,j,k}}{2h} \right) + O\left(h^2\right),$$
$$\frac{\partial C}{\partial x} \approx \frac{2C_{i,j,k} - 2C_{i-1,j,k} + C_{i,j,k} - 2C_{i-1,j,k} + C_{i-2,j,k}}{2h} + O\left(h^2\right),$$
$$\frac{\partial C}{\partial x} \approx \frac{C_{i-2,j,k} - 4C_{i-1,j,k} + 3C_{i,j,k}}{2h} + O\left(h^2\right),$$
$$\frac{\partial C}{\partial x} \approx \frac{C^{n}_{i-2,j,k} - 4C^{n}_{i-1,j,k} + 3C^{n}_{i,j,k}}{2\triangle x}. \tag{2.8}$$

2.3.7 Forward difference in space for second derivative

From forward difference in space,

$$
\begin{aligned}
\frac{\partial^2 C}{\partial x^2} &= \frac{\partial}{\partial x}\left(\frac{\partial C}{\partial x}\right), \\
\frac{\partial^2 C}{\partial x^2} &\approx \frac{\partial}{\partial x}\left(\frac{C_{i+1,j,k}-C_{i,j,k}}{\triangle x}\right), \\
\frac{\partial^2 C}{\partial x^2} &\approx \frac{1}{\triangle x}\left(\frac{C_{i+2,j,k}-C_{i+1,j,k}}{\triangle x}-\frac{C_{i+1,j,k}-C_{i,j,k}}{\triangle x}\right), \\
\frac{\partial^2 C}{\partial x^2} &\approx \frac{1}{\triangle x}\left(\frac{C_{i+2,j,k}-C_{i+1,j,k}-C_{i+1,j,k}+C_{i,j,k}}{\triangle x}\right), \\
\frac{\partial^2 C}{\partial x^2} &\approx \frac{1}{\triangle x}\left(\frac{C_{i+2,j,k}-2C_{i+1,j,k}+C_{i,j,k}}{\triangle x}\right), \\
\frac{\partial^2 C}{\partial x^2} &\approx \frac{C^n_{i,j,k}-2C^n_{i+1,j,k}+C^n_{i+2,j,k}}{\left(\triangle x\right)^2}.
\end{aligned}
\tag{2.9}
$$

2.3.8 Backward difference in space for second derivative

From backward difference in space,

$$
\begin{aligned}
\frac{\partial^2 C}{\partial x^2} &= \frac{\partial}{\partial x}\left(\frac{\partial C}{\partial x}\right), \\
\frac{\partial^2 C}{\partial x^2} &\approx \frac{\partial}{\partial x}\left(\frac{C_{i,j,k}-C_{i-1,j,k}}{\triangle x}\right), \\
\frac{\partial^2 C}{\partial x^2} &\approx \frac{1}{\triangle x}\left(\frac{C_{i-2,j,k}-4C_{i-1,j,k}+3C_{i,j,k}}{2\triangle x}-\frac{C_{i-3,j,k}-4C_{i-2,j,k}+3C_{i-1,j,k}}{2\triangle x}\right), \\
\frac{\partial^2 C}{\partial x^2} &\approx \frac{1}{\triangle x}\left(\frac{C_{i-2,j,k}-4C_{i-1,j,k}+3C_{i,j,k}-C_{i-3,j,k}+4C_{i-2,j,k}-3C_{i-1,j,k}}{2\triangle x}\right), \\
\frac{\partial^2 C}{\partial x^2} &\approx \frac{1}{\triangle x}\left(\frac{3C_{i,j,k}-7C_{i-1,j,k}+5C_{i-2,j,k}-C_{i-3,j,k}}{2\triangle x}\right), \\
\frac{\partial^2 C}{\partial x^2} &\approx \frac{3C^n_{i,j,k}-7C^n_{i-1,j,k}+5C^n_{i-2,j,k}-C^n_{i-3,j,k}}{2\left(\triangle x\right)^2}.
\end{aligned}
\tag{2.10}
$$

2.3.9 Two backward difference in space for second derivative

From backward difference in space,

$$
\begin{aligned}
\frac{\partial^2 C}{\partial x^2} &= \frac{\partial}{\partial x}\left(\frac{\partial C}{\partial x}\right), \\
\frac{\partial^2 C}{\partial x^2} &\approx \frac{\partial}{\partial x}\left(\frac{C_{i,j,k}-C_{i-1,j,k}}{\triangle x}\right),
\end{aligned}
$$

$$\frac{\partial^2 C}{\partial x^2} \approx \frac{1}{\triangle x}\left(\frac{C_{i,j,k}-C_{i-1,j,k}}{\triangle x}-\frac{C_{i-3,j,k}-4C_{i-2,j,k}+3C_{i-1,j,k}}{2\triangle x}\right),$$
$$\frac{\partial^2 C}{\partial x^2} \approx \frac{1}{\triangle x}\left(\frac{2C_{i,j,k}-2C_{i-1,j,k}-C_{i-3,j,k}+4C_{i-2,j,k}-3C_{i-1,j,k}}{2\triangle x}\right),$$
$$\frac{\partial^2 C}{\partial x^2} \approx \frac{1}{\triangle x}\left(\frac{2C_{i,j,k}-5C_{i-1,j,k}+4C_{i-2,j,k}-C_{i-3,j,k}}{2\triangle x}\right),$$
$$\frac{\partial^2 C}{\partial x^2} \approx \left(\frac{2C^n_{i,j,k}-5C^n_{i-1,j,k}+4C^n_{i-2,j,k}-C^n_{i-3,j,k}}{2(\triangle x)^2}\right). \quad (2.11)$$

2.4 Governing equation

2.4.1 The advection-diffusion equation

The concentration of air pollutant can be described by the advection-diffusion equation:

$$\frac{\partial C}{\partial t}+V\cdot\nabla C=\nabla\cdot\left(\overline{K}\otimes\nabla C\right)+R, \quad (2.12)$$

where $C(x, y, z, t)$ is the air pollutant concentration at point (x, y, z, t) in Cartesian coordinates and at time t (kg/m^3). $\nabla=\frac{\partial}{\partial x}\vec{i}+\frac{\partial}{\partial y}\vec{j}+\frac{\partial}{\partial z}\vec{k}$, $\otimes$ is matrix multiplication. The vector V is the wind velocity field (m/s), $\overline{K}$ is the eddy-diffusivity or dispersion tensor (m^2/s) and $R(x, y, z, t)$ describes sources or sinks of the quantity of air pollutant concentration (s^{-1}). For a chemical species, $R>0$ means that a chemical reaction is creating more of the species and $R<0$ means that a chemical reaction is destroying the species. Therefore Eq. (2.12), can be rearrangement as follow:

$$\frac{\partial C}{\partial t}+V\cdot\left(\frac{\partial}{\partial x}\vec{i}+\frac{\partial}{\partial y}\vec{j}+\frac{\partial}{\partial z}\vec{k}\right)C(x,y,z)$$
$$=\left(\frac{\partial}{\partial x}\vec{i}+\frac{\partial}{\partial y}\vec{j}+\frac{\partial}{\partial z}\vec{k}\right)\cdot\left(\overline{K}\otimes\left(\frac{\partial}{\partial x}\vec{i}+\frac{\partial}{\partial y}\vec{j}+\frac{\partial}{\partial z}\vec{k}\right)C(x,y,z)\right)+R,$$
$$\frac{\partial C}{\partial t}+V(u,v,w)\cdot\left(\frac{\partial C}{\partial x}+\frac{\partial C}{\partial y}+\frac{\partial C}{\partial z}\right)$$
$$=\left(\frac{\partial}{\partial x}\vec{i}+\frac{\partial}{\partial y}\vec{j}+\frac{\partial}{\partial z}\vec{k}\right)\cdot\left(K(x,y,z)\otimes\left(\frac{\partial C}{\partial x}+\frac{\partial C}{\partial y}+\frac{\partial C}{\partial z}\right)\right)+R,$$
$$\frac{\partial C}{\partial t}+\left(u\frac{\partial C}{\partial x}+v\frac{\partial C}{\partial y}+w\frac{\partial C}{\partial z}\right)$$
$$=\left(\frac{\partial}{\partial x}\vec{i}+\frac{\partial}{\partial y}\vec{j}+\frac{\partial}{\partial z}\vec{k}\right)\cdot\left(K_x\frac{\partial C}{\partial x}+K_y\frac{\partial C}{\partial y}+K_z\frac{\partial C}{\partial z}\right)+R,$$

$$\begin{aligned}
&\frac{\partial C}{\partial t}+u\frac{\partial C}{\partial x}+v\frac{\partial C}{\partial y}+w\frac{\partial C}{\partial z}\\
&\qquad=\left(\frac{\partial}{\partial x}\left(K_x\frac{\partial C}{\partial x}\right)+\frac{\partial}{\partial y}\left(K_y\frac{\partial C}{\partial y}\right)+\frac{\partial}{\partial z}\left(K_z\frac{\partial C}{\partial z}\right)\right)+R,\\
&\frac{\partial C}{\partial t}+u\frac{\partial C}{\partial x}+v\frac{\partial C}{\partial y}+w\frac{\partial C}{\partial z}\\
&\qquad=K_x\frac{\partial^2 C}{\partial x^2}+K_y\frac{\partial^2 C}{\partial y^2}+K_z\frac{\partial^2 C}{\partial z^2}+R.
\end{aligned} \tag{2.13}$$

We set $D_x = K_x$, $D_y = K_y$, and $D_z = K_z$. Then the three-dimensional advection-diffusion equation in Eq. (2.13), can be written as

$$\frac{\partial C}{\partial t}+u\frac{\partial C}{\partial x}+v\frac{\partial C}{\partial y}+w\frac{\partial C}{\partial z}=D_x\frac{\partial^2 C}{\partial x^2}+D_y\frac{\partial^2 C}{\partial y^2}+D_z\frac{\partial^2 C}{\partial z^2}+R, \tag{2.14}$$

where

u is a constant wind speed in the x-direction,

v is a constant wind speed in the y-direction,

w is a constant wind speed in the z-direction,

D_x is a constant dispersion coefficient in the x-direction,

D_y is a constant dispersion coefficient in the y-direction,

D_z is a constant dispersion coefficient in the z-direction.

The assumptions of Eq. (2.14) are defined that the wind in flow in x- and y-directions are the horizontal direction and in z-direction is the vertical direction. Consequently, the three-dimensional advection-diffusion equation in Eq. (2.14) can be written as:

$$\frac{\partial C}{\partial t}+u\frac{\partial C}{\partial x}+v\frac{\partial C}{\partial y}=D_h\frac{\partial^2 C}{\partial x^2}+D_h\frac{\partial^2 C}{\partial y^2}+D_v\frac{\partial^2 C}{\partial z^2}+R(x,y,z,t), \tag{2.15}$$

where D_h is a constant dispersion coefficient in in the horizontal direction and$d$ D_v is the constant dispersion coefficient in the vertical direction. If we assume no sources or sinks in Eq. (2.15), we have

$$\frac{\partial C}{\partial t}+u\frac{\partial C}{\partial x}+v\frac{\partial C}{\partial y}=D_h\frac{\partial^2 C}{\partial x^2}+D_h\frac{\partial^2 C}{\partial y^2}+D_v\frac{\partial^2 C}{\partial z^2}. \tag{2.16}$$

2.4.2 Wind inflow of street tunnel configuration

A street tunnel is a place for foot or vehicular road traffic, and is enclosed except for the entrance and exit. The street is flanked by buildings on both sides, including the top area, which is also closed. A street tunnel configuration is shown in Figure 2.15. An overhead part of the street is a skytrain platform, and both sides of the street are composed of sections of building.

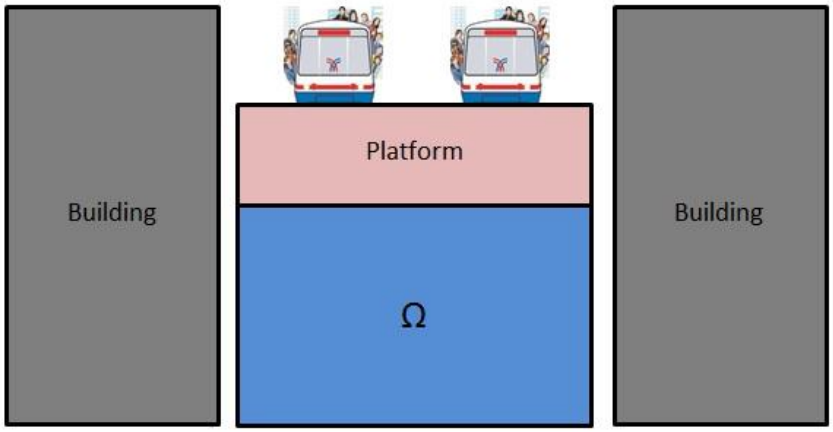

Figure 2.15 The simple street tunnel

In this research, the simulation of the simple street tunnel is divided into two cases:

2.4.2.1 Case I: Wind inflow only in x-direction

Assume that the wind is flowing only the x-direction. The considered street tunnel is illustrated in Figure 2.16(a). The wind direction field is shown in Figure 2.16(b).

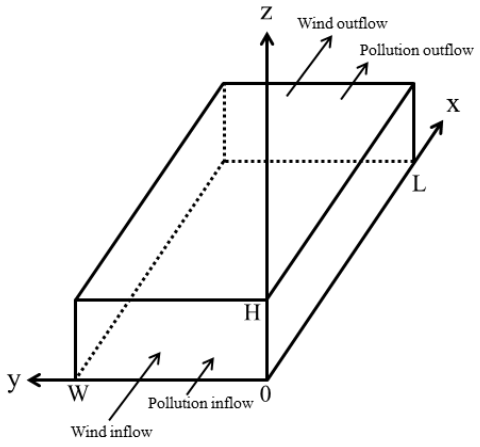

(a)

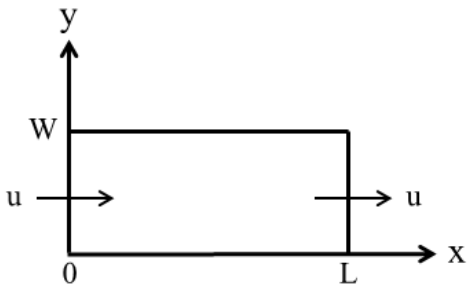

(b)

Figure 2.16 (a) The domain for street tunnel (Case I);
(b) The wind direction (Case I)

2.4.2.2 Case II: Wind inflow in x- and y-directions

Assume that the wind is flowing in the x- and y-directions. The considered street tunnel is illustrated in Figure 2.17(a). The wind direction field is shown in Figure 2.17(b).

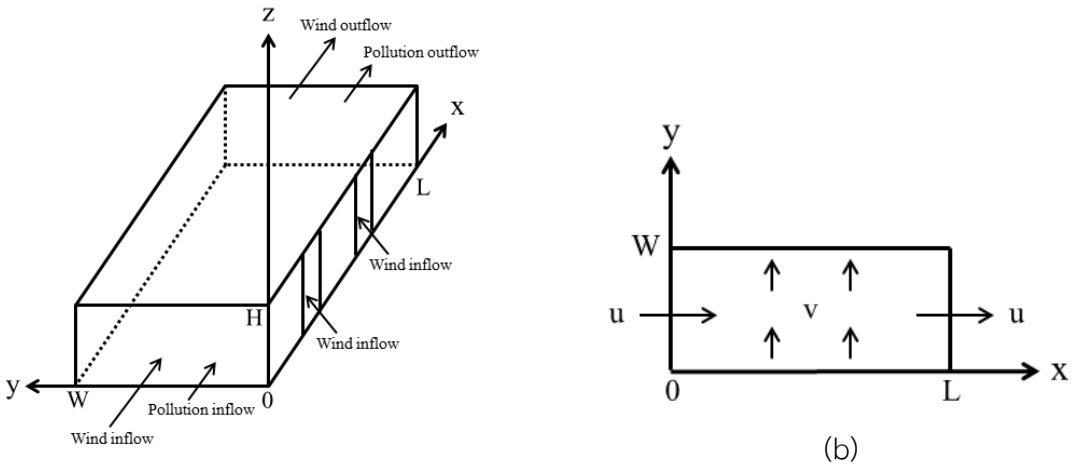

Figure 2.17 (a) The domain for street tunnel (CaseII);
(b) The wind directions CaseII)

The problem domain of this study is:

$$\Omega = \{(x, y, z);\ 0 \le x \le L,\ 0 \le y \le W,\ 0 \le z \le H\},$$

where

L is the length of tunnel (m),

W is the width of tunnel (m),

H is the height of tunnel (m).

Chapter 3
Three-dimensional Air Quality Model in an Area under a Bangkok Skytrain Platform

3.1 A numerical simulation of a three-dimensional air quality model in an area under a Bangkok skytrain platform using an explicit finite difference scheme

One of the air pollution problems in areas under Bangkok skytrain platforms is caused by pollutants coming from the entrance to the tunnel. This increases the concentration of pollutants, and affects the well-being of humans and the environment. In this research, the governing equation of the air quality model in the considered area is a three-dimensional advection-diffusion equation with time dependence. A finite difference technique is employed to approximate the solution of the governing equation. This model is solved by using an explicit forward difference in time and central difference in space (FTCS) scheme. We consider the wind inflow in two cases: wind inflow only in the x-direction, and wind inflow in the x- and y-directions. In addition, we add obstacles, such as columns, along the middle into the tunnel.

The tunnel is an underground passageway, which is enclosed except for the entrance and exit. In this research, a physical model of the steet tunnel with obstacles is shown in Figure 3.1. Above the street is the skytrain platform, and both sides of the street are sections of buildings.

Figure 3.1 Physical model of the steet tunnel with obstacles

3.1.1 Initial and boundary conditions setting techniques for street tunnel without chemical reaction

The initial condition, using the cold start technique, of the air pollutant concentration is assumed to be zero for the whole domain. It is obtained that $C(x,y,z,0)=0,$ for all $0\le x\le L,\ 0\le y\le W,\ 0\le z\le H,$ where $L,\ W$ and H are the length, width, and height of the tunnel, respectively. For the boundary conditions, we distinguish three different cases in the considered domain, as per the following:

3.1.1.1 Case I: One-direction wind inflow

Assuming that there is wind inflow only in the x-direction. In Figure 3.2, a model for Case I, for one-direction wind inflow, is shown.

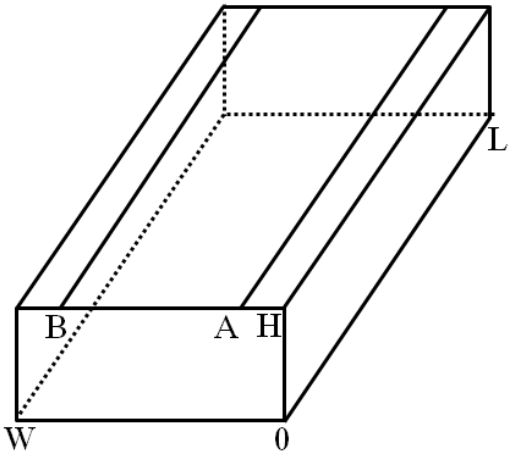

Figure 3.2 Model of the Case I: One-direction wind flowing in

The boundary conditions of Case I are as follows:

Entrance gate: $C(0,y,z,t)=c_1.$

Exit gate: $\frac{\partial C}{\partial x}(L,y,z,t)=c_2.$

Side walls: $\frac{\partial C}{\partial y}(x,0,z,t)=\frac{\partial C}{\partial y}(x,W,z,t)=0.$

Ground: $\frac{\partial C}{\partial z}(x,y,0,t)=0.$

Platform ceiling: $\frac{\partial C}{\partial z}(x,y,H,t)=0,\ A<y<B.$

Parallel gaps: $\frac{\partial C}{\partial z}(x,y,H,t)=c_3,$ otherwise,

where c_1 is the inflow air pollutant concentration in the x-direction, c_2 is the average rate of change of air pollutant concentration at the exit gate, c_3 is the average rate of change of air pollutant concentration along the both parallel gaps, A is the right parallel gap size along the ceiling, and B is the left parallel gap size along the ceiling.

3.1.1.2 Case II: One-direction wind inflow with column obstacles

Assume that there are obstacles, such as platform columns. A model of Case II, one-direction wind inflow with column obstacles, is shown in Figure 3.3.

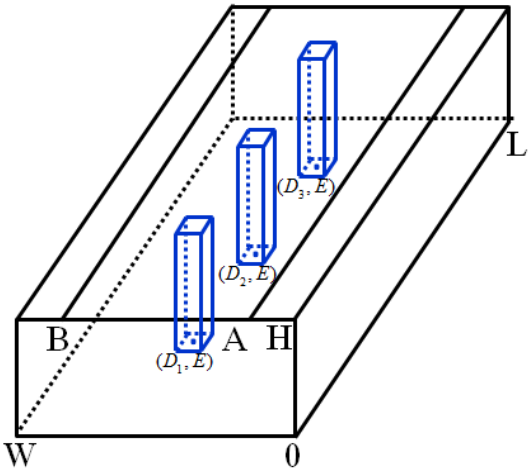

Figure 3.3 Model of the Case II: One-direction wind inflow with column obstacles

The boundary conditions of Case II are as follows:

Entrance gate: $C(0,y,z,t)=c_1.$

Exit gate: $\frac{\partial C}{\partial x}(L,y,z,t)=c_2.$

Side walls: $\frac{\partial C}{\partial y}(x,0,z,t)=\frac{\partial C}{\partial y}(x,W,z,t)=0.$

Ground: $\frac{\partial C}{\partial z}(x,y,0,t)=0.$

Platform ceiling: $\frac{\partial C}{\partial z}(x,y,H,t)=0,\ A<y<B.$

Parallel gaps: $\frac{\partial C}{\partial z}(x,y,H,t)=c_3,$ otherwise.

Center column: $C(D_i,E,z,t)=0,\ 0\le z\le H.$

Front and back column: $\frac{\partial C}{\partial x}(D_i-1,y,z,t)=\frac{\partial C}{\partial x}(D_i+1,y,z,t)=0,$
$E-1\le y\le E+1,\ t>0.$

Left and right column: $\frac{\partial C}{\partial y}(x,E-1,z,t)=\frac{\partial C}{\partial y}(x,E+1,z,t)=0,$
$D_i-1\le x\le D_i+1,\ t>0,$

where (D_i,E) is a center point of the platform column in the x- and y-directions for $i=1,2,...,ncl,$ and where ncl is the number of platform column.

3.1.1.3 Case III: Two-direction wind inflow

Assume that there is wind inflow in the x- and y-directions. In Figure 3.4, a model of Case III, for two-direction wind inflow, is shown.

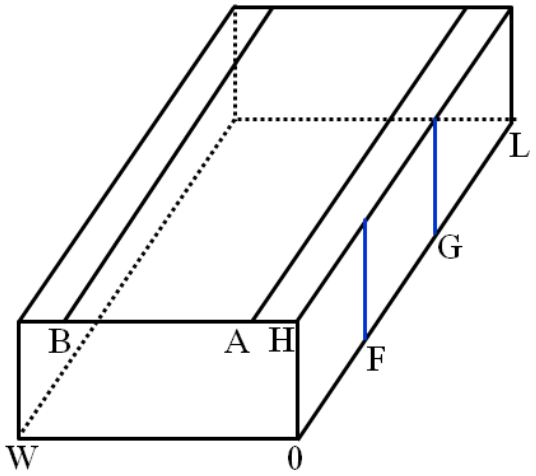

Figure 3.4 Model of the Case III: Two-directions wind inflow

The boundary conditions of Case III are as follows:

Entrance gate: $C(0,y,z,t)=c_1.$

Exit gate: $\frac{\partial C}{\partial x}(L,y,z,t)=c_2.$

Ground: $\frac{\partial C}{\partial z}(x,y,0,t)=0.$

Platform ceiling: $\frac{\partial C}{\partial z}(x,y,H,t)=0,\ A<y<B.$

Parallel gaps: $\frac{\partial C}{\partial z}(x,y,H,t)=c_3,$ otherwise.

Left side wall: $\frac{\partial C}{\partial y}(x,W,z,t)=0.$

Right side wall gap: $C(x,0,z,t)=c_4,\ F\le x\le G,\ 0\le z\le H.$

Right side wall: $\frac{\partial C}{\partial y}(x,0,z,t)=0,$ otherwise,

where c_4 is the inflow air pollutant concentration in the y-direction, and $F-G$ is the side wall gap beside the considered domain.

3.1.2 Finite difference techniques for street tunnel without chemical reaction

We use the finite difference method to approximate the solution of the three-dimensional advection-diffusion equation. The solution domain of the problem over a time $0\le t\le T$ is covered by a mesh of grid-lines: $x_i=i\Delta x,\ i=0,1,2,...,M,$

$y_j = j\Delta y,\ j = 0,1,2,...,N;\ z_k = k\Delta z,\ k = 0,1,2,...,P;\ t_n = n\Delta t,\ n = 0,1,2,...,Q$ over three spaces and time coordinate axes, respectively.

The approximate air pollutant concentration at point $(i\Delta x, j\Delta y, k\Delta z, n\Delta t)$ is denoted by $C^n_{i,j,k} = C(i\Delta x, j\Delta y, k\Delta z, n\Delta t)$ at the grid point (i, j, k, n). The constant spatial and temporal grid-spacing are $\Delta x = \frac{L}{M}$, $\Delta y = \frac{W}{N}$, $\Delta z = \frac{H}{P}$, and $\Delta t = \frac{T}{Q}$, respectively, where L, W and H are the length, width, and height of the tunnel, respectively.

The finite difference scheme approximates the solution of the three-dimensional advection-diffusion equation in equation (2.16), that is:

$$\frac{\partial C}{\partial t} + u\frac{\partial C}{\partial x} + v\frac{\partial C}{\partial y} = D_h\frac{\partial^2 C}{\partial x^2} + D_h\frac{\partial^2 C}{\partial y^2} + D_v\frac{\partial^2 C}{\partial z^2}.$$

We use an explicit forward-difference approximation for the time-derivative (FT), and central-difference approximations for the space-derivatives (CS). This is called FTCS. The approximate solution of the governing equation in equation (2.16) uses the finite difference scheme satisfies:

$$\begin{aligned}
&\frac{C^{n+1}_{i,j,k} - C^n_{i,j,k}}{\triangle t} + u\left(\frac{C^n_{i+1,j,k} - C^n_{i-1,j,k}}{2\triangle x}\right) + v\left(\frac{C^n_{i,j+1,k} - C^n_{i,j-1,k}}{2\triangle y}\right) \\
&\quad = D_h\left(\frac{C^n_{i+1,j,k} - 2C^n_{i,j,k} + C^n_{i-1,j,k}}{(\triangle x)^2}\right) + D_h\left(\frac{C^n_{i,j+1,k} - 2C^n_{i,j,k} + C^n_{i,j-1,k}}{(\triangle y)^2}\right) \\
&\quad + D_v\left(\frac{C^n_{i,j,k+1} - 2C^n_{i,j,k} + C^n_{i,j,k-1}}{(\triangle z)^2}\right).
\end{aligned} \tag{3.1}$$

Rearrangement of equation (3.1) gives,

$$\begin{aligned}
C^{n+1}_{i,j,k} &= \left(\frac{D_h\triangle t}{(\triangle x)^2} + \frac{u\triangle t}{2\triangle x}\right)C^n_{i-1,j,k} + \left(\frac{D_h\triangle t}{(\triangle y)^2} + \frac{v\triangle t}{2\triangle y}\right)C^n_{i,j-1,k} + \left(\frac{D_v\triangle t}{(\triangle z)^2}\right)C^n_{i,j,k-1} \\
&+ \left(\frac{D_h\triangle t}{(\triangle x)^2} - \frac{u\triangle t}{2\triangle x}\right)C^n_{i+1,j,k} + \left(\frac{D_h\triangle t}{(\triangle y)^2} - \frac{v\triangle t}{2\triangle y}\right)C^n_{i,j+1,k} + \left(\frac{D_v\triangle t}{(\triangle z)^2}\right)C^n_{i,j,k+1} \\
&+ \left(1 - 2\frac{D_h\triangle t}{(\triangle x)^2} - 2\frac{D_h\triangle t}{(\triangle y)^2} - 2\frac{D_v\triangle t}{(\triangle z)^2}\right)C^n_{i,j,k}.
\end{aligned} \tag{3.2}$$

Simplification of equation (3.2), we get

$$\begin{aligned} C_{i,j,k}^{n+1} &= \left(s_x + \frac{r_x}{2}\right) C_{i-1,j,k}^{n} + \left(s_y + \frac{r_y}{2}\right) C_{i,j-1,k}^{n} + \left(s_z\right) C_{i,j,k-1}^{n} \\ &+ \left(s_x - \frac{r_x}{2}\right) C_{i+1,j,k}^{n} + \left(s_y - \frac{r_y}{2}\right) C_{i,j+1,k}^{n} + \left(s_z\right) C_{i,j,k+1}^{n} \\ &+ \left(1 - 2s_x - 2s_y - 2s_z\right) C_{i,j,k}^{n}, \end{aligned} \tag{3.3}$$

in which $r_x = \frac{u\Delta t}{\Delta x}$, $r_y = \frac{v\Delta t}{\Delta y}$, $s_x = \frac{D_h \Delta t}{(\Delta x)^2}$, $s_y = \frac{D_h \Delta t}{(\Delta y)^2}$ and $s_z = \frac{D_v \Delta t}{(\Delta z)^2}$. The stability of this three-dimensional finite difference method may be investigated by using the von Neumann method, showing that [4, 15] are stable if both

$$s_x + s_y + s_z \le \frac{1}{2}, \tag{3.4}$$

and

$$\frac{r_x^2}{s_x} + \frac{r_y^2}{s_y} \le 3, \tag{3.5}$$

are satisfied.

The finite difference scheme for the left-hand side $(x = 0)$ and the right-hand side $(x = L)$ are as follows:

$$\frac{\partial C}{\partial x}(x_0, y_j, z_k) \approx \frac{-3C_{0,j,k}^{n} + 4C_{1,j,k}^{n} - C_{2,j,k}^{n}}{2\Delta x}, \tag{3.6}$$

$$\frac{\partial C}{\partial x}(x_M, y_j, z_k) \approx \frac{3C_{M,j,k}^{n} - 4C_{M-1,j,k}^{n} + C_{M-2,j,k}^{n}}{2\Delta x}, \tag{3.7}$$

$$\frac{\partial C}{\partial y}(x_i, y_0, z_k) \approx \frac{-3C_{i,0,k}^{n} + 4C_{i,1,k}^{n} - C_{i,2,k}^{n}}{2\Delta y}, \tag{3.8}$$

$$\frac{\partial C}{\partial y}(x_i, y_N, z_k) \approx \frac{3C_{i,N,k}^{n} - 4C_{i,N-1,k}^{n} + C_{i,N-2,k}^{n}}{2\Delta y}, \tag{3.9}$$

$$\frac{\partial C}{\partial z}(x_i, y_j, z_0) \approx \frac{-3C_{i,j,0}^{n} + 4C_{i,j,1}^{n} - C_{i,j,2}^{n}}{2\Delta z}, \tag{3.10}$$

$$\frac{\partial C}{\partial z}(x_i, y_j, z_P) \approx \frac{3C_{i,j,P}^{n} - 4C_{i,j,P-1}^{n} + C_{i,j,P-2}^{n}}{2\Delta z}. \tag{3.11}$$

The stencil diagram for FTCS scheme shown in Figure 3.5.

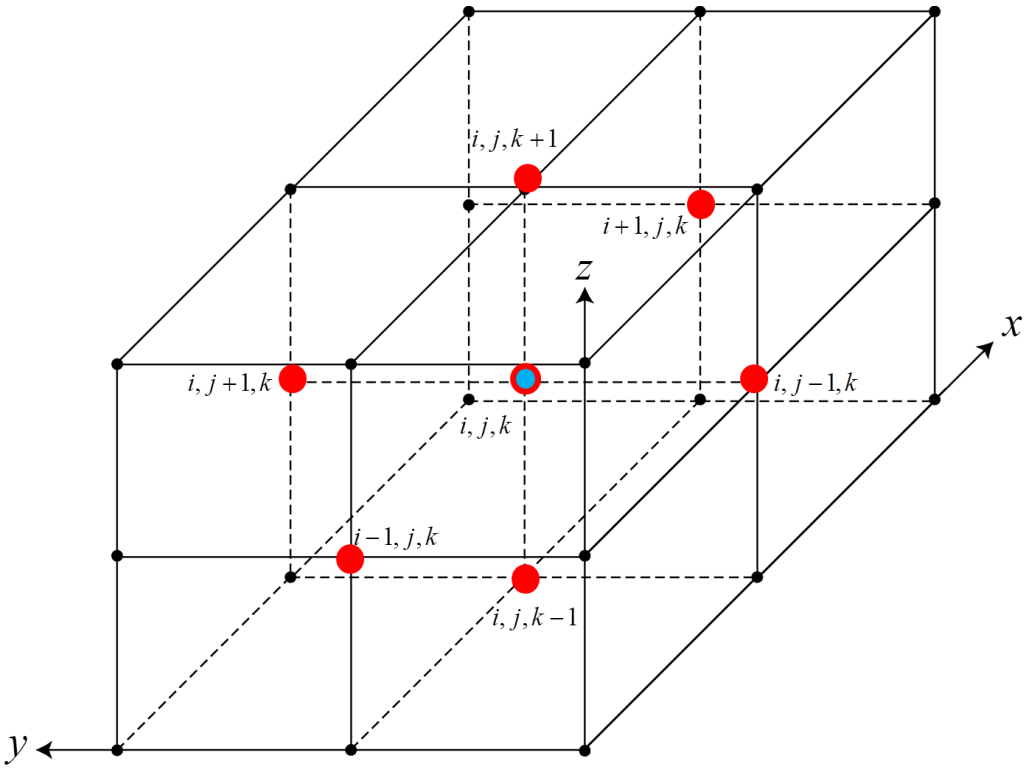

Figure 3.5 The stencil diagram for FTCS scheme

3.1.3 Numerical experiments and results for street tunnel without chemical reaction

We will show 3 cases, as already mentioned in the previous section, i.e., an area under the skytrain of the Bangkok Transit System (BTS). For Case I and Case II, we assume that there is wind inflow only in the x-direction. Case II is similar to Case I, but we add the boundary conditions of obstacles in the tunnel. For Case III, we assume that there is wind inflow in the x- and y-directions. We consider the length, width and height of tunnel to be 192, 26, and 6 meters, respectively. Then, the problem domain is $\Omega = \{(x, y, z);\ 0 \le x \le 192,\ 0 \le y \le 26,\ 0 \le z \le 6\}$.

3.1.3.1 Results for Case I

Case I: for more realistic problem, the parallel gaps along the tunnel between the ceiling and their building of the both sides are added in to the domain. It is assumed that the rate of change are decreased at the parallel gaps and the exit gate. We consider the three-dimensional advection-diffusion equation in equation (3.3) and we assume that $c_1 = 1,\ c_2 = c_3 = -0.01,\ A = 4,\ B = 24,\ \Delta x = \Delta y = \Delta z = 2\ m,\ \Delta t = 0.06\ s,\ D_h = 0.1592\ m^2/s,\ D_v = 0.05\ m^2/s,\ u = 2.7778\ m/s,\ v = 0\ m/s,$ and $z = 4m.$

The numerical results of Case I are shown in Table 3.1 and Figure 3.6-Figure 3.9. Figure 3.6 and Figure 3.7 show the air pollutant concentration levels after 30 second have passed in a contour plot and surface plot, respectively. Figure 3.8 and Figure 3.9 show the air pollutant concentration levels after 120 second have passed in a contour plot and surface plot, respectively. If we increase the time in our system, the concentration of pollutant will be reduced.

Table 3.1 The air pollutant concentration for Case I at $z = 4\ m$ and $T = 30\ s$

$y(m) \setminus x(m)$	30	60	90	120	150
6	0.8949	0.6173	0.0390	-0.0005	-0.0010
10	0.9278	0.6704	0.0454	-0.0001	-0.0006
14	0.9288	0.6727	0.0460	-0.0000	-0.0004
18	0.9287	0.6724	0.0459	-0.0000	-0.0005
22	0.9229	0.6599	0.0436	-0.0003	-0.0009

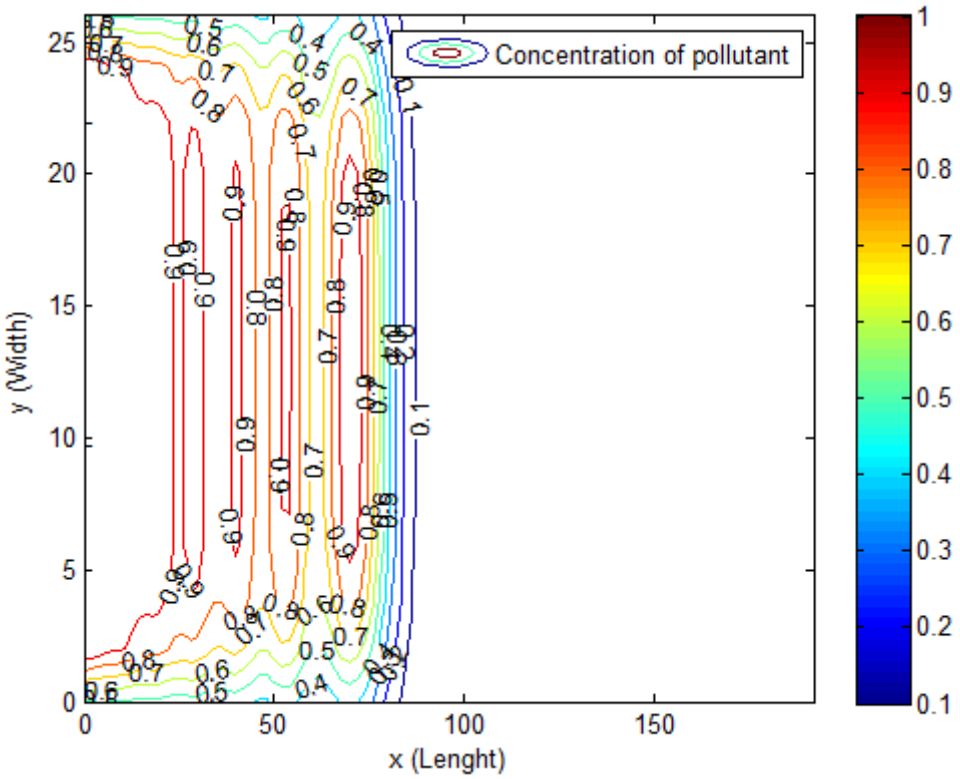

Figure 3.6 Contour plot of concentration of air pollutant levels for Case I after passed 30 second

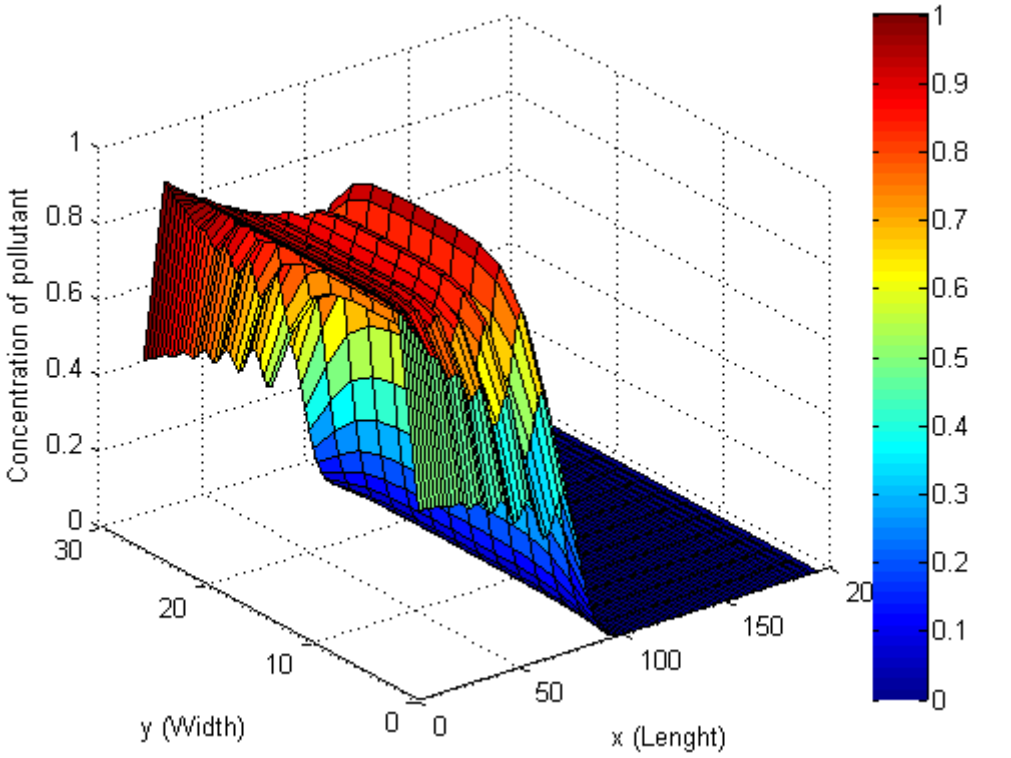

Figure 3.7 Surface plot of concentration of air pollutant levels for Case I after passed 30 second

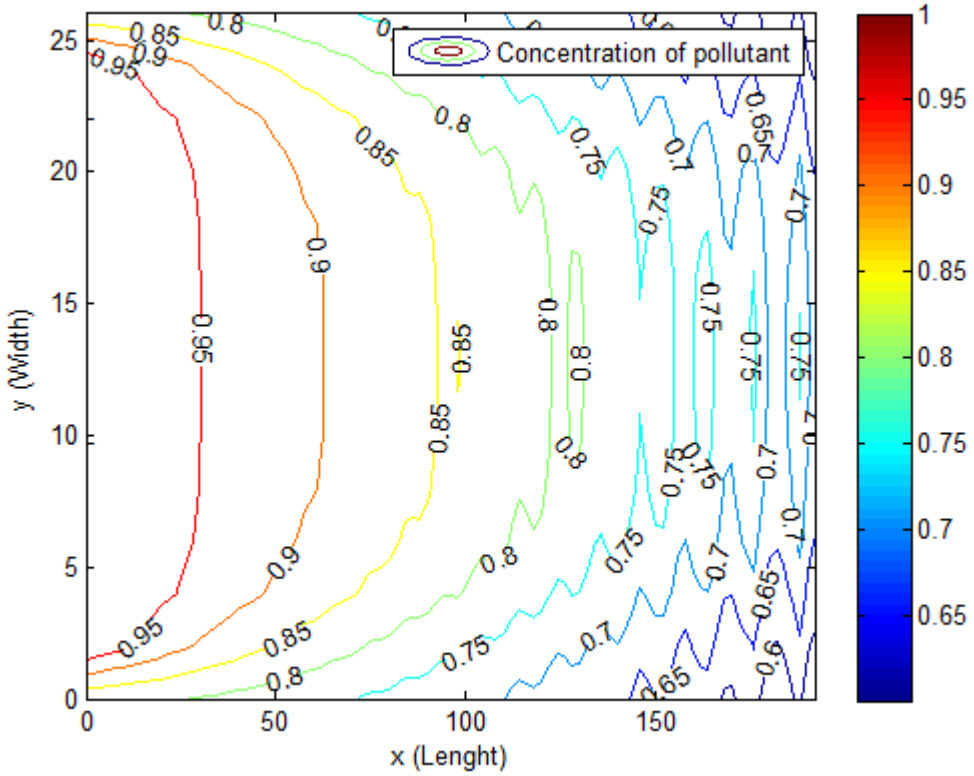

Figure 3.8 Contour plot of concentration of air pollutant levels for Case I after passed 120 second

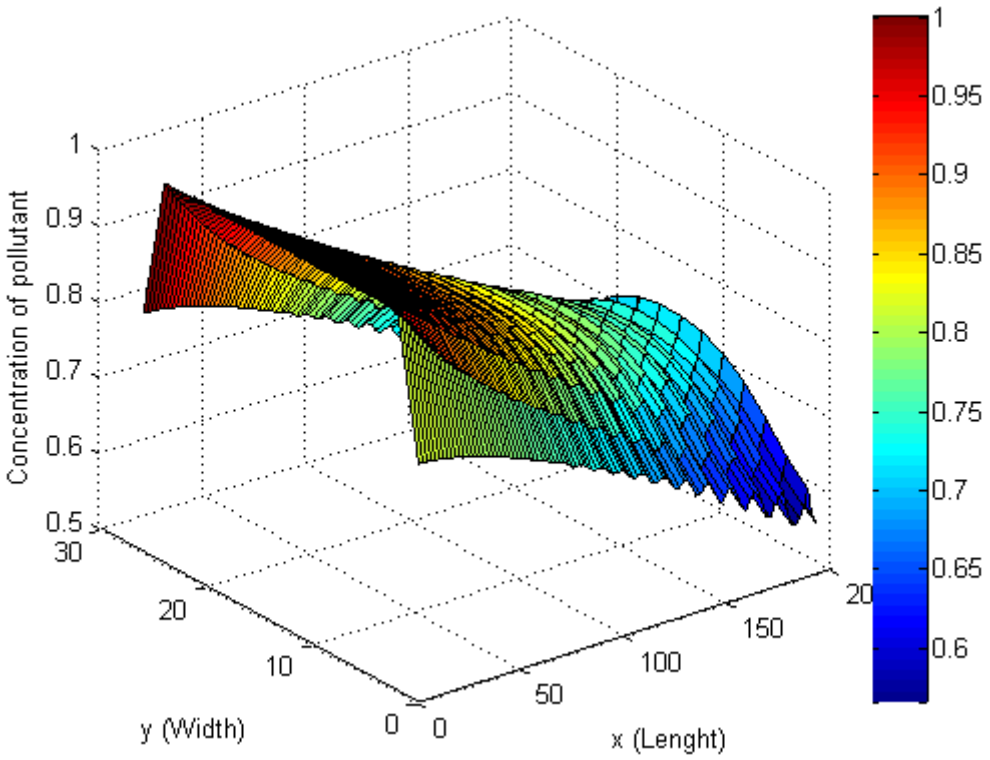

Figure 3.9 Surface plot of concentration of air pollutant levels for Case I after passed 120 second

3.1.3.2 Results for Case II

Case II: in reality, there are obstacles, such as columns. Therefore, we will add the boundary conditions of obstacles in the tunnel. It is assumed that there is no rate of change at the columns. We consider the three-dimensional advection-diffusion equation in equation (3.3) and we assume that $c_1 = 1,\ c_2 = c_3 = -0.01,\ A = 4,$ $B = 24,\ D_1 = 41,\ D_2 = 101,\ D_3 = 161,\ E = 14,\ \Delta x = \Delta y = \Delta z = 2\ m,\ \Delta t = 0.06\ s,\ D_h = 0.1592\ m^2/s,$ $D_v = 0.05\ m^2/s,\ ncl = 3,\ u = 2.7778\ m/s,\ v = 0\ m/s,$ and $z = 4\ m.$

The numerical results of Case II are shown in Table 3.2 and Figure 3.10-Figure 3.13. That is Figure 3.10 and Figure 3.11 show the air pollutant concentration levels after 30 second have passed in a contour plot and surface plot, respectively. Figure 3.12 and Figure 3.13 show the air pollutant concentration levels after 120 second have passed in a contour plot and surface plot, respectively. The results are agreeable, and the concentration of pollutant is decreased away from the source.

Table 3.2 The air pollutant concentration for Case II at $z = 4\ m$ and $T = 30\ s$

$y(m) \setminus x(m)$	30	60	90	120	150
6	0.9435	0.7615	0.0165	-0.0001	-0.0001
10	0.9353	0.6499	0.0131	-0.0000	-0.0000
14	0.8718	0.2665	0.0085	-0.0000	-0.0000
18	0.9432	0.7561	0.0161	-0.0000	-0.0000
22	0.9406	0.7469	0.0152	-0.0003	-0.0003

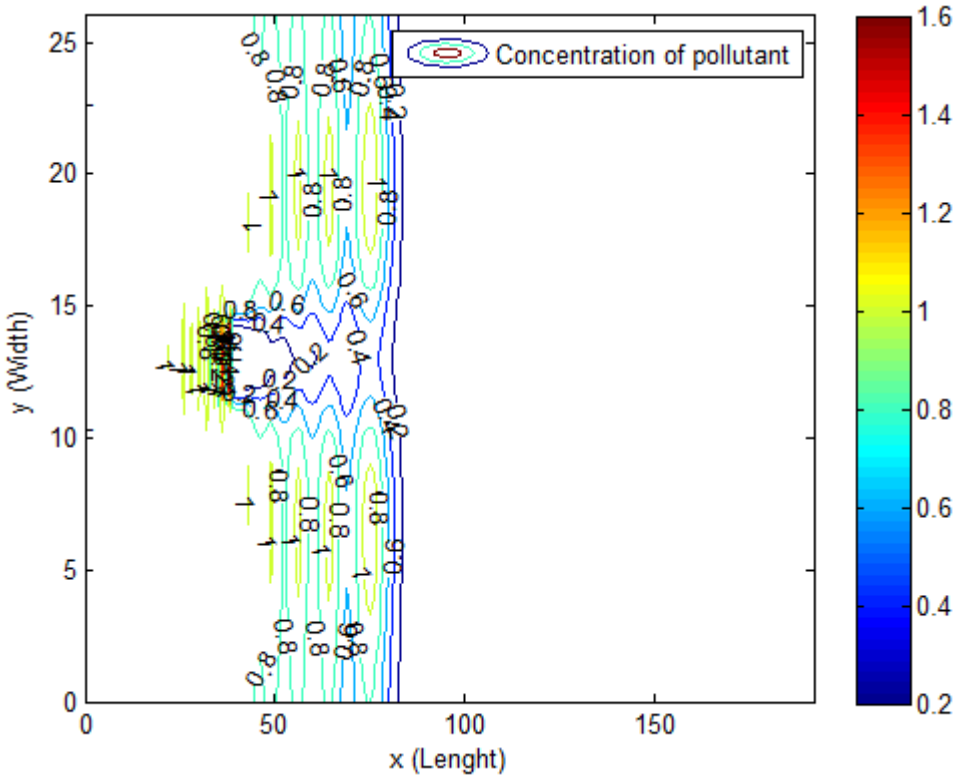

Figure 3.10 Contour plot of concentration of air pollutant levels for Case II after passed 30 second

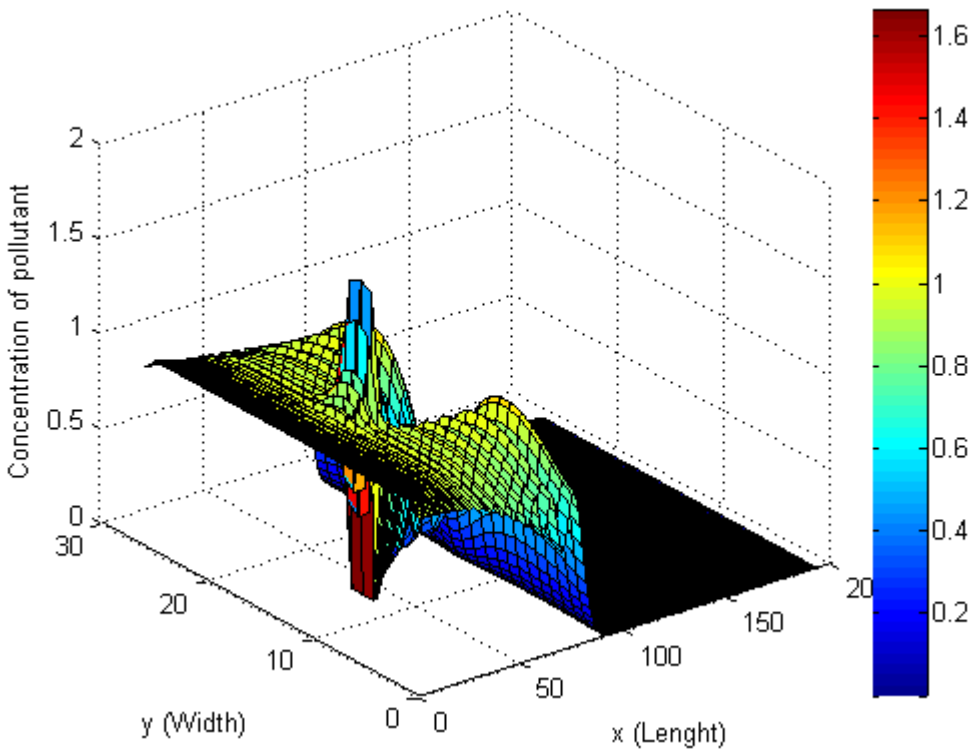

Figure 3.11 Surface plot of concentration of air pollutant levels for Case II after passed 30 second

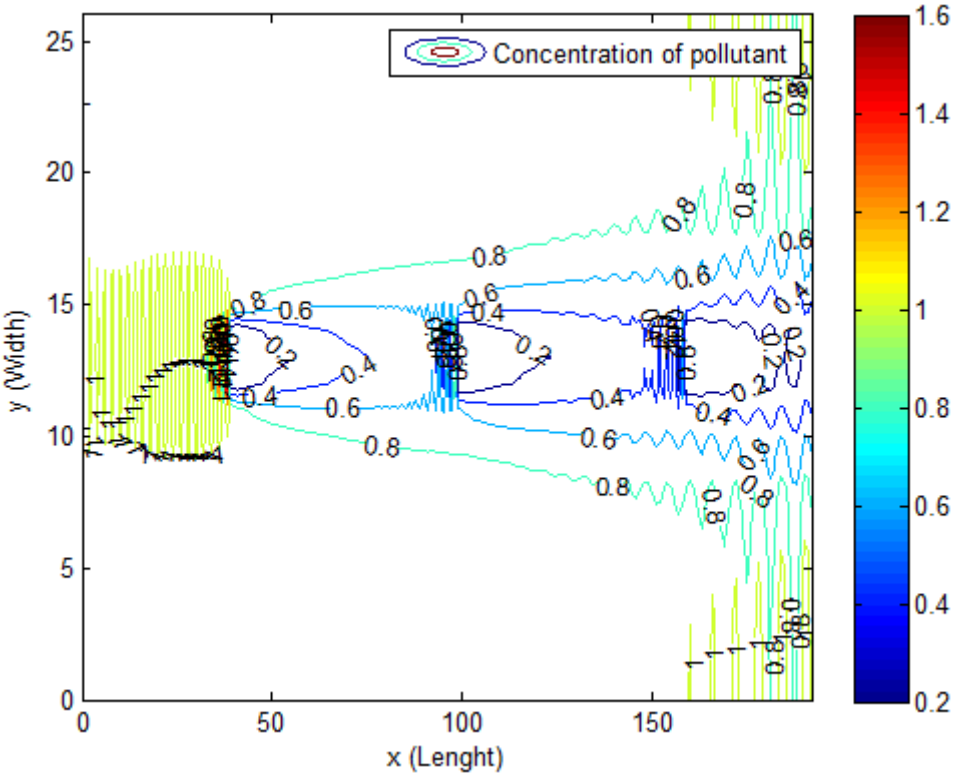

Figure 3.12 Contour plot of concentration of air pollutant levels for Case II after passed 120 second

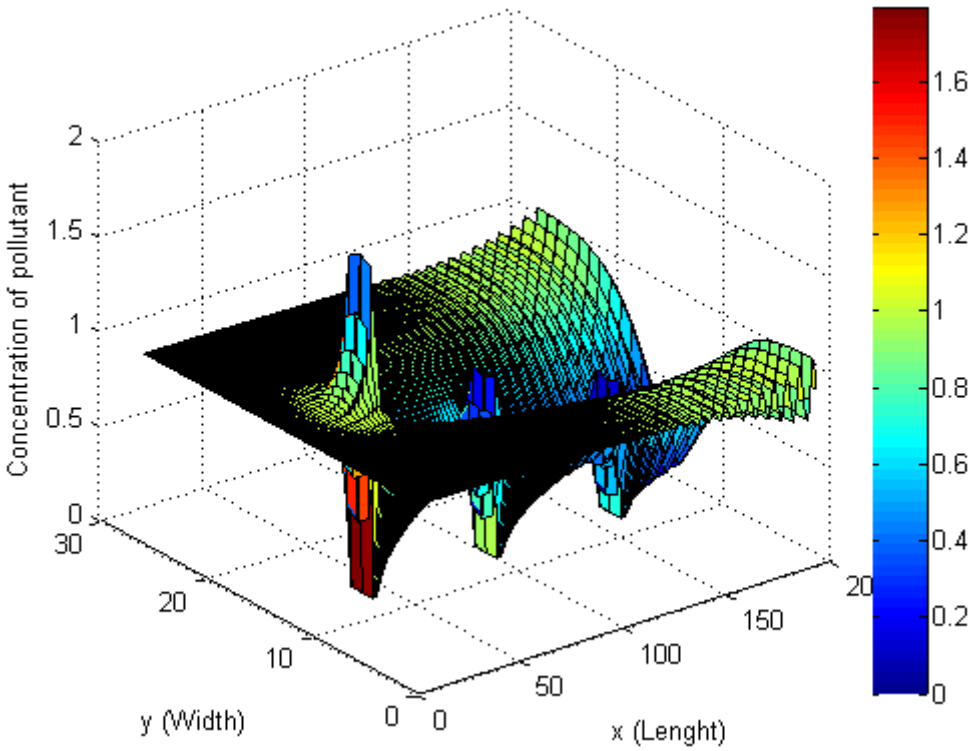

Figure 3.13 Surface plot of concentration of air pollutant levels for Case II after passed 120 second

3.1.3.3 Results for Case III

Case III: in this example, we consider the wind inflow in the x- and y-directions. That is, we will add u in x-direction and v in y-direction. We consider the three-dimensional advection-diffusion equation in equation (3.3) and we assume, $c_1 = 1,\ c_2 = c_3 = -0.01,\ c_4 = 0.5,\ A = 4,\ B = 24,\ F = 64,\ G = 129,\ \Delta x = \Delta y = \Delta z = 2m,\ \Delta t = 0.06\ s,$ $D_h = 0.1592\ m^2/s,\ D_v = 0.05\ m^2/s,\ u = 2.7778\ m/s,\ v = \frac{u}{20}\ m/s,$ and $z = 4\ m.$

The numerical results of Case III are shown in Table 3.3 and Figure 3.14-Figure 3.17. That is Figure 3.14 and Figure 3.15 show the air pollutant concentration levels after 30 second have passed in a in contour plot and surface plot, respectively. Figure 3.16 and Figure 3.17 show the air pollutant concentration levels after 120 second have passed in a contour plot and surface plot, respectively. The results are reasonable, and the concentration of pollutants are decreased away from the source.

Table 3.3 The air pollutant concentration for Case III at $z = 4\ m$ and $T = 30\ s$

$y(m) \setminus x(m)$	30	60	90	120	150
6	0.7350	0.3842	0.0936	0.1909	0.2055
10	0.9141	0.6336	0.0417	0.0284	0.0653
14	0.9278	0.6710	0.0451	0.0021	0.0083
18	0.9288	0.6727	0.0460	0.0001	0.0002
22	0.9287	0.6725	0.0458	-0.0001	-0.0006

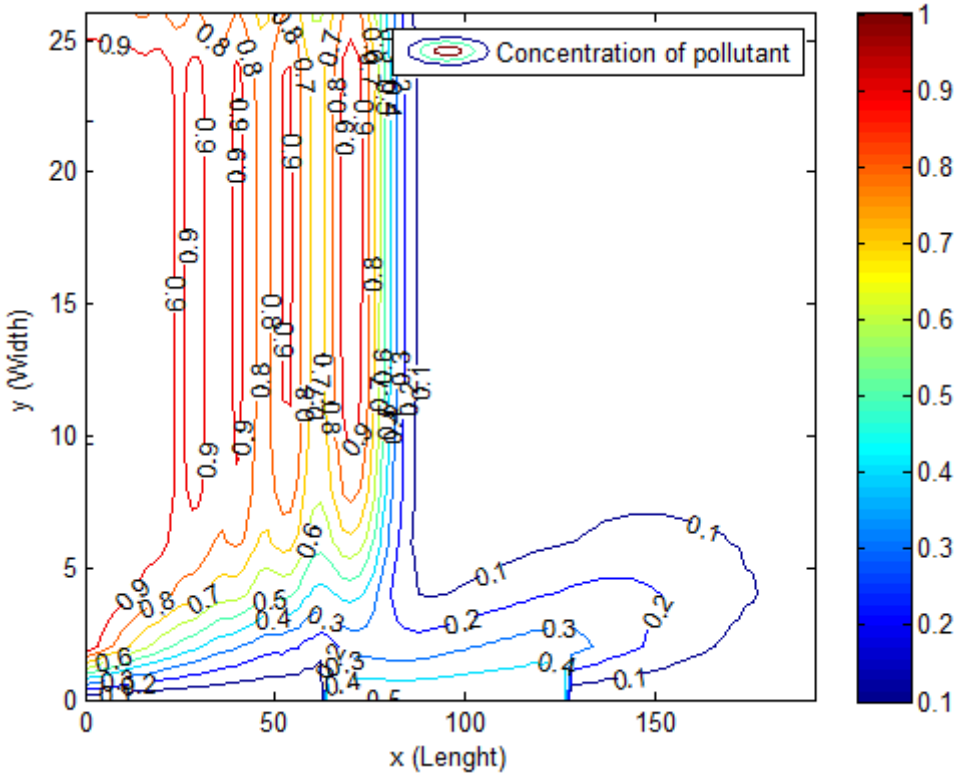

Figure 3.14 Contour plot of concentration of air pollutant levels for Case III after passed 30 second

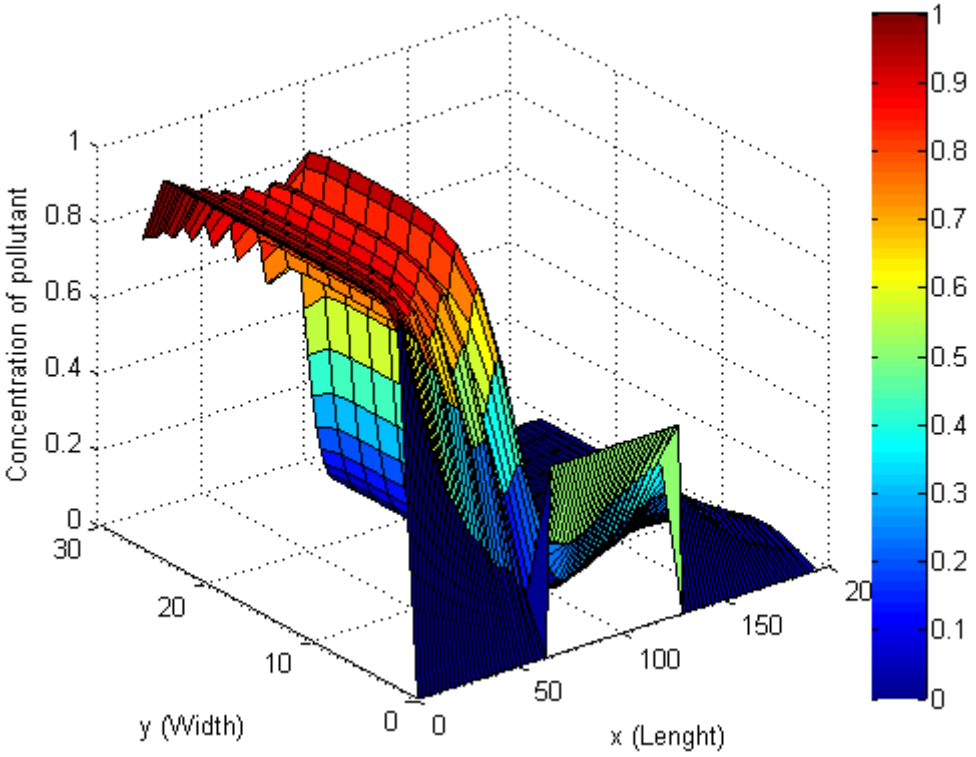

Figure 3.15 Surface plot of concentration of air pollutant levels for Case III after passed 30 second

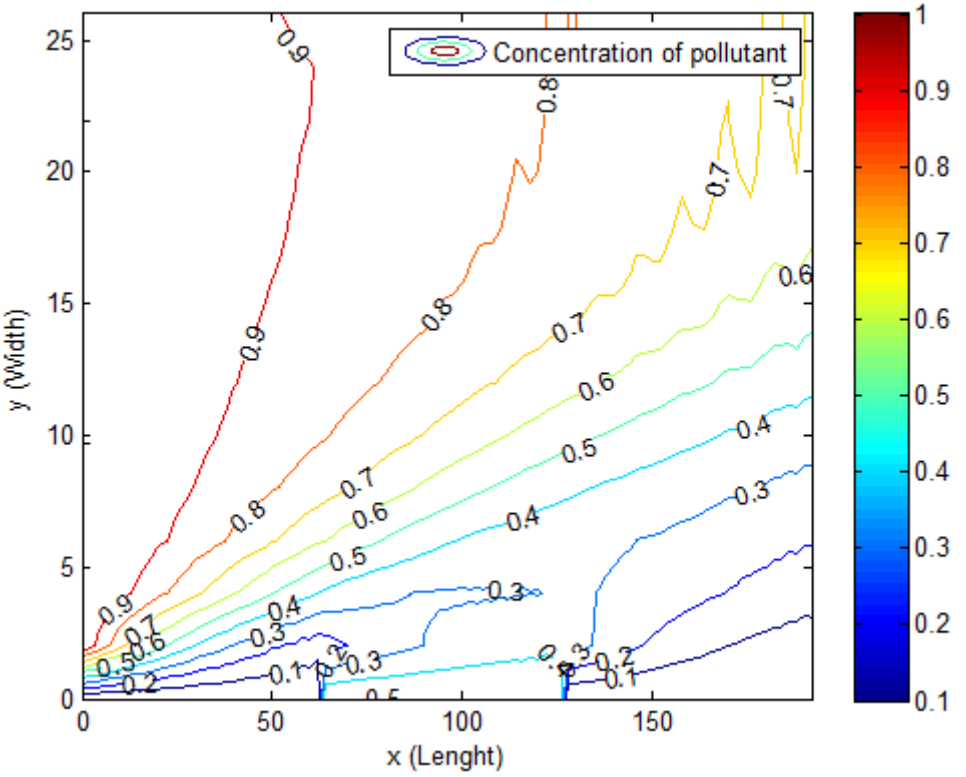

Figure 3.16 Contour plot of concentration of air pollutant levels for Case III after passed 120 second

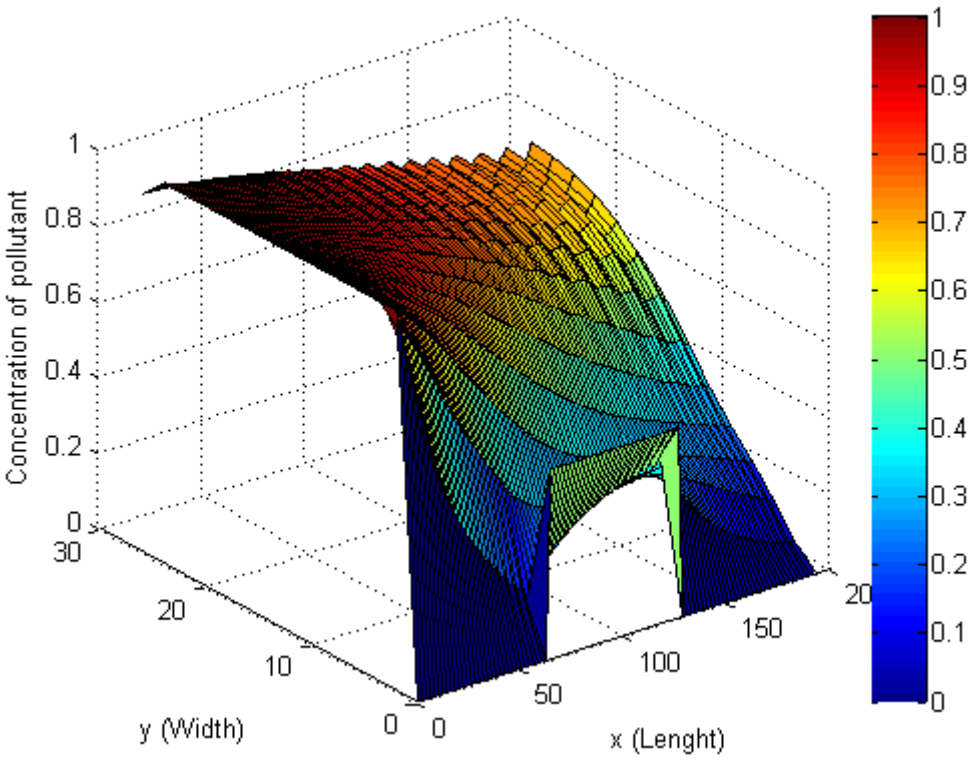

Figure 3.17 Surface plot of concentration of air pollutant levels for Case III after passed 120 second

3.2 Numerical simulation for a three-dimensional air pollution measurement model in a heavy traffic area under the Bangkok skytrain platform

Air pollutant levels in Bangkok are generally high in street tunnels. They are particularly elevated in almost closed street tunnels, such as areas under Bangkok skytrain platforms with high traffic volume, where dispersion is limited. There are no air quality measurement stations in the vicinities where human residence is high. In this research, numerical simulation is used to measure the air pollutant levels. A three-dimensional air pollution measurement model in a heavy traffic area under a Bangkok skytrain platform is proposed. The finite difference techniques are employed to approximate the modelled solutions. Vehicle air pollutant emissions due to the high traffic volume are mathematically assumed by the pollutant sources term. The simulation is also considered in averaged and moving pollutant sources, due to the manner of vehicle emissions. A physical model of the street tunnel is shown in Figure 3.18.

Figure 3.18 Physical model of the street tunnel

3.2.1 Initial and boundary conditions setting techniques for street tunnel with chemical reaction

We consider the components of the tunnel in Figure 3.19; the model of the problem can be divided into three zones, as shown in Figure 3.20.

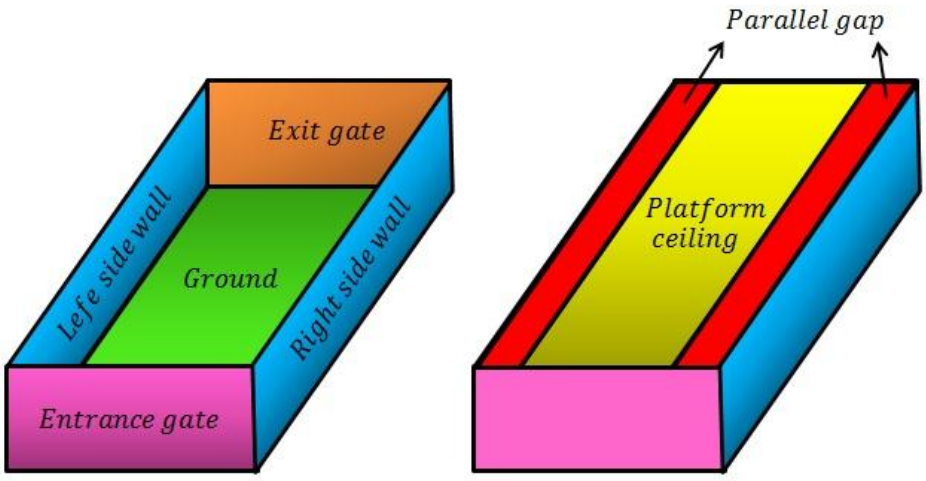

Figure 3.19 Components of the street tunnel

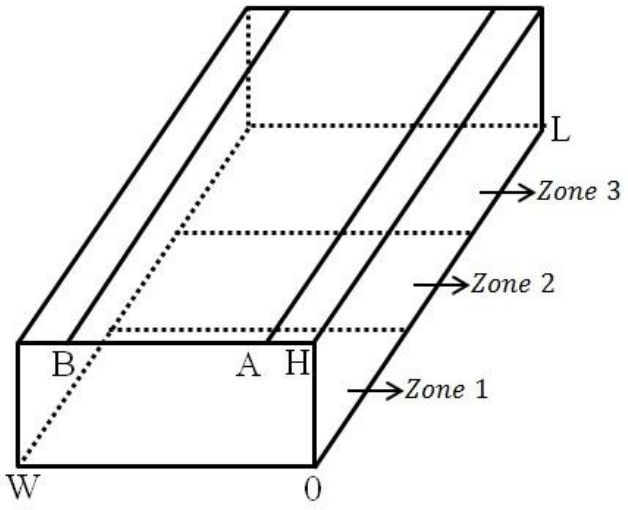

Figure 3.20 Model of the problem for three zones

The initial conditions of air pollutant concentration can be described by $C(x,y,z,0) = f(x,y,z)$, for all $(x,y,z) \in \Omega = \{(x,y,z);\ 0 \le x \le L,\ 0 \le y \le W,\ 0 \le z \le H\}$, where L is the length, W is the width, and H is the height of the tunnel. The boundary conditions are as follows:

Entrance gate: $C(0,y,z,t) = c_{N_1},\ 0 < y < W,\ 0 < z < H$

Margin of entrance gate: $\frac{\partial C}{\partial x}(0,y,z,t) = c_{N_2},\ y = 0, W,\ z = 0, H$

Exit gate: $\frac{\partial C}{\partial x}(L,y,z,t) = c_X.$

Both side walls: $\frac{\partial C}{\partial y}(x,0,z,t) = c_{W_1},\ \frac{\partial C}{\partial y}(x,W,z,t) = c_{W_2}.$

Ground: $\frac{\partial C}{\partial z}(x,y,0,t) = c_F.$

Platform ceiling: $\frac{\partial C}{\partial z}(x,y,H,t) = c_T,\ A < y < B.$

Ceiling Parallel gaps: $\frac{\partial C}{\partial z}(x,y,H,t) = c_{G_1},\ 0 \le y \le A,$

$\frac{\partial C}{\partial z}(x,y,H,t) = c_{G_2},\ B \le y \le W,$

where c_{N_1} is the inflow air pollutant concentration at the entrance gate c_{N_2}, c_X, c_{W_1}, c_{W_2}, c_F, c_T, c_{G_1}, c_{G_2} are the averaged rates of change of air pollutant concentration at the margin of the entrance gate, exit gate, both side walls, ground, platform ceiling, and both ceiling parallel gaps, respectively. A is the distance from the right wall to the right-ended platform ceiling, and B is the distance from the right wall to the left-ended platform ceiling, seen in Figure 3.20.

3.2.2 Finite difference techniques for street tunnel with chemical reaction

We use the finite difference method to approximate the solution of the three-dimensional advection-diffusion equation. The solution domain of the problem over time $0 \le t \le T$ is covered by a mesh of grid-lines: $x_i = i\Delta x,\ i = 0,1,2,...,M,\ y_j = j\Delta y,$ $j = 0,1,2,...,N,\ z_k = k\Delta z,\ k = 0,1,2,...,P,$ and $t_n = n\Delta t,\ n = 0,1,2,...,Q$ over three spaces and time coordinate axes, respectively. The approximate air pollutant concentration at point $(i\Delta x, j\Delta y, k\Delta z, n\Delta t)$ is denoted by $C^n_{i,j,k} = C(i\Delta x, j\Delta y, k\Delta z, n\Delta t)$ at the grid point (i, j, k, n). The constant spatial and temporal grid-spacing are $\Delta x = \frac{L}{M},\ \Delta y = \frac{W}{N},\ \Delta z = \frac{H}{P},$ and $\Delta t = \frac{T}{Q},$ respectively, where L is the length, W is the width, and H is the height of the tunnel.

The finite difference scheme approximates the solution of the three-dimensional advection-diffusion equation in equation (2.15), that is

$$\frac{\partial C}{\partial t} + u\frac{\partial C}{\partial x} + v\frac{\partial C}{\partial y} = D_h\frac{\partial^2 C}{\partial x^2} + D_h\frac{\partial^2 C}{\partial y^2} + D_v\frac{\partial^2 C}{\partial z^2} + R(x,y,z,t).$$

In this research, an explicit forward time central space (FTCS) method is employed. Consequently, the finite difference equation to equation (*2.15*) becomes

$$\begin{aligned}
&\frac{C^{n+1}_{i,j,k} - C^n_{i,j,k}}{\Delta t} + u\left(\frac{C^n_{i+1,j,k} - C^n_{i-1,j,k}}{2\Delta x}\right) + v\left(\frac{C^n_{i,j+1,k} - C^n_{i,j-1,k}}{2\Delta y}\right) \\
&= D_h\left(\frac{C^n_{i+1,j,k} - 2C^n_{i,j,k} + C^n_{i-1,j,k}}{(\Delta x)^2}\right) + D_h\left(\frac{C^n_{i,j+1,k} - 2C^n_{i,j,k} + C^n_{i,j-1,k}}{(\Delta y)^2}\right) \\
&+ D_v\left(\frac{C^n_{i,j,k+1} - 2C^n_{i,j,k} + C^n_{i,j,k-1}}{(\Delta z)^2}\right) + R^n_{i,j,k}.
\end{aligned} \tag{3.12}$$

Rearrangement of equation (3.12) gives,

$$\begin{aligned}
C^{n+1}_{i,j,k} &= \left(\frac{D_h\Delta t}{(\Delta x)^2} + \frac{u\Delta t}{2\Delta x}\right)C^n_{i-1,j,k} + \left(\frac{D_h\Delta t}{(\Delta y)^2} + \frac{v\Delta t}{2\Delta y}\right)C^n_{i,j-1,k} + \left(\frac{D_v\Delta t}{(\Delta z)^2}\right)C^n_{i,j,k-1} \\
&+ \left(\frac{D_h\Delta t}{(\Delta x)^2} - \frac{u\Delta t}{2\Delta x}\right)C^n_{i+1,j,k} + \left(\frac{D_h\Delta t}{(\Delta y)^2} - \frac{v\Delta t}{2\Delta y}\right)C^n_{i,j+1,k} + \left(\frac{D_v\Delta t}{(\Delta z)^2}\right)C^n_{i,j,k+1} \\
&+ \left(1 - 2\frac{D_h\Delta t}{(\Delta x)^2} - 2\frac{D_h\Delta t}{(\Delta y)^2} - 2\frac{D_v\Delta t}{(\Delta z)^2}\right)C^n_{i,j,k} + (\Delta t)R^n_{i,j,k}.
\end{aligned} \tag{3.13}$$

Simplification of equation (3.13), we get

$$\begin{aligned} C_{i,j,k}^{n+1} &= \left(s_x + \frac{r_x}{2}\right)C_{i-1,j,k}^{n} + \left(s_y + \frac{r_y}{2}\right)C_{i,j-1,k}^{n} + \left(s_z\right)C_{i,j,k-1}^{n} \\ &+ \left(s_x - \frac{r_x}{2}\right)C_{i+1,j,k}^{n} + \left(s_y - \frac{r_y}{2}\right)C_{i,j+1,k}^{n} + \left(s_z\right)C_{i,j,k+1}^{n} \\ &+ \left(1 - 2s_x - 2s_y - 2s_z\right)C_{i,j,k}^{n} + \left(\Delta t\right)R_{i,j,k}^{n}, \end{aligned} \tag{3.14}$$

in which $r_x = \dfrac{u\Delta t}{\Delta x}$, $r_y = \dfrac{v\Delta t}{\Delta y}$, $s_x = \dfrac{D_h \Delta t}{(\Delta x)^2}$, $s_y = \dfrac{D_h \Delta t}{(\Delta y)^2}$ and $s_z = \dfrac{D_v \Delta t}{(\Delta z)^2}$.

The finite difference scheme for the left-hand side and the right-hand side of the fictitious points are as follows:

$$\frac{\partial C}{\partial x}(x_0, y_j, z_k, t_n) \approx \frac{-3C_{0,j,k}^{n} + 4C_{1,j,k}^{n} - C_{2,j,k}^{n}}{2\Delta x} = c_{N_2}, \tag{3.15}$$

$$\frac{\partial C}{\partial y}(x_i, y_0, z_k, t_n) \approx \frac{-3C_{i,0,k}^{n} + 4C_{i,1,k}^{n} - C_{i,2,k}^{n}}{2\Delta y} = c_{W_1}, \tag{3.16}$$

$$\frac{\partial C}{\partial z}(x_i, y_i, z_0, t_n) \approx \frac{-3C_{i,j,0}^{n} + 4C_{i,j,1}^{n} - C_{i,j,2}^{n}}{2\Delta z} = c_F, \tag{3.17}$$

$$\frac{\partial C}{\partial x}(x_M, y_j, z_k, t_n) \approx \frac{3C_{M,j,k}^{n} - 4C_{M-1,j,k}^{n} + C_{M-2,j,k}^{n}}{2\Delta x} = c_X, \tag{3.18}$$

$$\frac{\partial C}{\partial y}(x_i, y_N, z_k, t_n) \approx \frac{3C_{i,N,k}^{n} - 4C_{i,N-1,k}^{n} + C_{i,N-2,k}^{n}}{2\Delta y} = c_{W_2}, \tag{3.19}$$

$$\frac{\partial C}{\partial z}(x_i, y_j, z_P, t_n) \approx \frac{3C_{i,j,P}^{n} - 4C_{i,j,P-1}^{n} + C_{i,j,P-2}^{n}}{2\Delta z} = c_T = c_{G_2} = c_{G_2}. \tag{3.20}$$

3.2.3 Numerical experiments and results for street tunnel with chemical reaction

In this section, there are three simulations of released air pollutant phenomena, demonstrated by using the finite difference in equation (3.14). In all simulations, the air flows along the x-direction from the entrance to the exit gates. There are two parallel gaps along the celling, as seen in Figure 3.18 and Figure 3.19. There is no potential ambient air pollution. There are two buildings that brace the areas, as seen in Figure 3.18. All of the building walls are made of non-absorbing air pollution materials. Since there is no potential air pollution, the initial conditions are assumed by $f(x, y, z) = 0$.

For three simulation, the experimented area has dimensions such that the length, width and height are 192, 26, and 6 meters, respectively. Then, the simulated

domain is defined by $\Omega = \{(x, y, z);\ 0 \le x \le 192,\ 0 \le y \le 26,\ 0 \le z \le 6\}$. We assume:, $c_{N_1} = 1,\ c_{N_2} = c_{W_1} = c_{W_2} = c_F = c_T = 0,\ c_X = c_{G_1} = c_{G_2} = -0.01,\ A = 4,$ and $B = 24.$ When we consider the model of problem as shown in Figure 3.20, $0 \le x < 64,\ 64 \le x \le 128$ and $128 < x \le 192$ are zones 1, zones 2, and zones 3, respectively. The grid spacing: $\Delta x = \Delta y = \Delta z = 2\ m,\ \ z = 4\ m,\ \Delta t = 0.06\ s$ and for the time $T = 30\ s.$ We choose the diffusion coefficient in x- and z-directions are 0.1592 and $0.05\ m^2/s,$ respectively with diffusion coefficient in x- and y-directions are equal. The wind velocity in x- and y-directions are 2.7778 and $0\ m/s,$ respectively.

3.2.3.1 Simulation A : Source or sink emissions are averaged

In this example, we consider two cases. In the first case, R is the constant of source $(R > 0)$, which are $0.001, 0.004$ and $0.007\ s^{-1}$. The results are shown in Figure 3.21-Figure 3.24. The second case, R is the constant of sink $(R < 0),$ which are $-0.001,\ -0.004,$ and $-0.007\ s^{-1}$. The results are shown in Figure 3.25-Figure 3.28.

Morover, Figure 3.21-Figure 3.22 and Figure 3.25-Figure 3.26 show the air pollutant concentration levels after passing 30 second in contour plot and surface plot between $R = 0.007$ (Source) and $R = -0.007$ (Sink), respectively. Figure 3.23 and Figure 3.27 compare the air pollutant concentration levels where R is the constant in first case and second case of Simulation $A,$ respectively. From the results, if we take more source rates into our system, we can see that the concentration of air pollutant levels increases (see Figure 3.23). Therefore, the concentration varies with the sources. Furthermore, the sink can lower the concentration of the air pollutant levels (see Figure 3.27). Finally of Simulation $A,$ Figure 3.24 and Figure 3.28 are compared the concentration of air pollutant at $x = 60\ m,\ y = 14\ m,$ and $z = 4\ m$ in different time of sources and sinks, respectively.

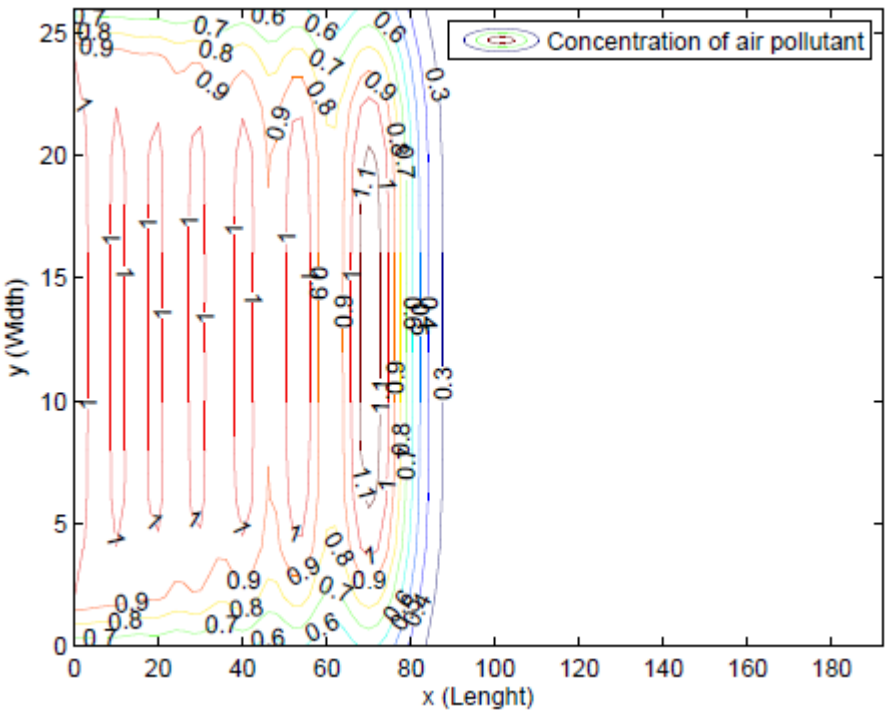

Figure 3.21 Contour plot of concentration of air pollutant levels for $R = 0.007$ sec^{-1}

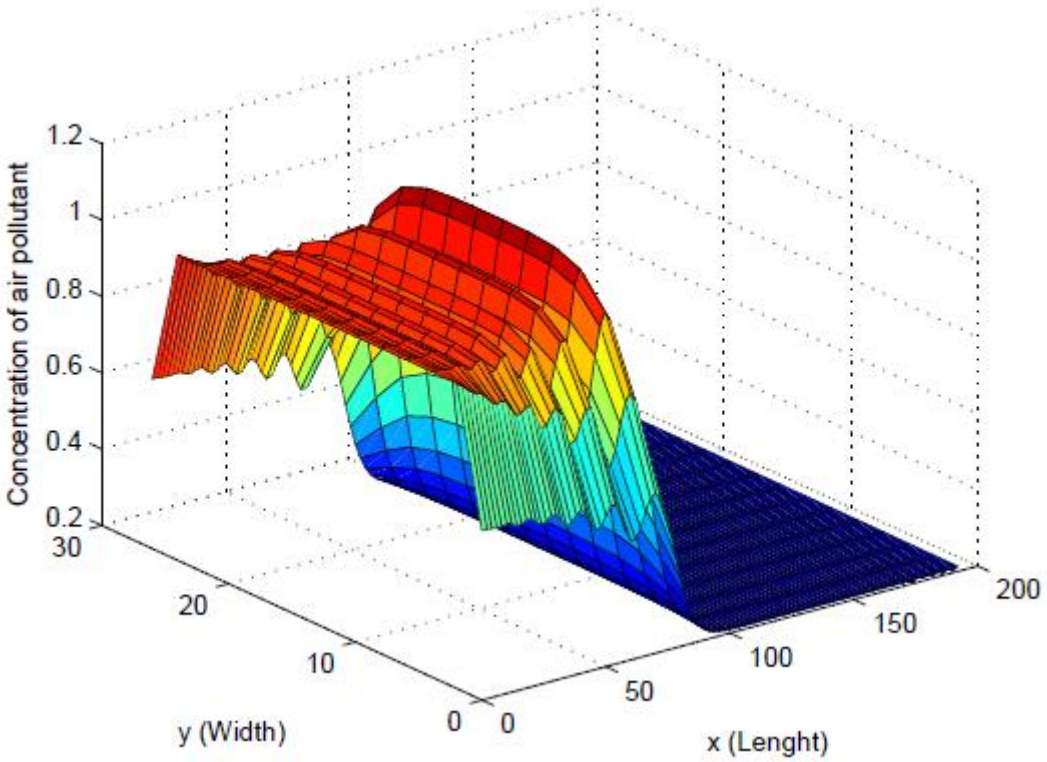

Figure 3.22 Surface plot of concentration of air pollutant levels for $R = 0.007$ sec^{-1}

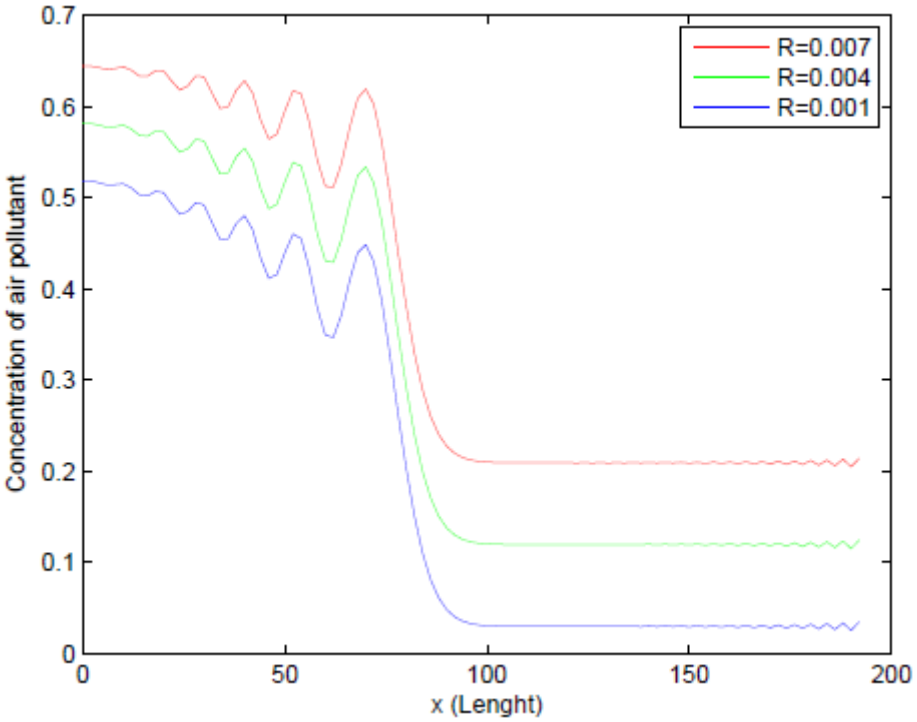

Figure 3.23 Compare the concentration of air pollutant where $R = 0.001,\ R = 0.004,$ and $R = 0.007$ $\sec^{-1}$

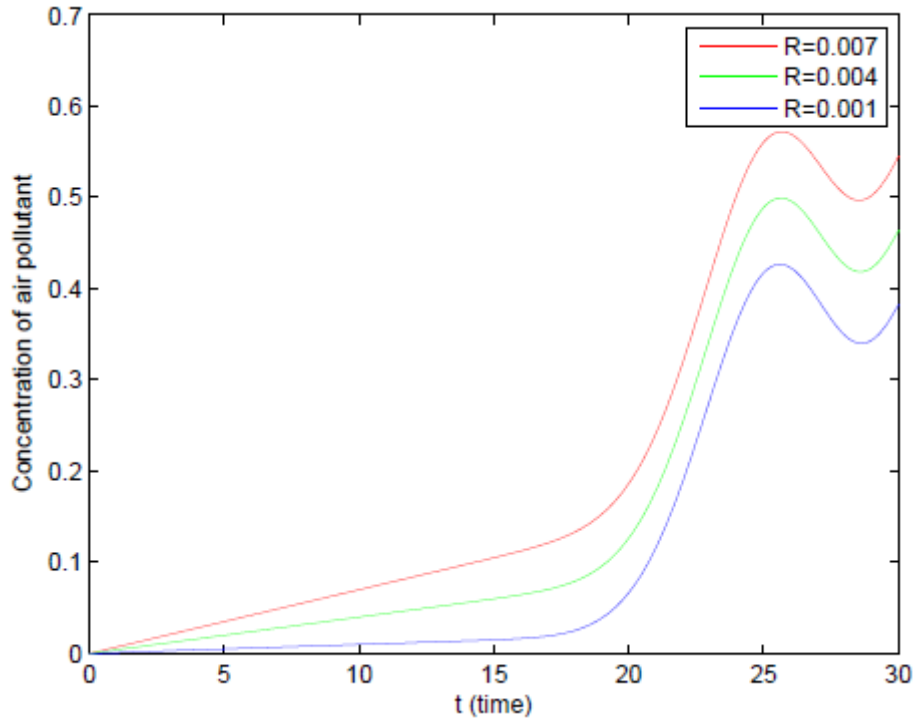

Figure 3.24 Compare the concentration of air pollutant at $x = 60\ m,\ y = 14\ m,\ z = 4\ m$ of sources in different time

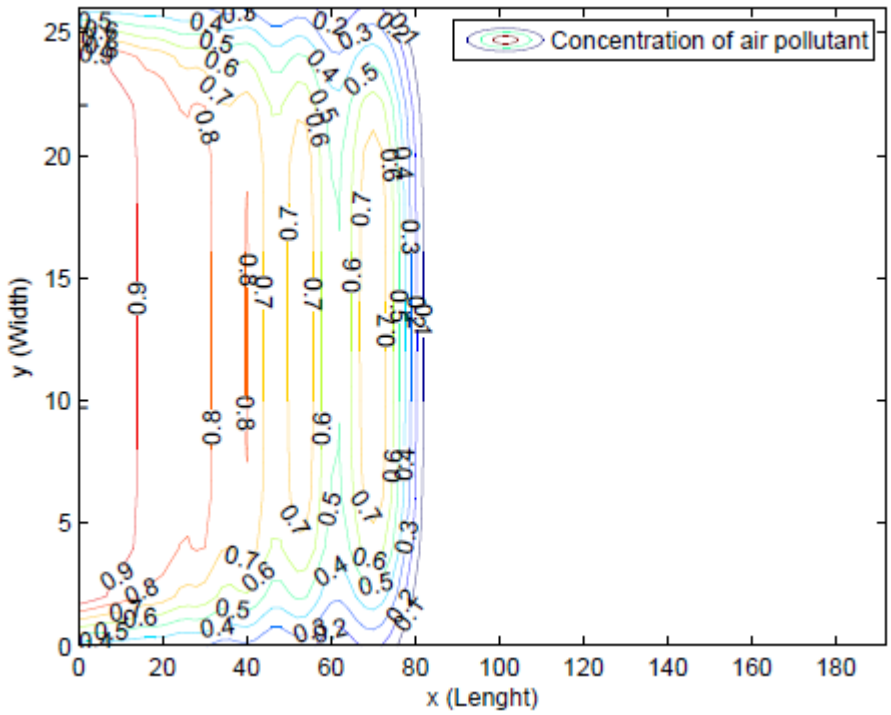

Figure 3.25 Contour plot of concentration of air pollutant levels for $R = -0.007$ sec^{-1}

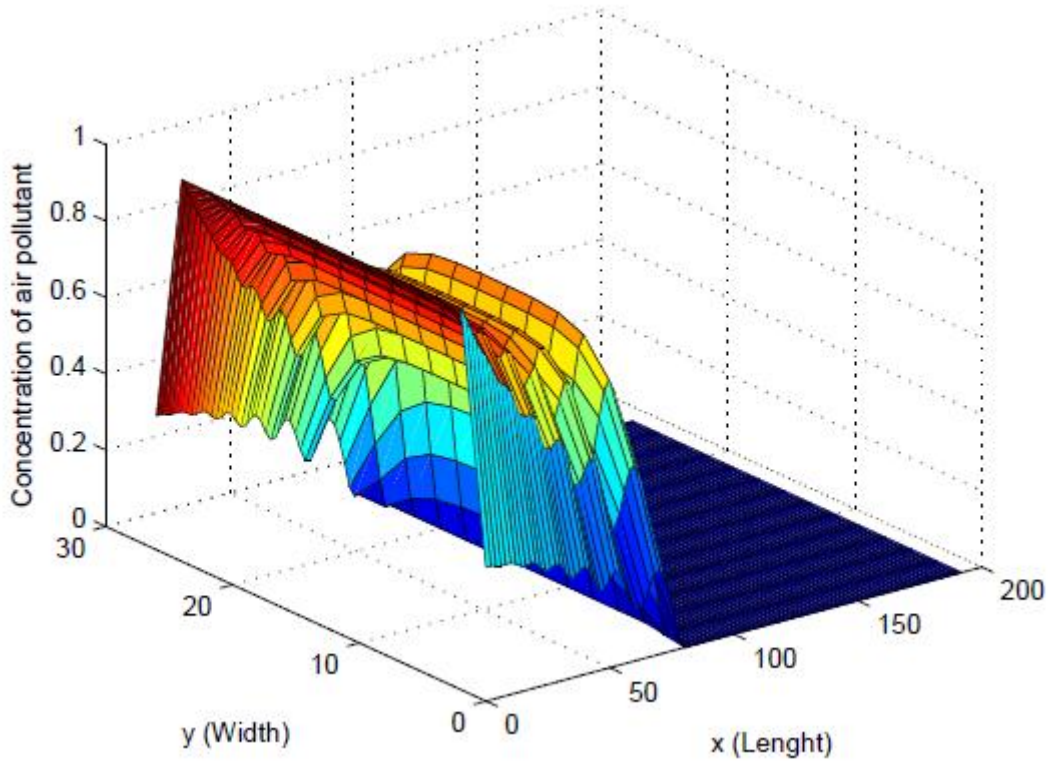

Figure 3.26 Surface plot of concentration of air pollutant levels for $R = -0.007$ sec^{-1}

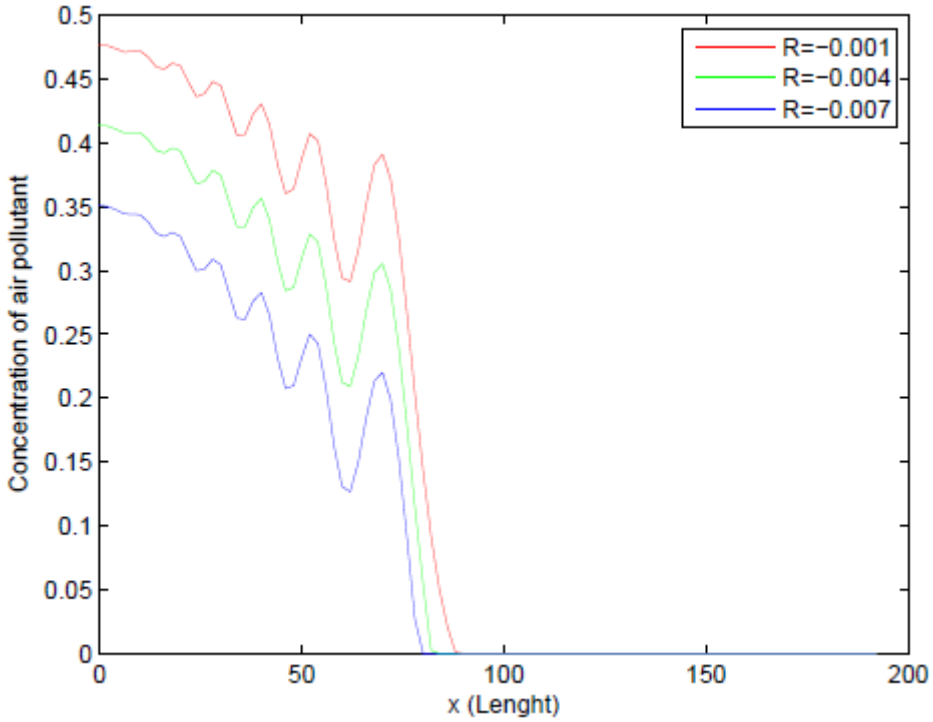

Figure 3.27 Compare the concentration of air pollutant where $R = -0.001$, $R = -0.004$, and $R = -0.007$ $\sec^{-1}$

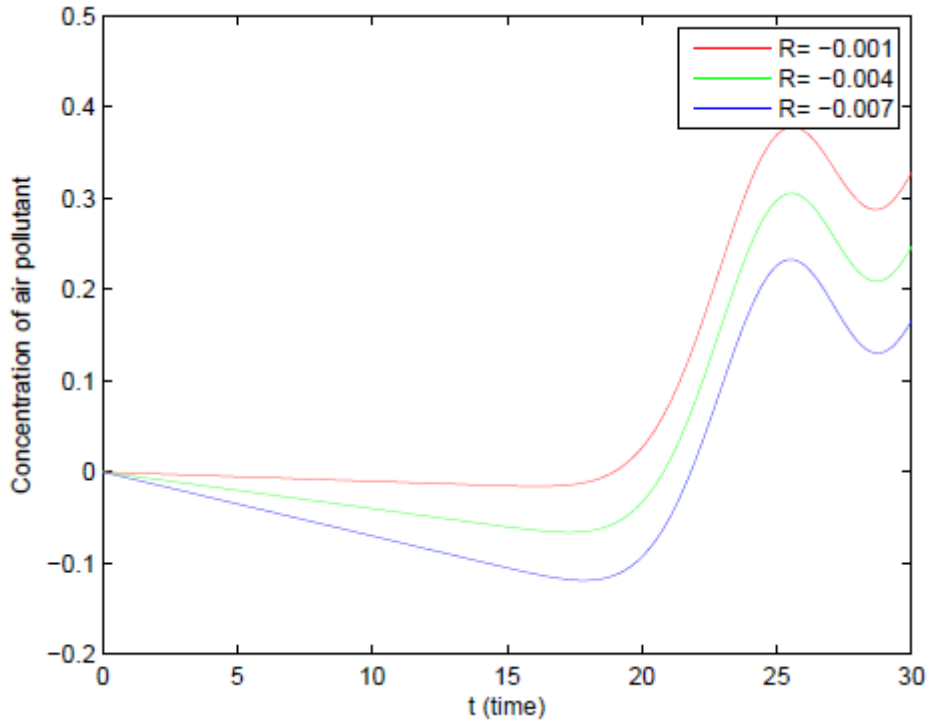

Figure 3.28 Compare the concentration of air pollutant at $x = 60\ m$, $y = 14\ m$, $z = 4\ m$ of sinks in different time

3.2.3.2 Simulation B : Source or sink emissions are moving

In this example, we consider two cases. In the first case, R is the function of source and sink $(R>0,\ R<0)$. That is $0.001\sin(xt)$, $0.003\sin(xt)$, and $0.005\sin(xt)\ s^{-1}$. The results are shown in Figure 3.29-Figure 3.31. The second case, R is the function of source $(R>0)$, which are $0.001|\sin(xt)|$, $0.003|\sin(xt)|$, and $0.005|\sin(xt)\ s^{-1}$. The results are shown in Figure 3.32-Figure 3.35.

Furthermore, Figure 3.29-Figure 3.30 and Figure 3.32-Figure 3.33 show the air pollutant concentration levels after passing 30 second in contour plot and surface plot between $R=0.001\sin(xt)$ (source-sink) and $R=0.003|\sin(xt)|$ (source), respectively. Figure 3.31 and Figure 3.34 compare the air pollutant concentration levels where R is the constant in first case and second case of Simulation B, respectively. As a results, R is a function of both source and sink and the concentration of air pollutant has increased and decreased (see Figure 3.31). That is, it is increased when R is the source but, on the other hand, if R is sink, the concentration of air pollutant is decreased. Finally of Simulation B, Figure 3.35 is compared the concentration of air pollutant at $x=60\ m$, $y=14\ m$, and $z=4\ m$ in different time of moving sources (vehicle sources).

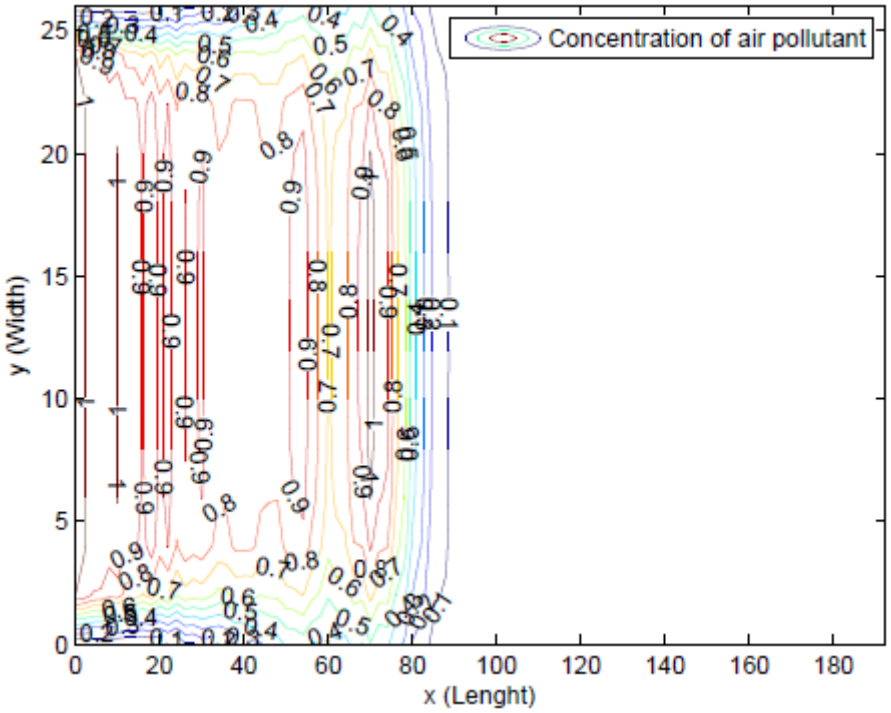

Figure 3.29 Contour plot of concentration of air pollutant levels for $R=0.001\sin(xt)$ sec^{-1}

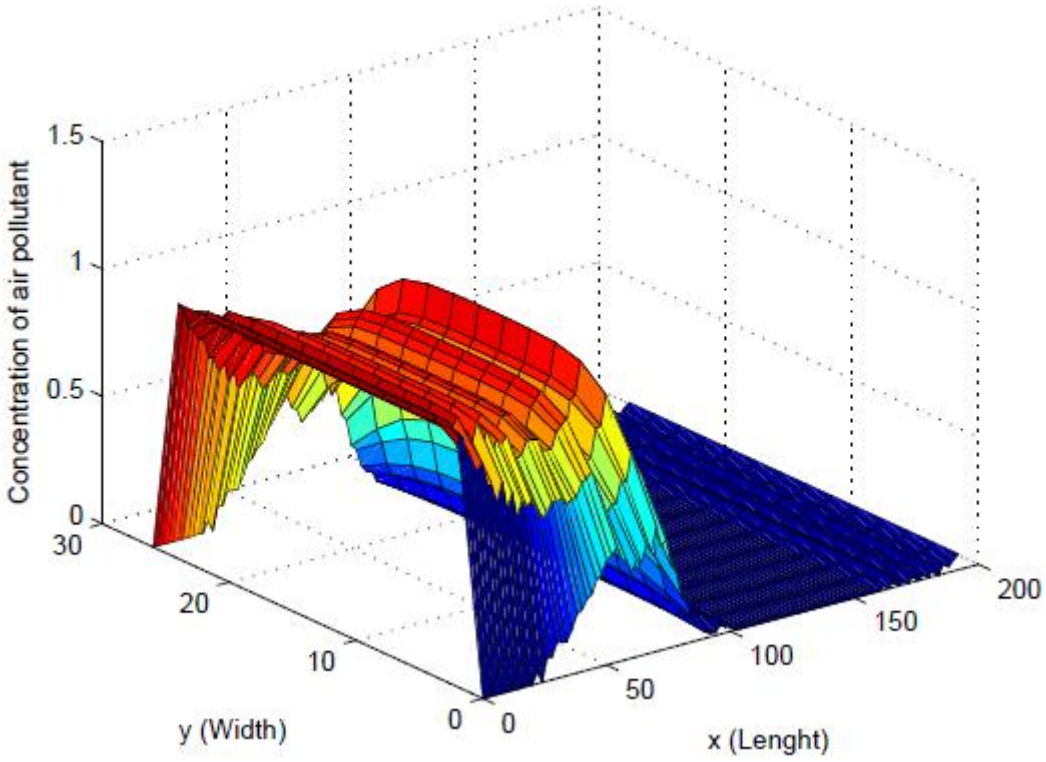

Figure 3.30 Surface plot of concentration of air pollutant levels for $R = 0.001\sin(xt)$ $\sec^{-1}$

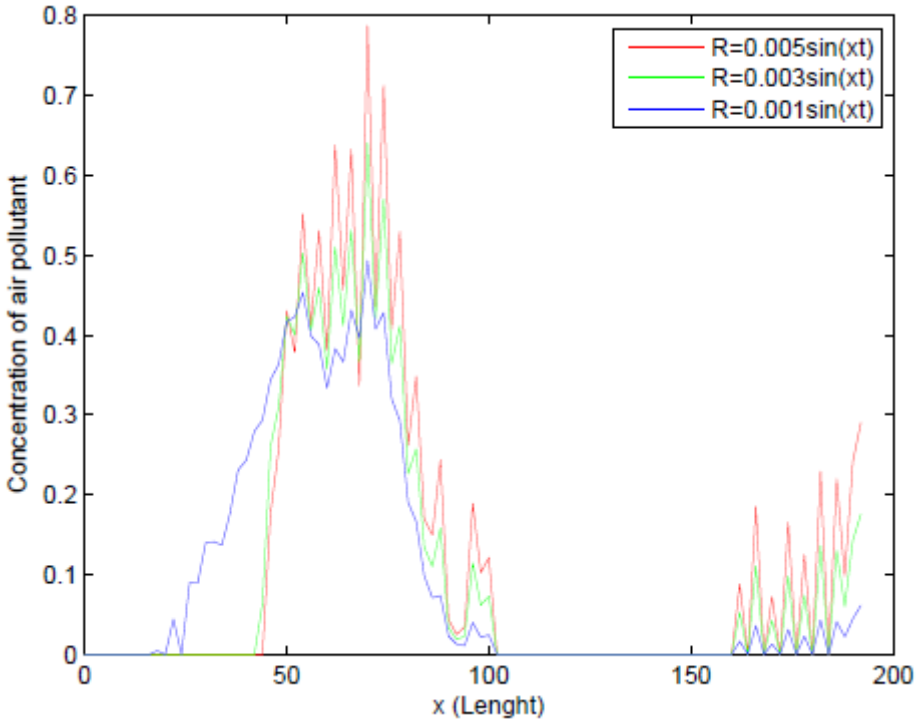

Figure 3.31 Compare the concentration of air pollutant where $R = 0.001\sin(xt)$, $R = 0.003\sin(xt)$, and $R = 0.005\sin(xt)$ $\sec^{-1}$

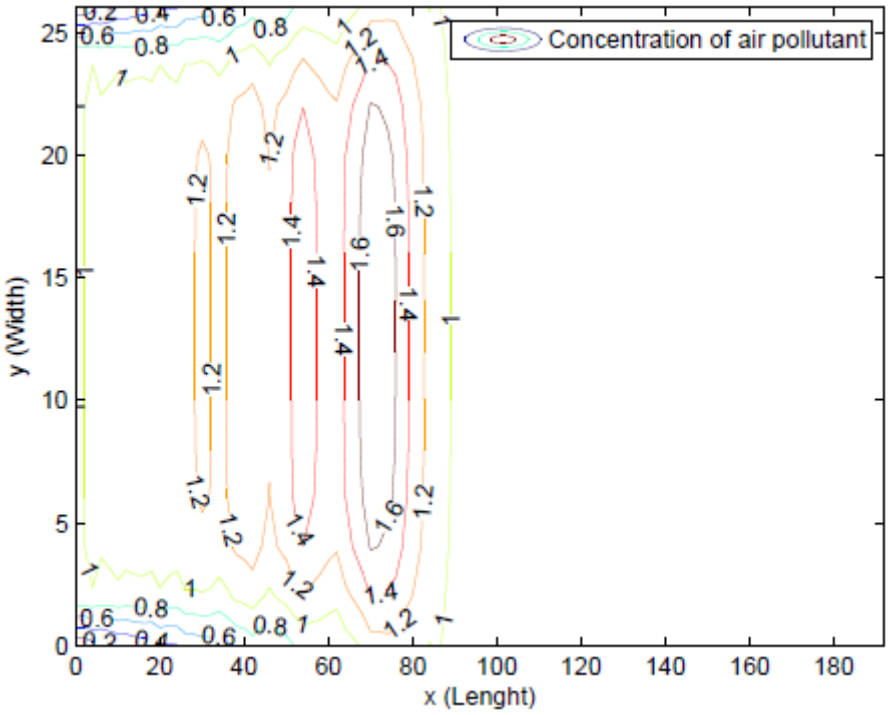

Figure 3.32 Contour plot of concentration of air pollutant levels for $R = 0.003|\sin(xt)|$ sec^{-1}

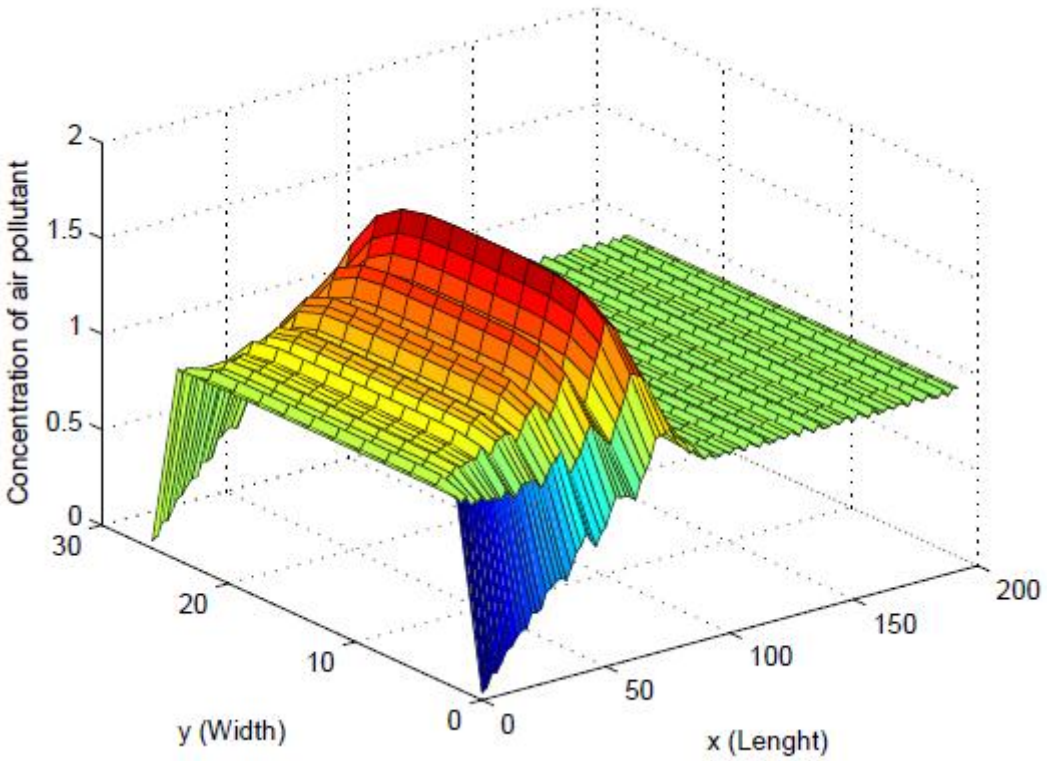

Figure 3.33 Surface plot of concentration of air pollutant levels for $R = 0.003|\sin(xt)|$ sec^{-1}

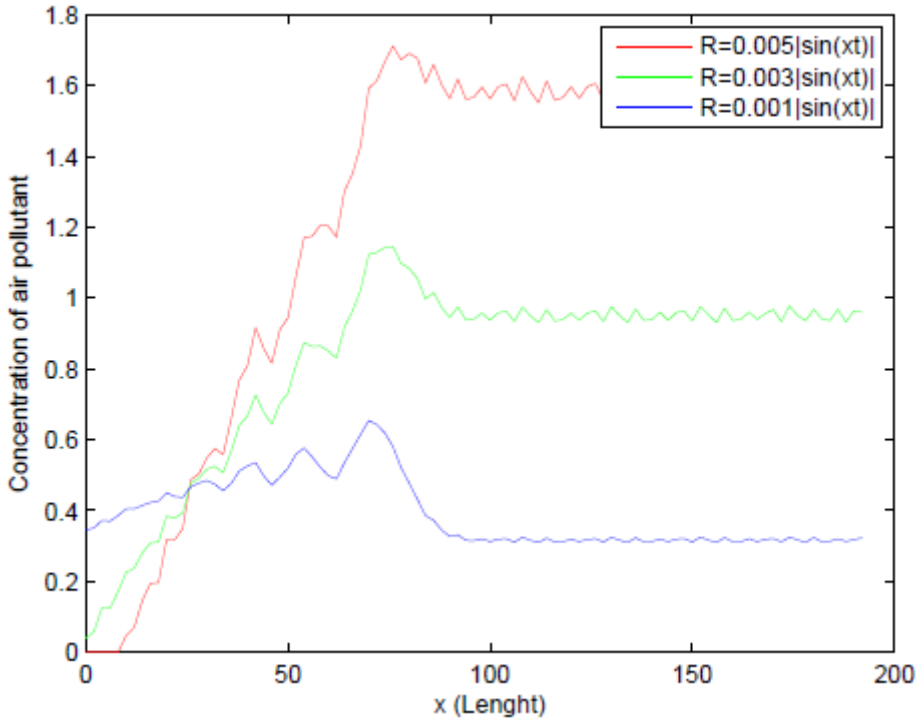

Figure 3.34 Compare the concentration of air pollutant where $R = 0.001|\sin(xt)|$, $R = 0.003|\sin(xt)|$, and $R = 0.005|\sin(xt)|$ $\sec^{-1}$

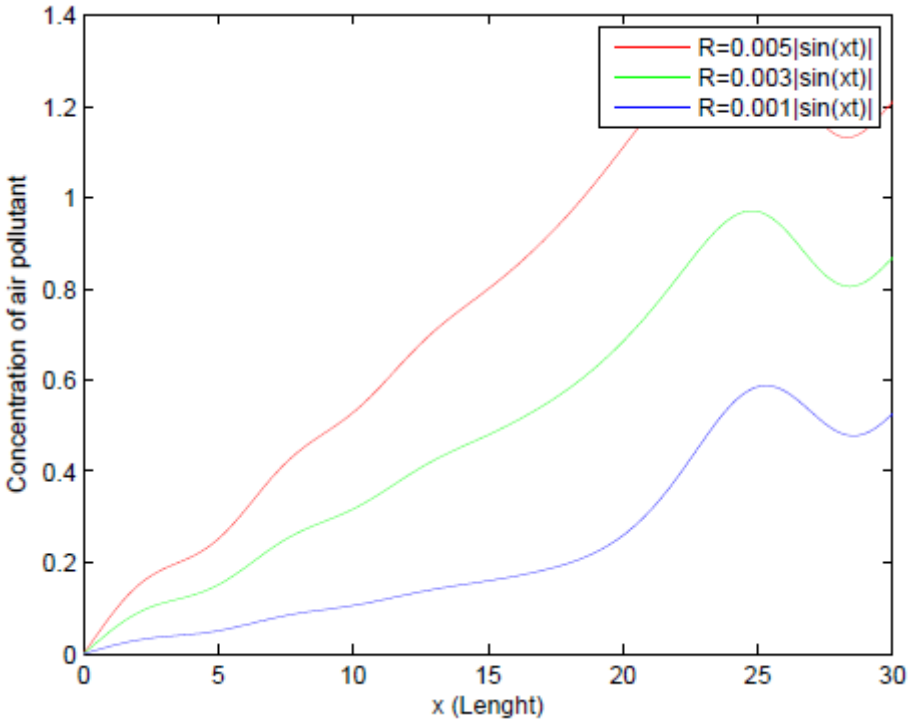

Figure 3.35 Compare the concentration of air pollutant at $x = 60\ m,\ y = 14\ m,\ z = 4\ m$ of moving sources (vehicle sources) in different time

3.2.3.3 Simulation C : Source or sink emissions are mixed

In this example, we divide R into 3 zones. R_1, R_2, and R_3 are sources of zone 1, zone 2, and zone 3, respectively. We consider three cases when R is the constant of the source. The first case, R is small and gradually increases, which are $R_1 = 0.01,\ R_2 = 0.03,$ and $R_3 = 0.05\ s^{-1}$. The second case, R is in the middle zone and is the most, which are $R_1 = 0.03,\ R_2 = 0.05,$ and $R_3 = 0.03\ s^{-1}$. The last case, R in zone 1 is the highest and gradually decreases, which are $R_1 = 0.05,\ R_2 = 0.03,$ and $R_3 = 0.01\ s^{-1}$. The result of simulation C are shown in Figure 3.36-Figure 3.40.

Moreover, Figure 3.36-Figure 3.38 show the air pollutant concentration levels after passing 30 second in surface plot where R is the constant in first, second and third case of Simulation C, respectively. Figure 3.39 compares the air pollutant concentration levels of three cases in Simulation C. As a result, it can be concluded that, if we add a large quantity of sources in at the beginning, it affects the concentration of pollutants. Therefore, the source is the cause of high concentrations of air pollutant. Finally of Simulation C, Figure 3.40 is compared the concentration of air pollutant at $x = 60\ m,\ y = 14\ m,$ and $z = 4\ m$ in different time of 3 averaged zone sources.

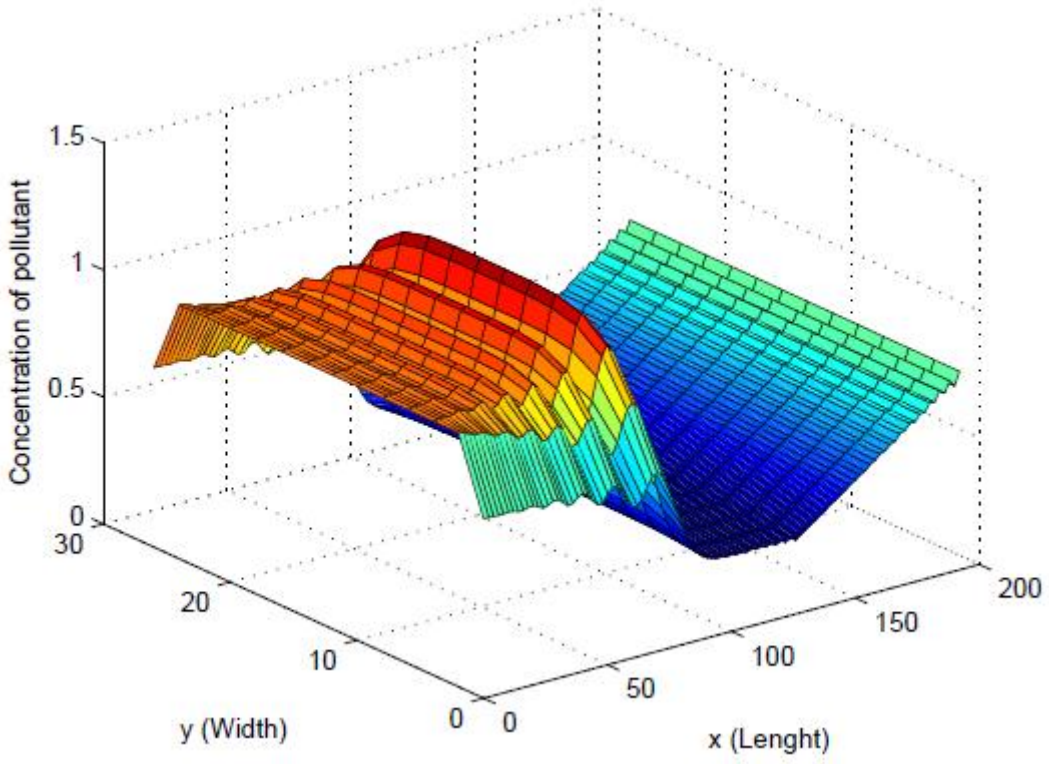

Figure 3.36 Surface plot of concentration of air pollutant levels for $R_1 = 0.01,\ R_2 = 0.03$ and $R_3 = 0.05$ sec^{-1}

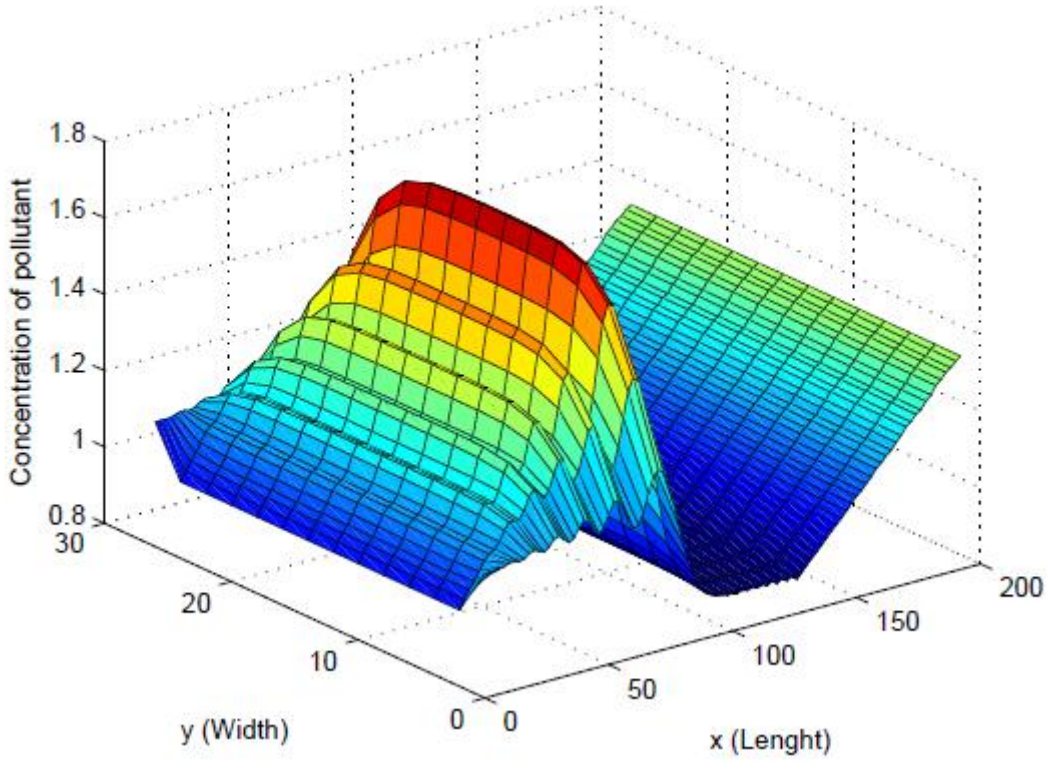

Figure 3.37 Surface plot of concentration of air pollutant levels for $R_1 = 0.03,\ R_2 = 0.05$ and $R_3 = 0.03$ $\sec^{-1}$

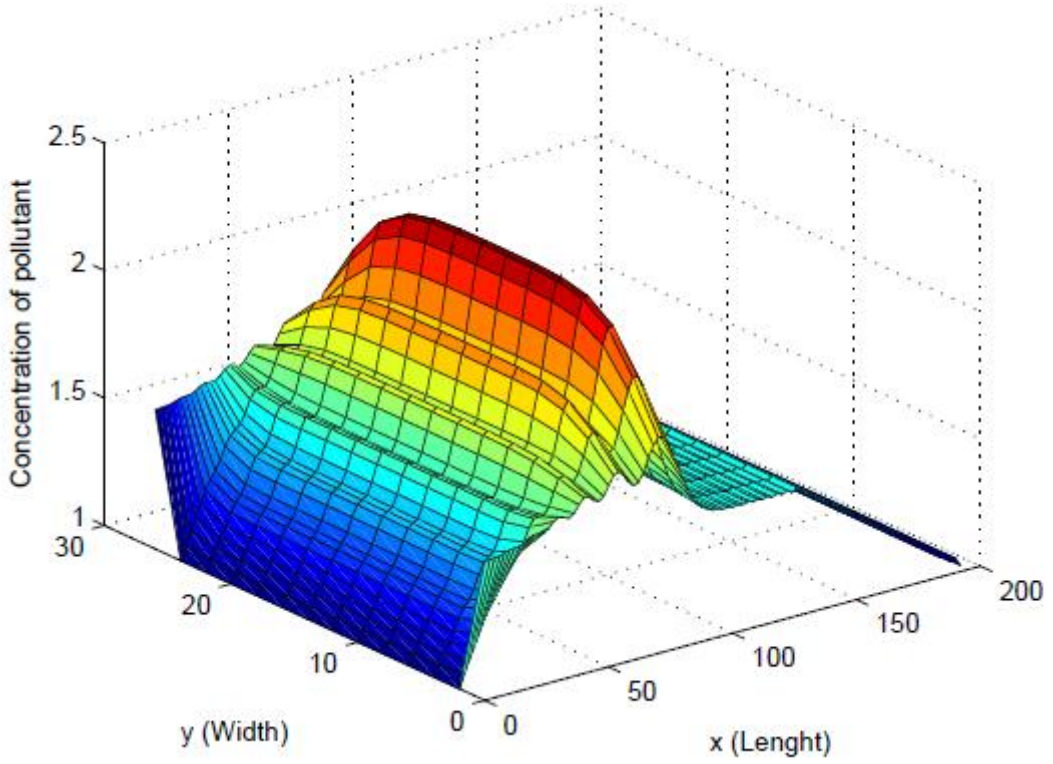

Figure 3.38 Surface plot of concentration of air pollutant levels for $R_1 = 0.05,\ R_2 = 0.03$ and $R_3 = 0.01$ $\sec^{-1}$

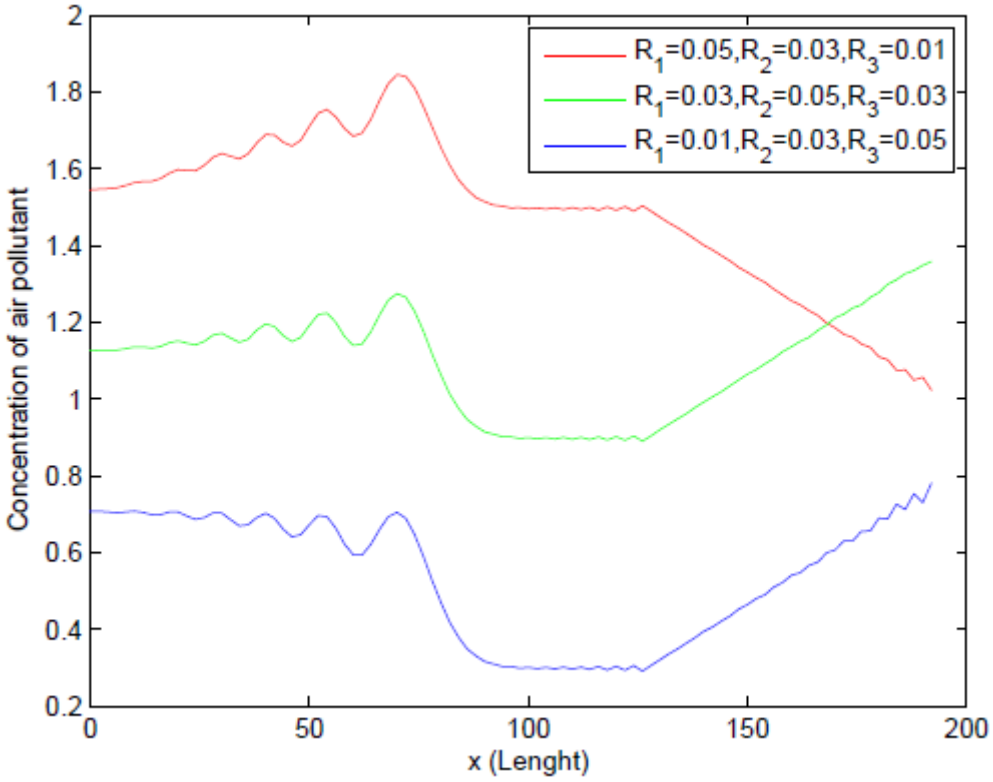

Figure 3.39 Compare the concentration of air pollutant where R_1, R_2, and R_3 are difference of three cases

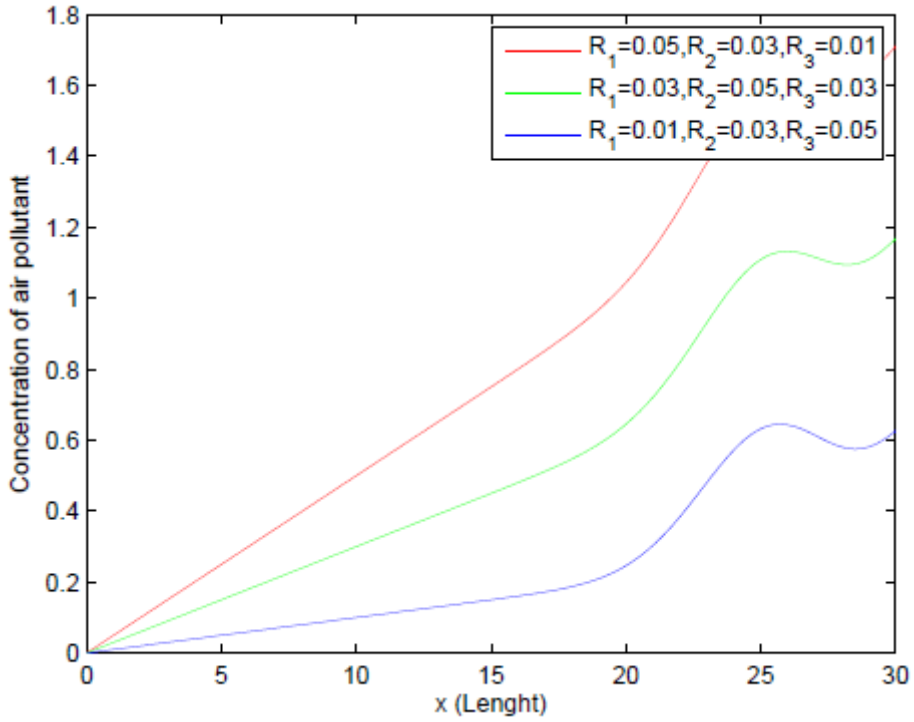

Figure 3.40 Compare the concentration of air pollutant at $x = 60\ m,\ y = 14\ m,\ z = 4\ m$ of 3 averaged zone sources in different time

The air pollutant concentrations are calculated by using a finite difference technique. Whether sources or sinks, it affected the air pollutant concentrations. The comparison of sources or sinks for simulation A, B and C are shown in Table 3.4.

Table 3.4 comparison of sources or sinks for simulation A, B and C

Simulation-cases	$R_1\ (0 \le x < 64)$	$R_2\ (64 \le x \le 128)$	$R_1\ (128 < x \le 192)$
A-1.1	0.001	0.001	0.001
A-1.2	0.004	0.004	0.004
A-1.3	0.007	0.007	0.007
A-2.1	-0.001	-0.001	-0.001
A-2.2	-0.004	-0.004	-0.004
A-2.3	-0.007	-0.007	-0.007
B-1.1	$0.001\sin(xt)$	$0.001\sin(xt)$	$0.001\sin(xt)$
B-1.2	$0.004\sin(xt)$	$0.004\sin(xt)$	$0.004\sin(xt)$
B-1.3	$0.007\sin(xt)$	$0.007\sin(xt)$	$0.007\sin(xt)$
B-2.1	$0.001\lvert\sin(xt)\rvert$	$0.001\lvert\sin(xt)\rvert$	$0.001\lvert\sin(xt)\rvert$
B-2.2	$0.004\lvert\sin(xt)\rvert$	$0.004\lvert\sin(xt)\rvert$	$0.004\lvert\sin(xt)\rvert$
B-2.3	$0.007\lvert\sin(xt)\rvert$	$0.007\lvert\sin(xt)\rvert$	$0.007\lvert\sin(xt)\rvert$
C-1	0.01	0.03	0.05
C-2	0.03	0.05	0.03
C-3	0.05	0.03	0.01

Chapter 4
Three-Dimensional Air Quality Assessment Simulations inside Skytrain Platform with Airflow Obstacles on Heavy Traffic Road

Air pollutant levels in Bangkok are generally high in street tunnels. They are particularly elevated in almost closed street tunnels, such as areas under a Bangkok skytrain platform with high traffic volume, where dispersion is limited. These areas have no air quality measurement stations, even though there is a high percentage of people living around this vicinity. We are interested in conducting research on Bangkok skytrain platforms, due to the traffic density and enormously polluted areas there. Therefore, we propose a numerical modeling of air pollution concentration under a skytrain platform with airflow obstacles on a heavy traffic road as an approximated solution of the three-dimensional advection-diffusion equation by using the finite difference methods. Our research presentation is based on how the air pollution model depends on the flow of air pollution and wind directions; the governing equation of the corresponding three-dimensional advection-diffusion equation is presented. This also includes the initial conditions and boundary conditions of traffic and polluted areas. In order to illustrate the performance of the model, numerical experiments are presented. The comparison between the two methods and the simulations of air pollution control are proposed. The three-dimensional advection-diffusion equation is solved by using the Forward Time, Centered Space (FTCS) and Forward Time, Backward Space (FTBS) schemes. The results obtained indicate that the FTCS method provides a better result than the FTBS method. Furthermore, the proposed experimental variations of the boundary conditions in the entrance gate affect the air pollutant concentrations of each floor.

4.1 Initial and boundary conditions setting techniques for multiple layers in street tunnel

We consider the components of the street tunnel with a right-side wall gap, shown in Figure 4.1. Figure 4.2 shows a model of the problem with obstacles, where A is the right parallel gap size along the ceiling, B is the left parallel gap size along the ceiling, and $G-F$ is the right-side wall gap beside the considered domain. (D_{cn}, E_{rn}) is the center point of the columns for $cn = 1,2,...,ncl$ and $rn = 1,2$, where ncl is the number of columns.

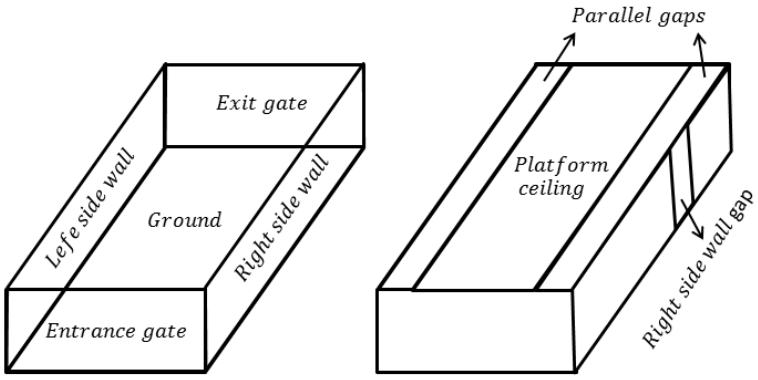

Figure 4.1 The components of the street tunnel with right side wall gap

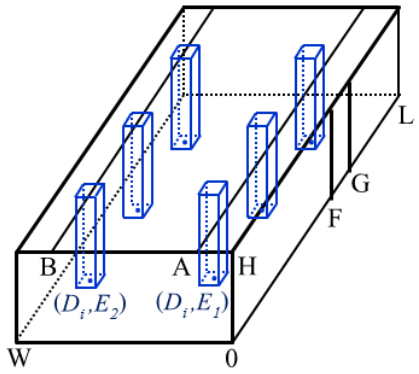

Figure 4.2 Model of the problem with obstacles

The initial condition, there is no initial pollutant $C(x,y,z,0)=0$, for all $(x,y,z)\in\Omega=\{(x,y,z);\ 0\le x\le L,\ 0\le y\le W,\ 0\le z\le H\}$, where L is the length, W is the width, and H is the height of the tunnel. For the boundary conditions are assumed that

Entrance gate: $C(0,y,z,t)=c_1.$

Margin of entrance gate: $\frac{\partial C}{\partial x}(0,y,z,t)=c_2,\ y=0,W,\ z=0,H.$

Exit gate: $\frac{\partial C}{\partial x}(L,y,z,t)=c_3.$

Left side wall: $\frac{\partial C}{\partial y}(x,W,z,t)=c_4.$

Right side wall gap: $C(x,0,z,t)=c_5,\ F\le x\le G.$

Right side wall: $\frac{\partial C}{\partial y}(x,0,z,t)=c_6,$ otherwise.

Ground: $\frac{\partial C}{\partial z}(x,y,0,t)=c_7.$

Platform ceiling: $\frac{\partial C}{\partial z}(x,y,H,t)=c_8,\ A<y<B.$

Parallel gaps: $\frac{\partial C}{\partial z}(x,y,H,t)=c_9,$ otherwise.

Center columns: $C(D_{cn},E_{rn},z,t)=0,\ 0\le z\le H.$

Front and back columns: $\frac{\partial C}{\partial x}(D_{cn}-1,y,z,t)=\frac{\partial C}{\partial x}(D_{cn}+1,y,z,t)=c_{10},$

$E_{rn}-1\le y\le E_{rn}+1,$ for all $t>0.$

Left and right columns: $\frac{\partial C}{\partial y}(x,E_{rn}-1,z,t)=\frac{\partial C}{\partial y}(x,E_{rn}+1,z,t)=c_{11},$

$D_{cn}-1\le x\le D_{cn}+1,$ for all $t>0.$

Where c_1 and c_5 are the air pollutant concentration inflow in x- and y-directions, respectively, c_2, c_3, c_4, c_6, c_7, c_8, c_9, c_{10}, and c_{11} are the rate of change of air pollutant concentration in each the boundary conditions.

4.2 Finite difference techniques for multiple layers in street tunnel

We use the finite difference method to approximate the solution of the three-dimensional advection-diffusion equation. The solution domain of the problem over a time $0\le t\le T$ is covered by a mesh of grid-lines: $x_i=i\Delta x,\ i=0,1,2,...,M$; $y_j=j\Delta y,\ j=0,1,2,...,N,\ z_k=k\Delta z,\ k=0,1,2,...,P,$ and $t_n=n\Delta t,\ n=0,1,2,...,Q$ over three spaces and time coordinate axes, respectively. The approximate air pollutant concentration at point $(i\Delta x, j\Delta y, k\Delta z, n\Delta t)$ is denoted by $C^n_{i,j,k}=C(i\Delta x, j\Delta y, k\Delta z, n\Delta t)$ at the grid point (i,j,k,n). The constant spatial and temporal grid-spacing are $\Delta x=\frac{L}{M},\ \Delta y=\frac{W}{N},\ \Delta z=\frac{H}{P},$ and $\Delta t=\frac{T}{Q},$ respectively. Where L is the length, W is the width, and H is the height of the tunnel.

We calculated by using an explicit forward-difference approximation for the time-derivative (FT), and central-difference approximations for the space-derivatives (CS). It is called FTCS in equation (3.3) and forward difference estimate for the time derivative (FT), and backward difference approximations for the space derivative (BS), so the acronym FTBS. The approximate solution of a three-dimensional advection-diffusion equation (2.16) use the FTBS scheme satisfies:

$$\begin{aligned}&\frac{C^{n+1}_{i,j,k}-C^n_{i,j,k}}{\Delta t}+u\left(\frac{C^n_{i,j,k}-C^n_{i-1,j,k}}{2\Delta x}\right)+v\left(\frac{C^n_{i,j,k}-C^n_{i,j-1,k}}{2\Delta y}\right)\\&=D_h\left(\frac{C^n_{i,j,k}-2C^n_{i-1,j,k}+C^n_{i-2,j,k}}{(\Delta x)^2}\right)+D_h\left(\frac{C^n_{i,j,k}-2C^n_{i,j-1,k}+C^n_{i,j-2,k}}{(\Delta y)^2}\right)\\&+D_v\left(\frac{C^n_{i,j,k}-2C^n_{i,j,k-1}+C^n_{i,j,k-2}}{(\Delta z)^2}\right).\end{aligned}\qquad (4.1)$$

Rearrangeme of equation (4.1) gives,

$$\begin{aligned} C_{i,j,k}^{n+1} &= \left(\frac{D_h \triangle t}{(\triangle x)^2}\right) C_{i-2,j,k}^{n} + \left(\frac{D_h \triangle t}{(\triangle y)^2}\right) C_{i,j-2,k}^{n} + \left(\frac{D_v \triangle t}{(\triangle z)^2}\right) C_{i,j,k-2}^{n} \\ &+ \left(\frac{u \triangle t}{\triangle x} - \frac{2D_h \triangle t}{(\triangle x)^2}\right) C_{i-1,j,k}^{n} + \left(\frac{v \triangle t}{\triangle y} - \frac{2D_h \triangle t}{(\triangle y)^2}\right) C_{i,j-1,k}^{n} - \left(\frac{2D_v \triangle t}{(\triangle z)^2}\right) C_{i,j,k-1}^{n} \\ &+ \left(1 + \frac{D_h \triangle t}{(\triangle x)^2} + \frac{D_h \triangle t}{(\triangle y)^2} + \frac{D_v \triangle t}{(\triangle z)^2} - \frac{u \triangle t}{\triangle x} - \frac{v \triangle t}{\triangle y}\right) C_{i,j,k}^{n}. \end{aligned} \tag{4.2}$$

Simplification of equation (4.2) we get,

$$\begin{aligned} C_{i,j,k}^{n+1} &= (s_x) C_{i-2,j,k}^{n} + (s_y) C_{i,j-2,k}^{n} + (s_z) C_{i,j,k-2}^{n} + (r_x - 2s_x) C_{i-1,j,k}^{n} \\ &+ (r_y - 2s_y) C_{i,j-1,k}^{n} - (2s_z) C_{i,j,k-1}^{n} \\ &+ (1 + s_x + s_y + s_z - r_x - r_y) C_{i,j,k}^{n}, \end{aligned} \tag{4.3}$$

where $r_x = \frac{u\Delta t}{\Delta x}$, $r_y = \frac{v\Delta t}{\Delta y}$, $s_x = \frac{D_h \Delta t}{(\Delta x)^2}$, $s_y = \frac{D_h \Delta t}{(\Delta y)^2}$ and $s_z = \frac{D_v \Delta t}{(\Delta z)^2}$.

The finite difference scheme for the left-hand side of the fictitious points are as follows:

$$C_{-1,j,k}^{n} = \frac{4C_{0,j,k}^{n} - C_{1,j,k}^{n} - 2c_2 \Delta x}{3}, \tag{4.4}$$

$$C_{-2,j,k}^{n} = \frac{13C_{0,j,k}^{n} - 4C_{1,j,k}^{n} - 14c_2 \Delta x}{9}, \tag{4.5}$$

$$C_{i,-1,k}^{n} = \frac{4C_{i,0,k}^{n} - C_{i,1,k}^{n} - 2c_6 \Delta y}{3}, \tag{4.6}$$

$$C_{i,-2,k}^{n} = \frac{13C_{i,0,k}^{n} - 4C_{i,1,k}^{n} - 14c_6 \Delta y}{9}, \tag{4.7}$$

$$C_{i,j,-1}^{n} = \frac{4C_{i,j,0}^{n} - C_{i,j,1}^{n} - 2c_7 \Delta z}{3}, \tag{4.8}$$

$$C_{i,j,-2}^{n} = \frac{13C_{i,j,0}^{n} - 4C_{i,j,1}^{n} - 14c_7 \Delta z}{9}. \tag{4.9}$$

The stencil diagram for FTBS scheme shown in Figure 4.3.

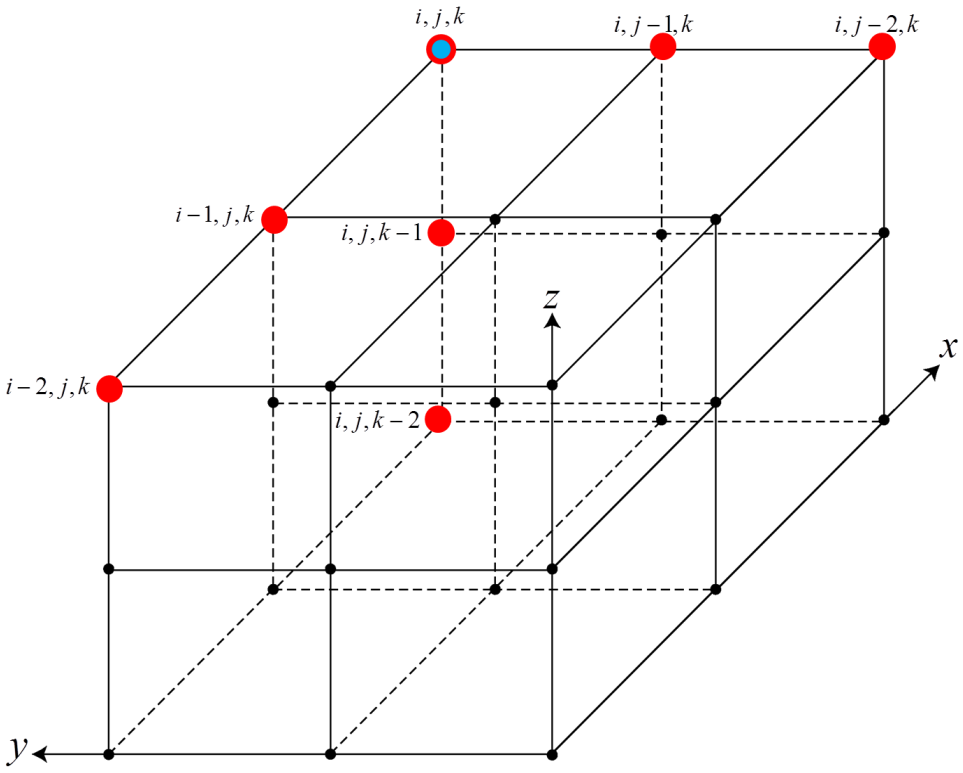

Figure 4.3 The stencil diagram for FTBS scheme

4.3 Numerical experiments and results for multiple layers in street tunnel

4.3.1 Comparison between FTCS and FTBS solutions in skytrain platform on a single layer

In this section, we describe about a comparision of some numerical methods for solving the three-dimensional advection-diffusion equation. There are two methods. These are forward time central space (FTCS) and forward time backward space (FTBS). We consider the domain as a single layer as shown in Figure 4.2 that the length(L), width(W), and height(H) of tunnel are 198, 21, and 28 meters, respectively. Then, the problem domain is $\Omega = \{(x,y,z);\ 0 \le x \le 198,\ 0 \le y \le 21,\ 0 \le z \le 28\}$. We assume that $\Delta x = \Delta y = \Delta z = 2\ m,\ \Delta t = 0.06\ s,\ T = 120\ s,\ u = 0.5\ m/s,\ v = 0\ m/s,\ D_h = D_v = 0.001\ m^2/s,\ c_1 = 0.5,\ c_5 = 0.2,\ c_3 = c_9 = -0.01,\ c_2 = c_4 = c_6 = c_7 = c_8 = c_{10} = c_{11} = 0,\ A = 4,\ B = 17,$ and $ncl = 9$. Figure 4.4-Figure 4.7 are solved by various methods. These are FTCS and FTBS methods, respectively. The solutions of air pollutant concentration by using the FTCS method in equation (3.3) are shown in Figure 4.4 and Figure 4.5. This figure show about contour and surface plots of air pollutant concentration levels after 2 minutes passed. You can be seen that the maximum value of air pollutant concentration is $0.6\ kg/m^3$.

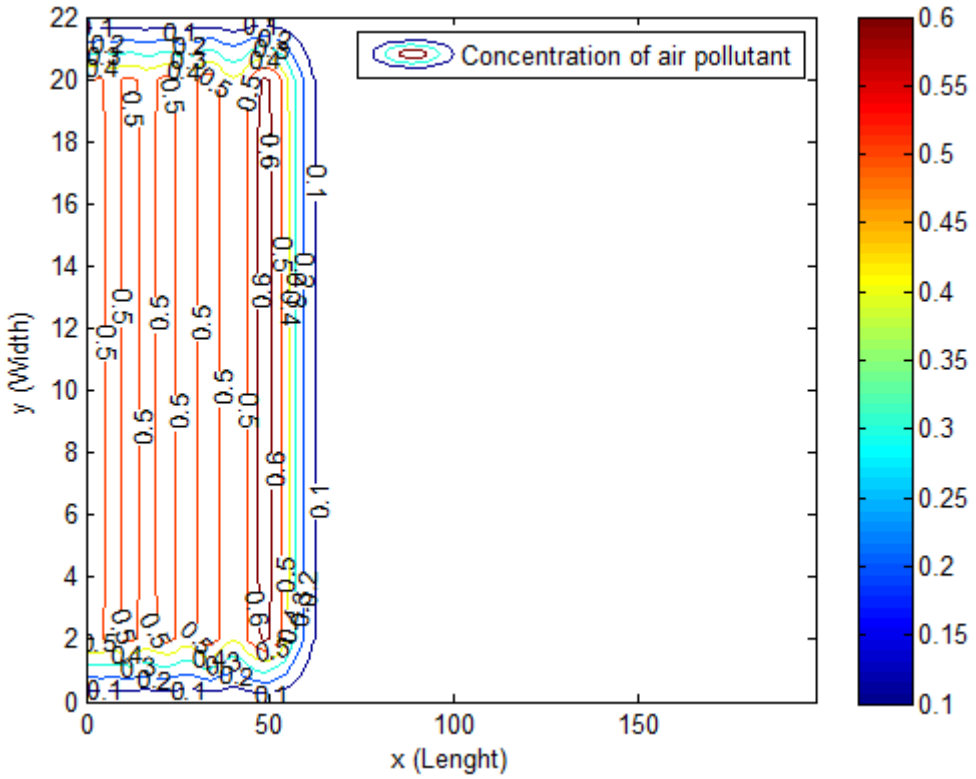

Figure 4.4 Contour plot of air pollutant concentration levels after the past 2 minutes computed by FTCS method

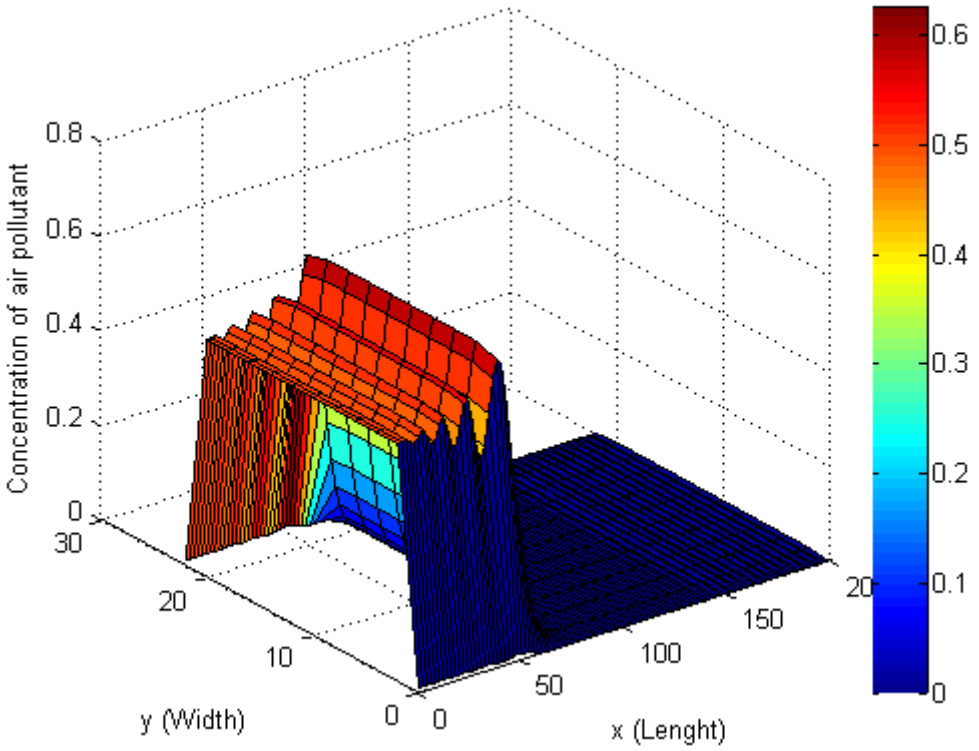

Figure 4.5 Surface plot of air pollutant concentration levels after the past 2 minutes computed by FTCS method

Furthermore, the contour and surface plots of air pollutant concentration levels after 2 minutes have passed for solutions of air pollutant concentration by using the FTBS method in equation (4.3) are shown in Figure 4.6 and Figure 4.7. The maximum value of air pollutant concentration is $0.5\ kg/m^3$.

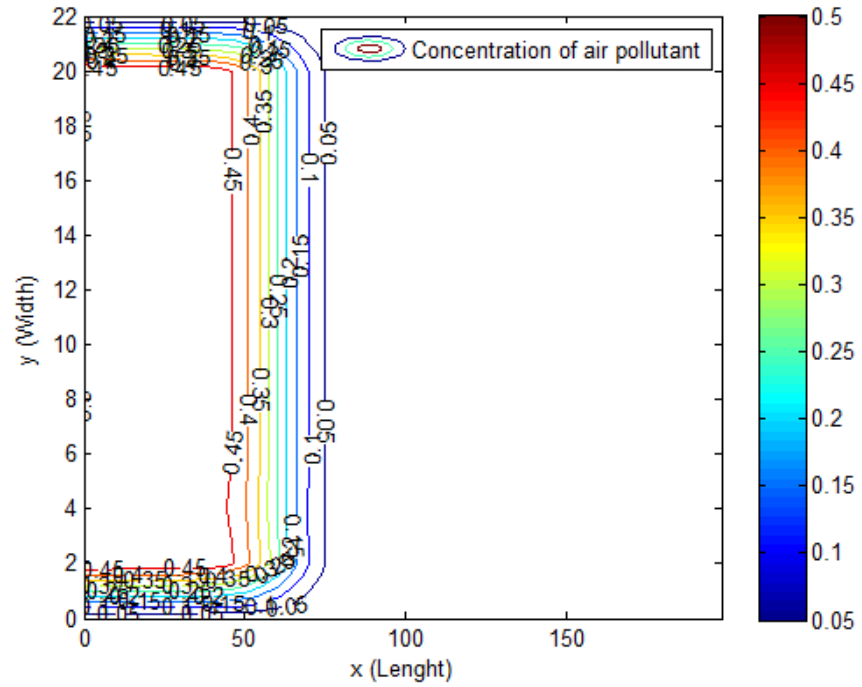

Figure 4.6 Contour plot of air pollutant concentration levels after the past 2 minutes computed by FTBS method

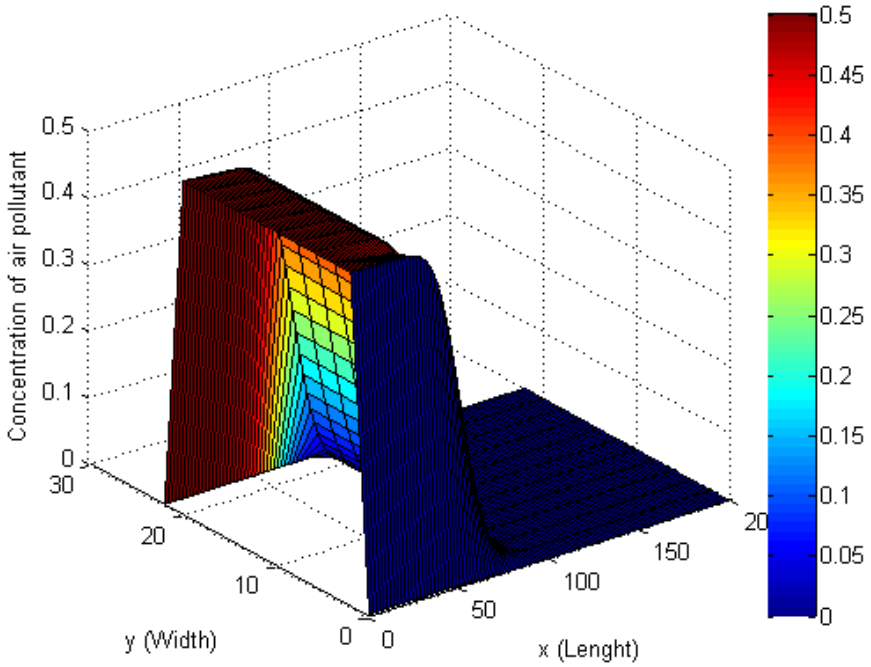

Figure 4.7 Surface plot of air pollutant concentration levels after the past 2 minutes computed by FTBS method

The approximations of air pollutant concentration for FTCS and FTBS methods are compared in Figure 4.8. We choose $\Delta x = \Delta y = \Delta z = 2\ m,\ \Delta t = 0.06\ s,\ T = 30\ s,$ $u = 0.1\ m/s,\ v = 0\ m/s,\ D_h = D_v = 0.001\ m^2/s,\ c_1 = 0.5, c_3 = c_9 = -0.001,\ c_2 = c_4 = c_5 = c_6 = c_7 = c_8 = c_{10} = c_{11} = 0,\ A = 4,\ B = 17,$ and $ncl = 9$. It can be seen that the trend of results from both methods is in the same direction. In order to identify which one is the best we will change the grid-spacing to see if the solution is stable. Table 4.1 shows the stability of the FTCS and FTBS approximate solutions. It can be seen that, if we choose $\lambda = \gamma = 0.03$ and $\lambda = 0.06$, then the solution of the FTBS method is unstable, but the FTCS method is stable. Consequently, the FTCS method gives a better solution than the FTBS method.

Table 4.1 The stable of FTCS and FTBS approximate solutions

$\lambda = \frac{\Delta t}{\Delta x}$	$\gamma = \frac{\Delta t}{(\Delta x^2)}$	Δx	Δy	Δz	Δt	*FTCS*	*FTBS*
0.02	0.0067	3.0	3.0	3.0	0.06	stable	stable
	0.0267	1.5	1.5	1.5	0.03	stable	stable
0.03	0.015	2.0	2.0	2.0	0.06	stable	stable
	0.03	1.0	1.0	1.0	0.03	stable	unstable
0.06	0.06	1.0	1.0	1.0	0.06	stable	unstable
	0.12	0.5	0.5	0.5	0.03	stable	unstable

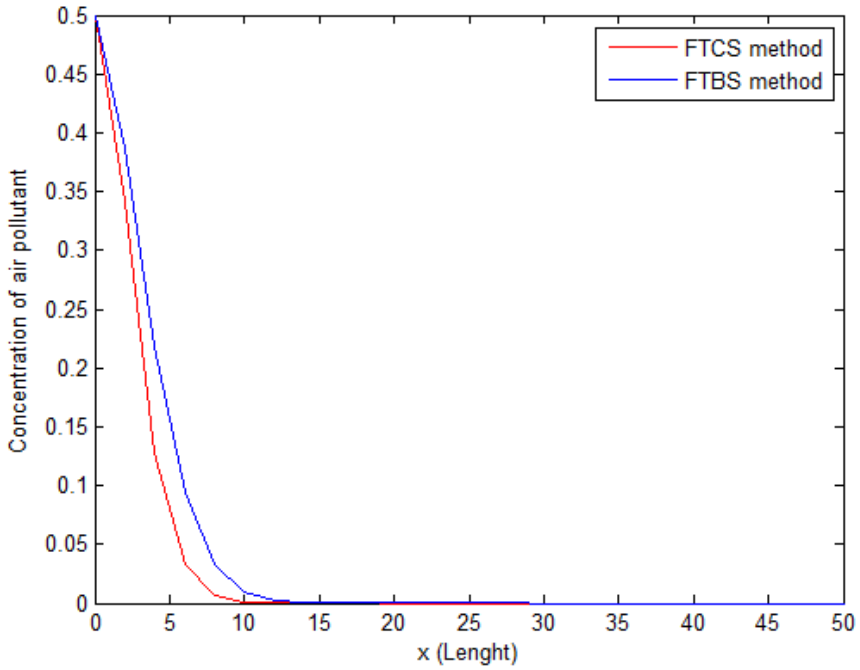

Figure 4.8 Comparison of air pollutant concentration between FTCS and FTBS methods after the past 30 seconds

4.3.2 Numerical simulations of air pollutant assessment in skytrain platform on triple layers

In this section, an explicit forward time and central space (FTCS) scheme is presented. We distinguish three scenarios of released air pollutant phenomena by using the finite difference in equation (3.3). In all scenarios, the air pollutant concentration is flowing along the x- and y-directions, which are constants or functions. In addition, there are two parallel gaps along the ceiling, and the rate of change are decreased at the parallel gaps. Moreover, both sides are flanked by buildings. All of the building walls are made from non-absorbing air pollution materials, and there is no rate of change.

For three scenarios, we consider the length, width and height of tunnel are $198,\ 21,$ and 28 meters, respectively. Then, the problem domain is $\Omega = \{(x,y,z);\ 0 \le x \le 198,\ 0 \le y \le 21,\ 0 \le z \le 28\}$, when $0 \le z < 9,\ 9 \le z < 22,\ 22 \le z \le 28$ are street floor, ticket floor and platform floor, respectively, see in Figure 4.9. We consider c_1 in the boundary conditions around the entrance gate of each floor, and we distinguish 3 scenarios in the considered domain, as per the following:

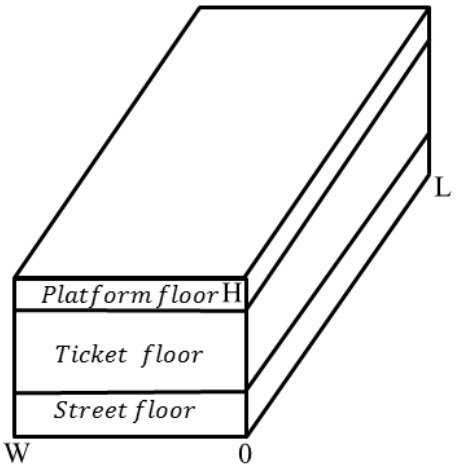

Figure 4.9 The problem domain with three floors

4.3.2.1 Scenario A: Air pollutant flowing into the street floor

If we consider the BTS station area, we will see that the street floor has a lot of cars. This causes heavy traffic and, as a result, air pollution is higher than on other floors. Therefore, we assume that the air pollutant concentration at the entrance gate of the street floor is constant. However, the ticket floor and platform floor are assumed to be areas that the pollution cannot reach. Therefore, we assume that there is no rate of change of air pollutant concentration at the entrance gates of the ticket and platform floors. Therefore, c_1 in the boundary conditions of all 3 floors are as follows:

Street floor: $c_1 = 0.5.$

Ticket floor: $c_1 = \dfrac{\partial C}{\partial x} = 0.$

Platform floor: $c_1 = \dfrac{\partial C}{\partial x} = 0.$

The problem domain is $\Omega = \{(x, y, z);\ 0 \le x \le 198,\ 0 \le y \le 21,\ 0 \le z < 9\}$. The grid spacing: $\Delta x = \Delta y = \Delta z = 1\ m,\ \Delta t = 0.06\ s,$ and for the time $T = 120\ s.$ We assume: $c_3 = c_9 = -0.01,\ c_5 = 0.2,\ c_2 = c_4 = c_6 = c_7 = c_8 = c_{10} = c_{11} = 0,\ A = 4,\ B = 17,\ F = 125,\ G = 135,$ and $ncl = 9.$ The wind velocity and diffusion coefficient are taken to be $u = 2.7778$, $v = \dfrac{u}{20}\ m/s$ and $D_h = 0.1592,\ D_v = 0.05\ m^2/\text{s},$ respectively. Therefore, the results of Scenario A for three different floors are shown in Figure 4.10. That is, in Figure 4.10(a), Figure 4.10(c), and Figure 4.10(e) show the contour plot of the air pollutant concentration levels for street, ticket and platform floors, respectively. Meanwhile, the surface plot of the air pollutant concentration levels for street, ticket and platform floors are shown in Figure 4.10(b), Figure 4.10(d), and Figure 4.10(f), respectively. It can be seen from Figure 4.10 that the air pollutant concentration in the platform floor is very low. This comes from only the pollution on the right side wall gap. Therefore, the air pollution on the platform floor is less than $0.2\ kg/m^3$.

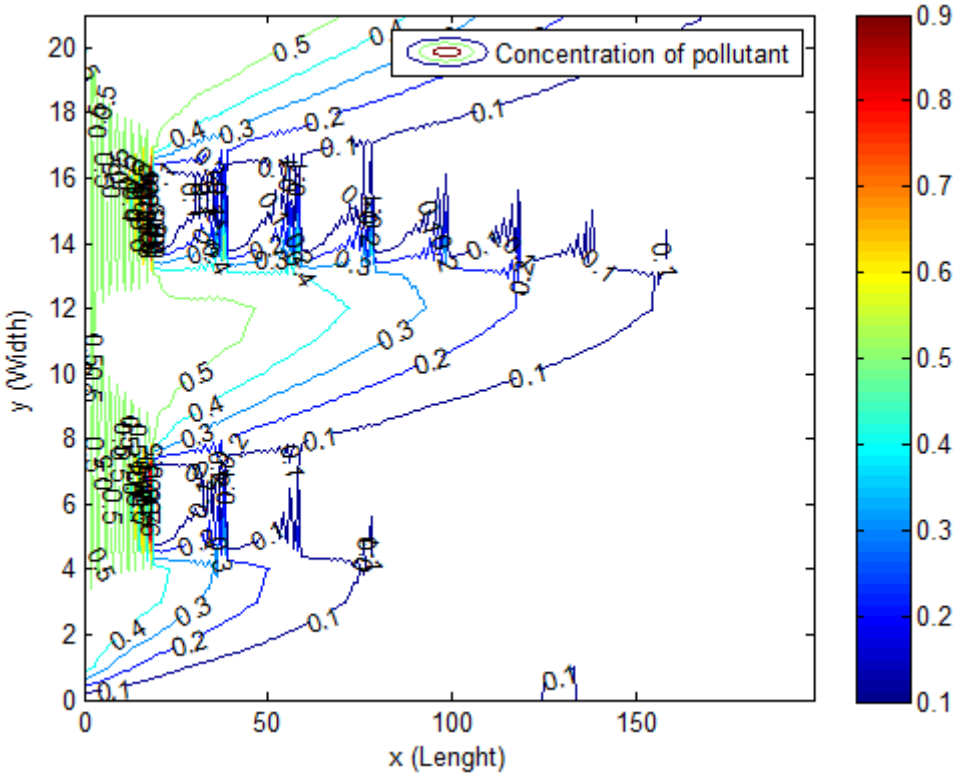

(a)

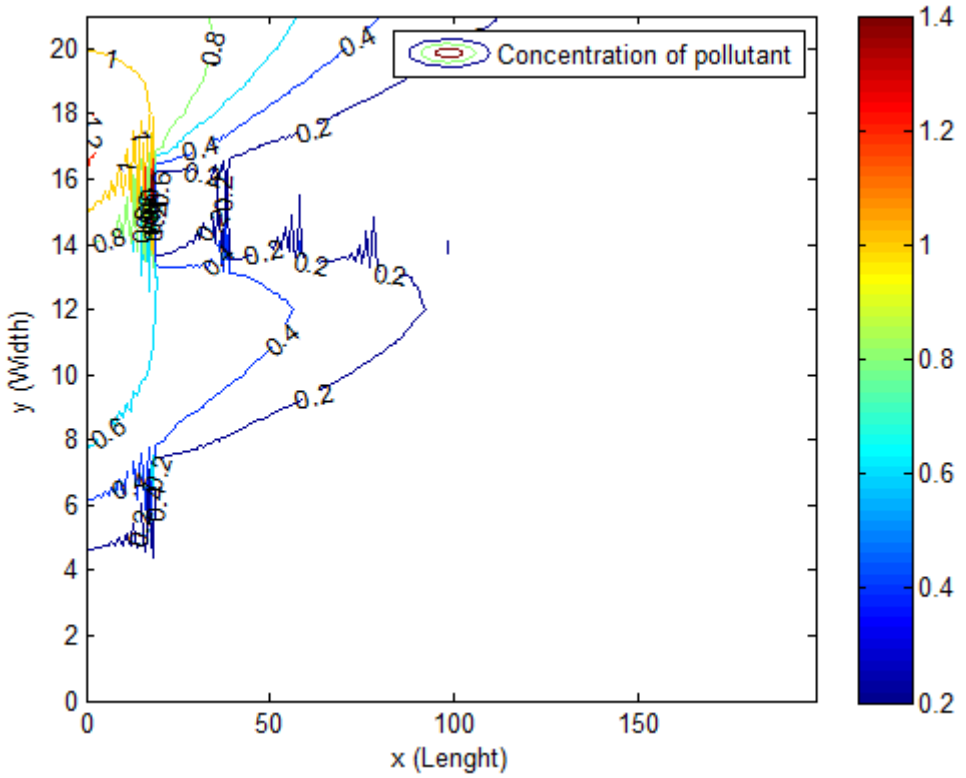
Concentration of pollutant
y (Width)
x (Lenght)
0
50
100
150
0
2
4
6
8
10
12
14
16
18
20
0.2
0.4
0.6
0.8
1
1.2
1.4

(b)

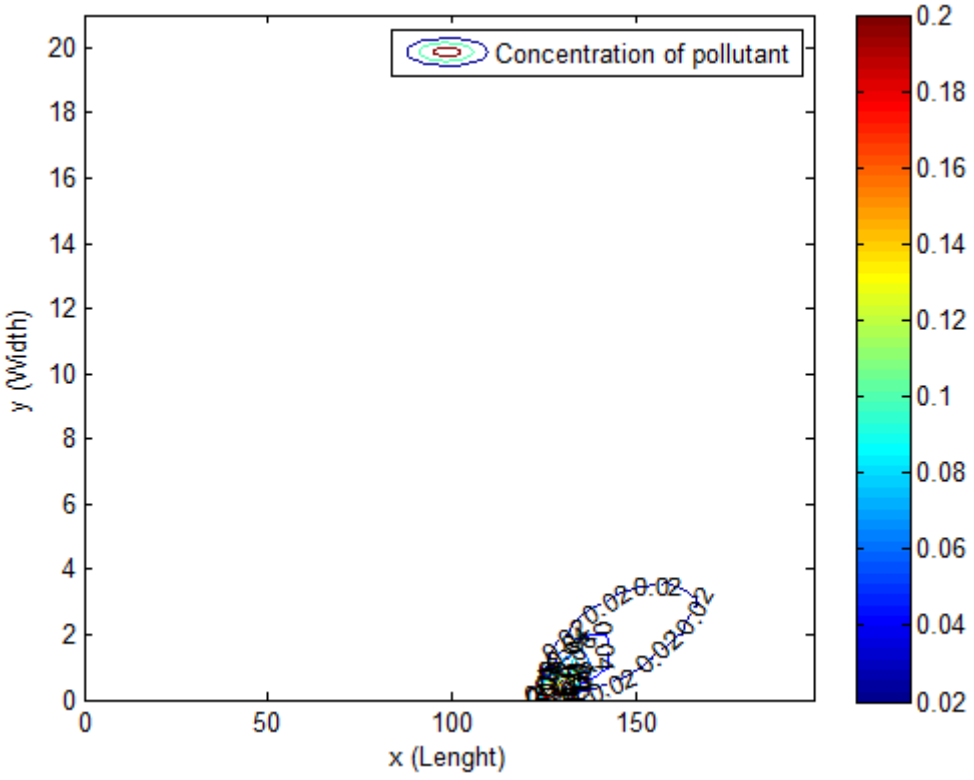
Concentration of pollutant
y (Width)
x (Lenght)
0
50
100
150
0
2
4
6
8
10
12
14
16
18
20
0.02
0.04
0.06
0.08
0.1
0.12
0.14
0.16
0.18
0.2

(c)

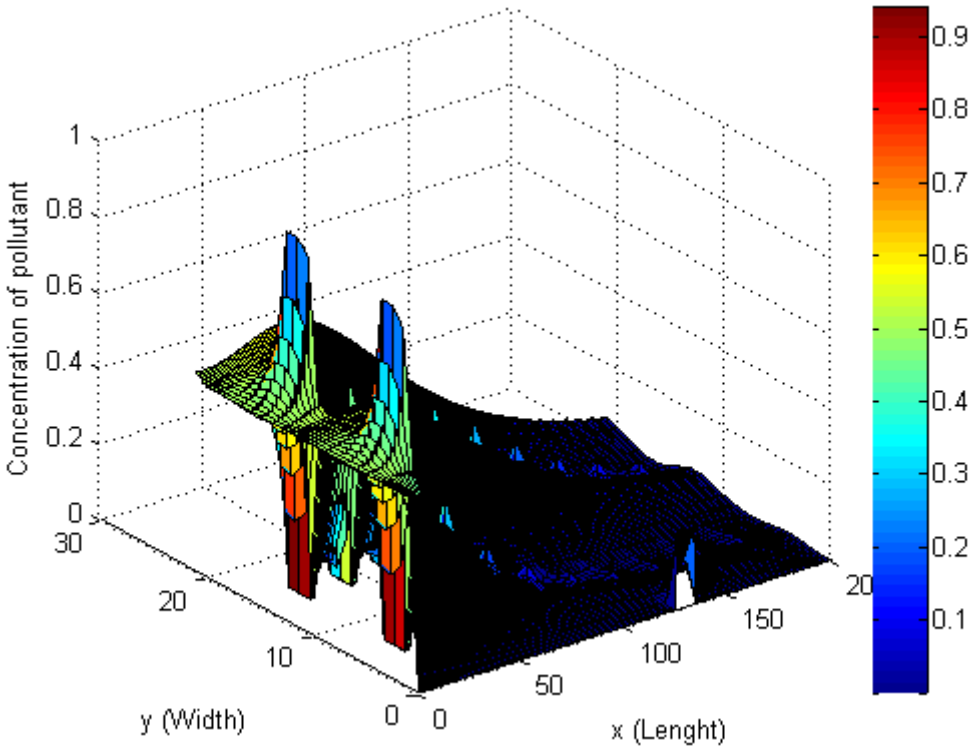
Concentration of pollutant
1
0.8
0.6
0.4
0.2
0
30
20
10
0
y (Width)
0
50
100
150
200
x (Lenght)
0.9
0.8
0.7
0.6
0.5
0.4
0.3
0.2
0.1

(d)

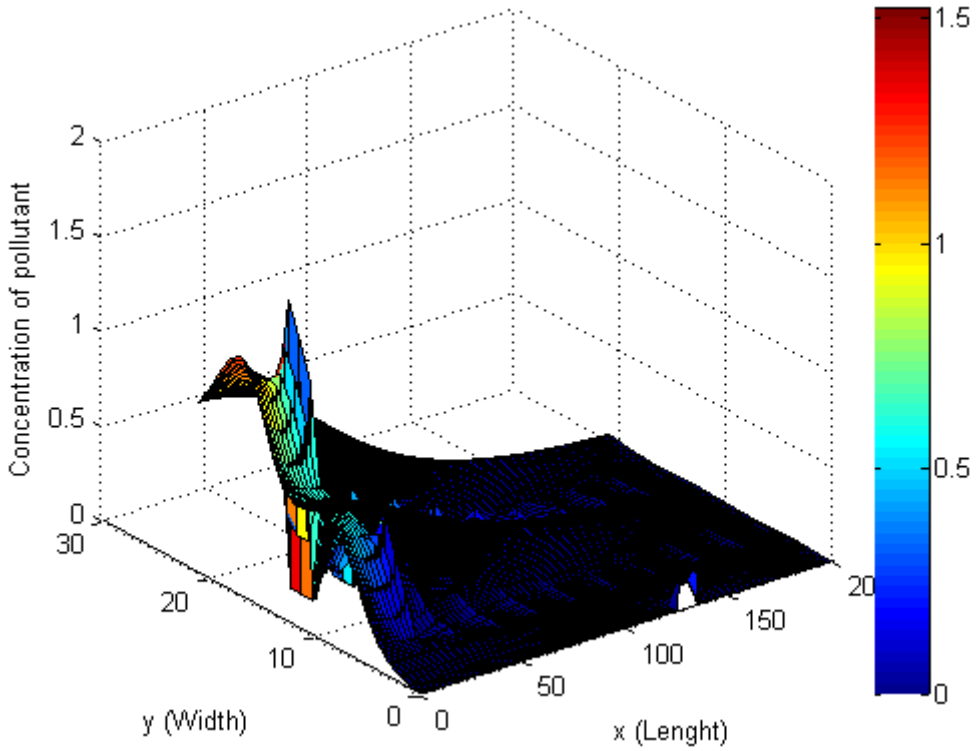
Concentration of pollutant
2
1.5
1
0.5
0
30
20
10
0
y (Width)
0
50
100
150
200
x (Lenght)
1.5
1
0.5
0

(e)

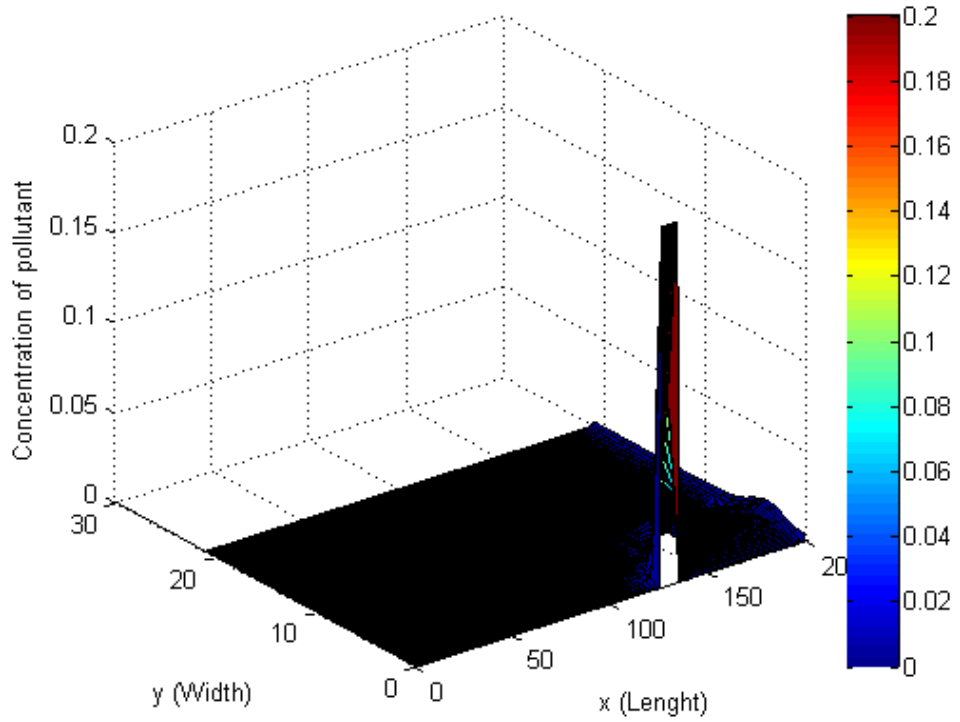

(f)

Figure 4.10 Contour and surface plot of air pollutant concentration levels after the past 2 minutes for the respective streets, tickets, and platform floors (Scenario A)

The air pollutant concentration of Scenario A with the different floors are shown in Figure 4.11.

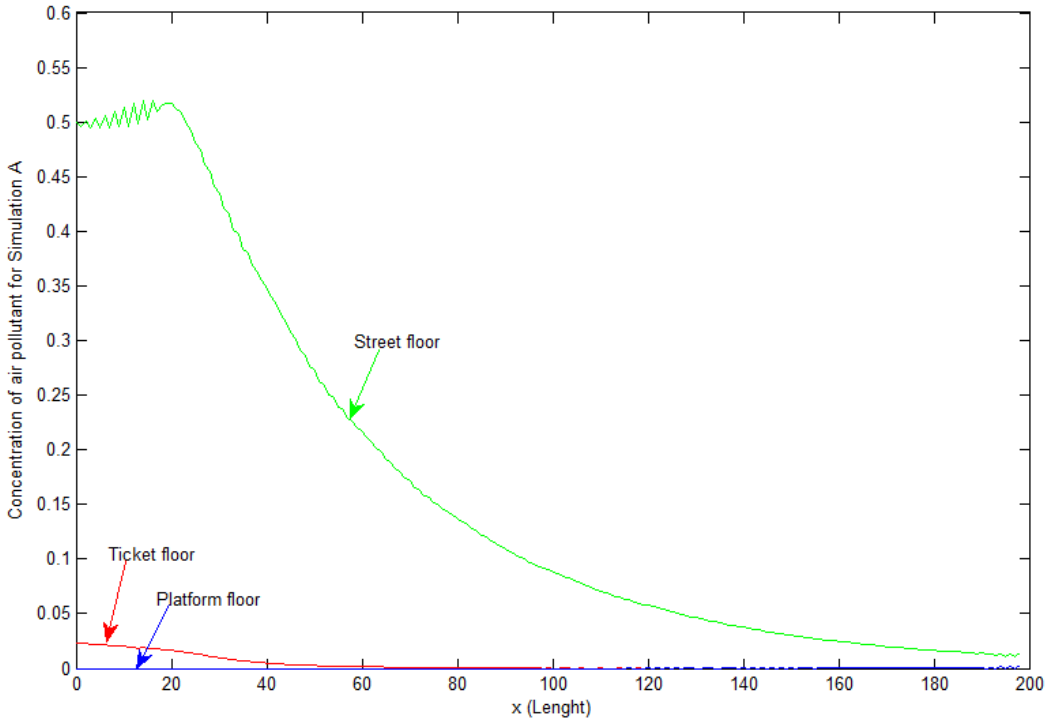

Figure 4.11 The air pollutant concentration with the different floors of Scenario A

4.3.2.2 Scenario B: Air pollutant flowing into every floors

In reality, we notice that the air pollutant concentration depends on the height of the tunnel; if the height increases, the air pollutant concentration will be less. Thus, the air pollutant concentration at the entrance gate for the street floor, ticket floor, and platform floor can be described as different decreasing functions varying with the height of the tunnel. Therefore, c_1 in the boundary conditions of all 3 floors are as follows:

Street floor: $c_1 = 0.5 - 0.02z.$
Ticket floor: $c_1 = 0.32 - 0.015z.$
Platform floor: $c_1 = 0.1 - 0.005z.$

The problem domain is $\Omega = \{(x, y, z);\ 0 \le x \le 198,\ 0 \le y \le 21,\ 9 \le z < 22\}$. The grid spacing: $\Delta x = \Delta y = \Delta z = 1\ m,\ \Delta t = 0.06\ s,$ and for the time $T = 120\ s.$ We assume: $c_3 = c_9 = -0.01,\ c_5 = 0.2,\ c_2 = c_4 = c_6 = c_7 = c_8 = c_{10} = c_{11} = 0,\ A = 4,\ B = 17,\ F = 125,\ G = 135,$ and $ncl = 9.$ We choose $u = 2.7778,\ v = u/20\ m/s,\ D_h = 0.1592,\ D_v = 0.05\ m^2/s.$ So, the results of Scenario B for three different floors are shown in Figure 4.12. That is, in Figure 4.12(a), Figure 4.12(c) and Figure 4.12(e) show the contour plot of the air pollutant concentration levels for street, ticket and platform floors, respectively. Meanwhile, the surface plot of the air pollutant concentration levels for street, ticket and platform floors are shown in Figure 4.12(b), Figure 4.12(d) and Figure 4.12(f), respectively. As seen in the results, the air pollution continues to be released as the functions decrease, but gradually decreases. Therefore, the air pollution on the three floors of this scenario is higher; especially, the air pollutant concentration on the street floor is as high as $0.7\ kg/m^3.$

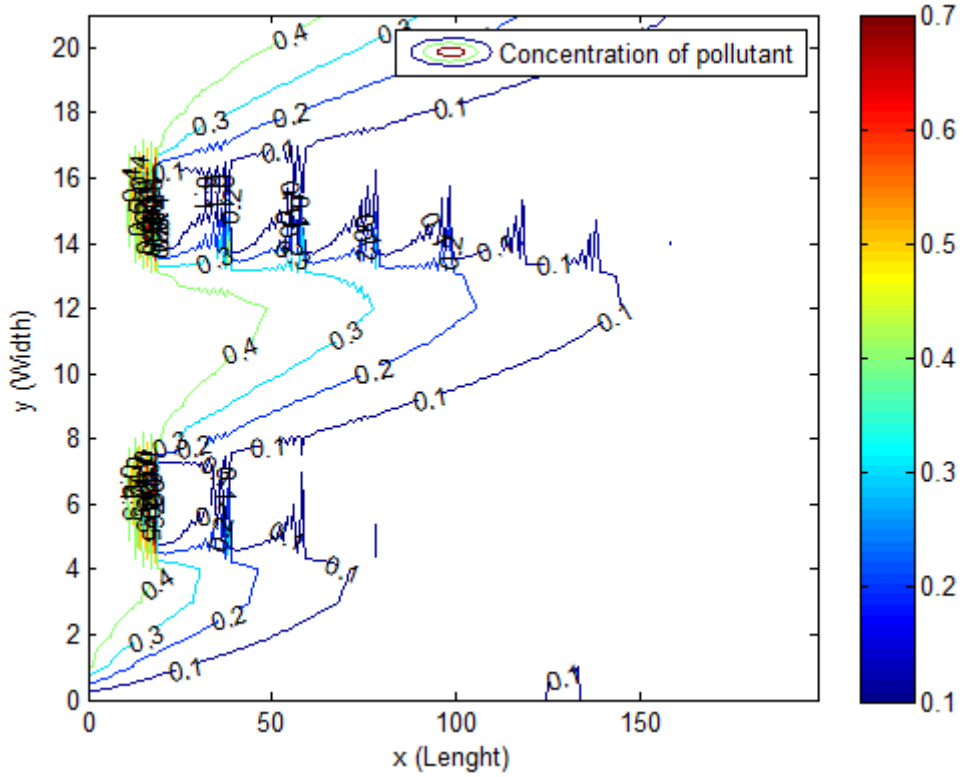
Concentration of pollutant
y (Width)
x (Lenght)
0
50
100
150
0
2
4
6
8
10
12
14
16
18
20
0.1
0.2
0.3
0.4
0.5
0.6
0.7

(a)

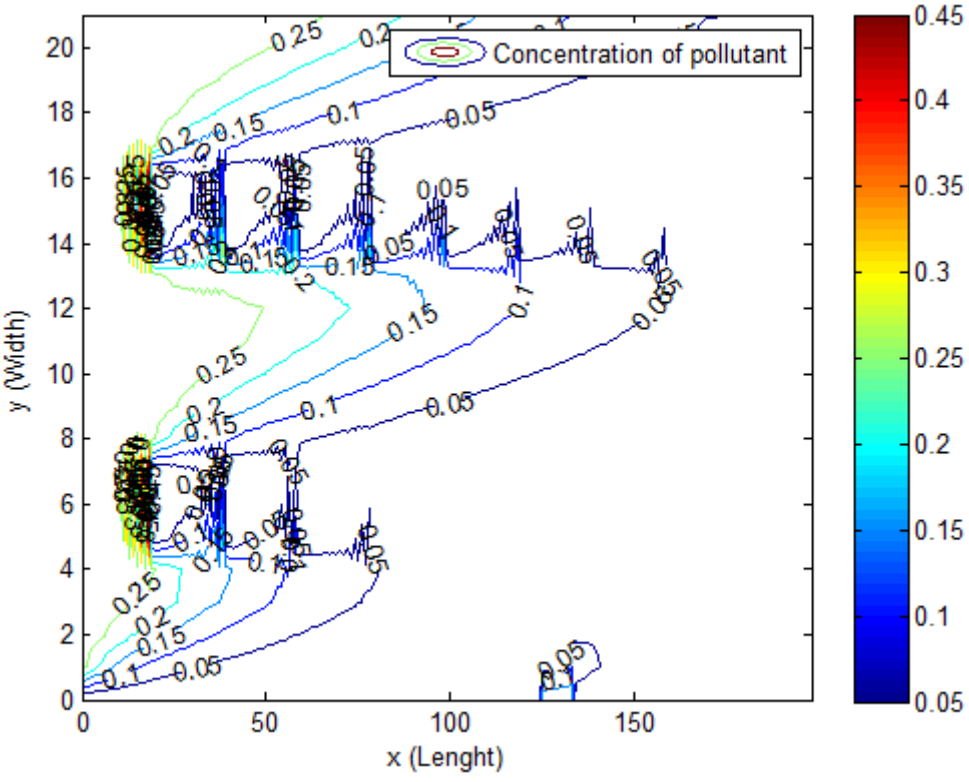
Concentration of pollutant
y (Width)
x (Lenght)
0
50
100
150
0
2
4
6
8
10
12
14
16
18
20
0.05
0.1
0.15
0.2
0.25
0.3
0.35
0.4
0.45

(b)

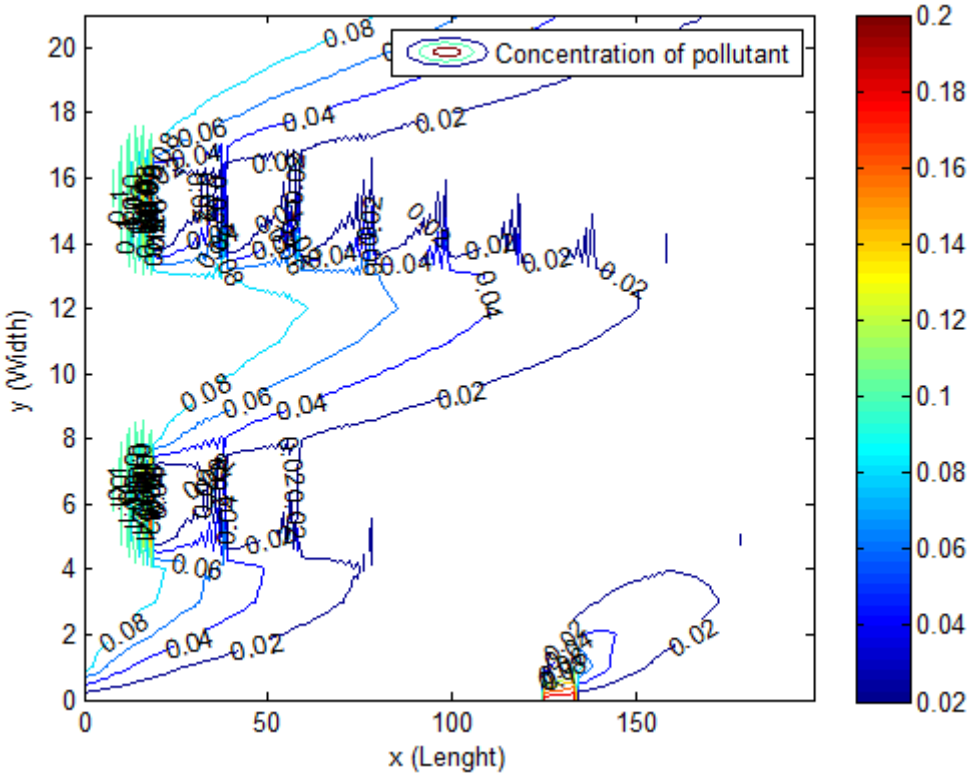
Concentration of pollutant
y (Width)
x (Lenght)
0
50
100
150
0
2
4
6
8
10
12
14
16
18
20
0.02
0.04
0.06
0.08
0.1
0.12
0.14
0.16
0.18
0.2

(c)

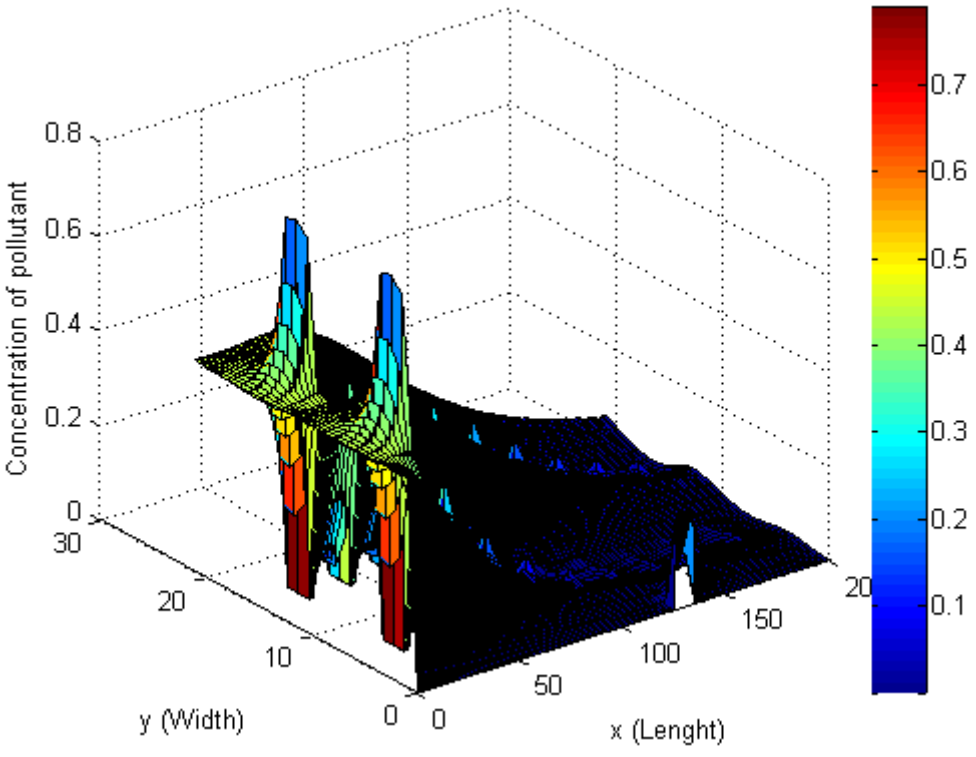
Concentration of pollutant
y (Width)
x (Lenght)
0
0.2
0.4
0.6
0.8
0
10
20
30
0
50
100
150
200
0.1
0.2
0.3
0.4
0.5
0.6
0.7

(d)

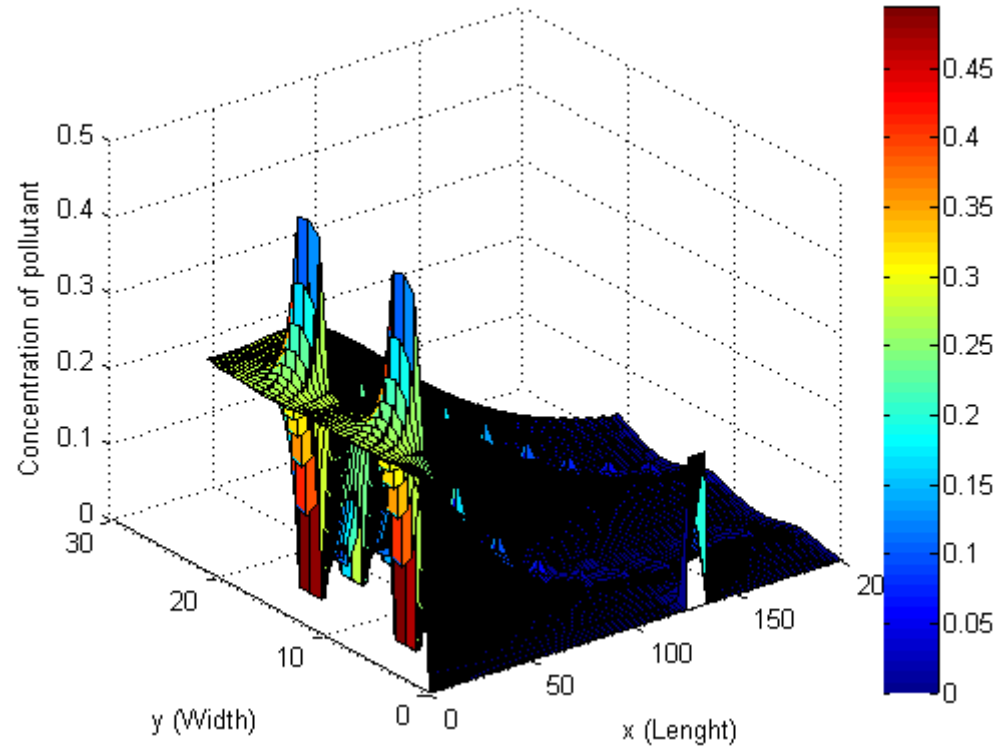

(e)

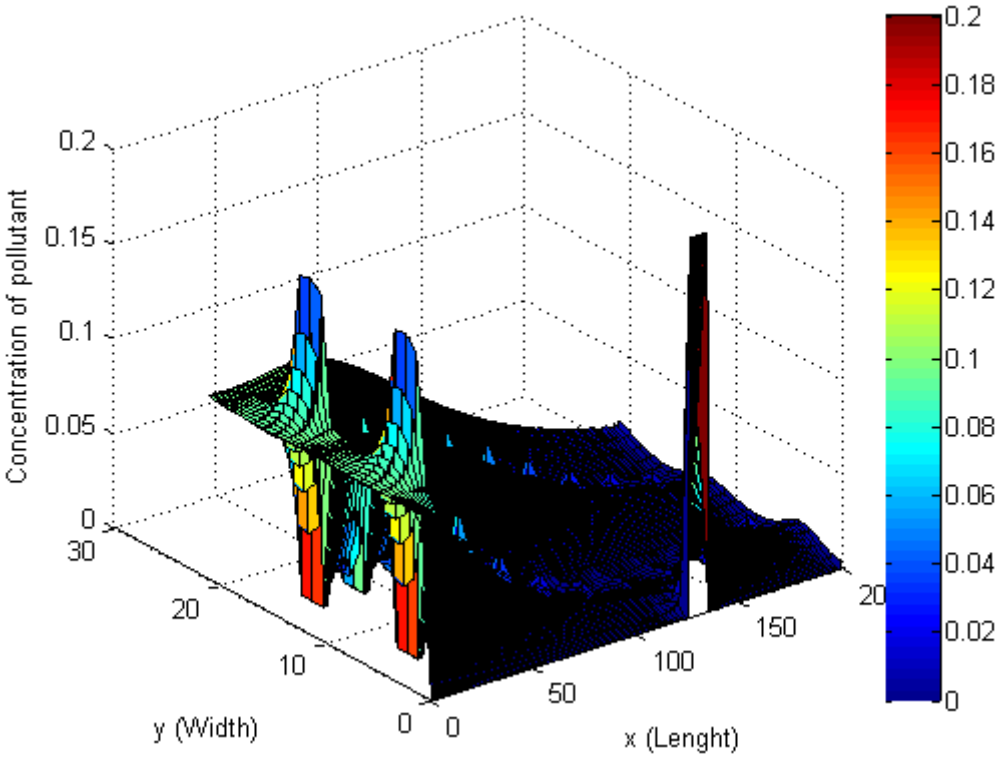

(f)

Figure 4.12 Contour and surface plot of air pollutant concentration levels after the past 2 minutes for the respective streets, tickets, and platform floors (Scenario B)

The air pollutant concentration of Scenario B with the different floors are shown in Figure 4.13.

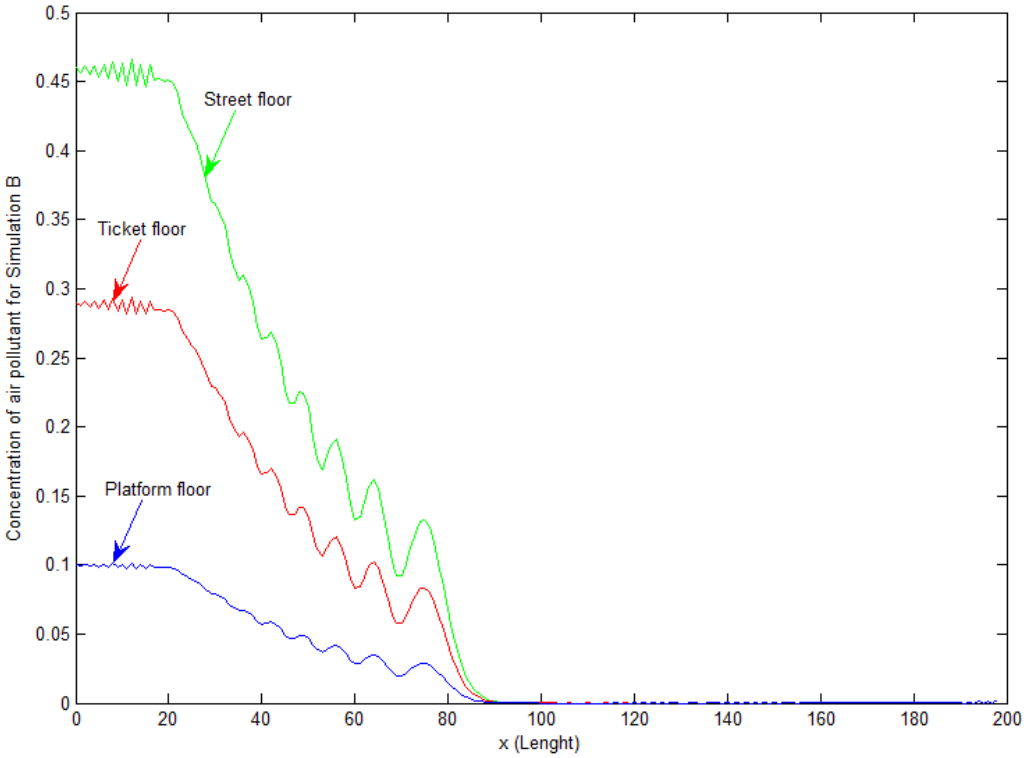

Figure 4.13 The air pollutant concentration with the different floors of Scenario B

4.3.2.3 Scenario C: Air pollutant flowing through the street floor and their gaps

The air pollutant concentration on the street floor is assumed to be a constant. Furthermore, for more realism, we can see that the air pollutant concentration from the previous floor impacts on the next floor. Therefore, we will define the pollution of the next floor by applying the principle of average. The air pollutant concentration at the entrance of the next floor is the average of the air pollutant concentration of gaps on the previous floor. Therefore, c_1 in the boundary conditions of all 3 floors are as follows:

Street floor : $c_1 = 0.5.$
Ticket floor : $c_1 = c_{avS}$.
Platform floor : $c_1 = c_{avT}$,

where c_{avS} and c_{avT} are the average of air pollutant concentration of gaps on the street floor and ticket floor, respectively.

The problem domain is $\Omega = \{(x, y, z);\ 0 \le x \le 198,\ 0 \le y \le 21,\ 22 \le z < 28\}$. The grid spacing: $\Delta x = \Delta y = \Delta z = 1\ m,\ \Delta t = 0.06\ s,$ and for the time $T = 120\ s.$ We assume: $c_3 = c_9 = -0.01,\ c_5 = 0.2,\ c_2 = c_4 = c_6 = c_7 = c_8 = c_{10} = c_{11} = 0,\ A = 4,\ B = 17,\ F = 125,\ G = 135,$ and $ncl = 9.$ We choose $u = 2.7778,\ v = u/20\ m/s,\ D_h = 0.1592,\ D_v = 0.05\ m^2/s.$ So, the results of Scenario C for three different floors are shown in Figure 4.14. That is, in Figure 4.14(a), Figure 4.14(c) and Figure 4.14(e) show the contour plot of the air pollutant concentration levels for street, ticket and platform floors, respectively. Meanwhile, the surface plot of the air pollutant concentration levels for street, ticket and platform floors are shown in Figure 4.14(b), Figure 4.14(d) and Figure 4.14(f), respectively. It can also be obtained by Figure 4.14 that the air pollutant concentration gradually decreases because we bring the value of the previous floor to the next floor. Therefore, the pollution on the platform floor is less than the pollution on other floors, as $0.5\ kg/m^3$.

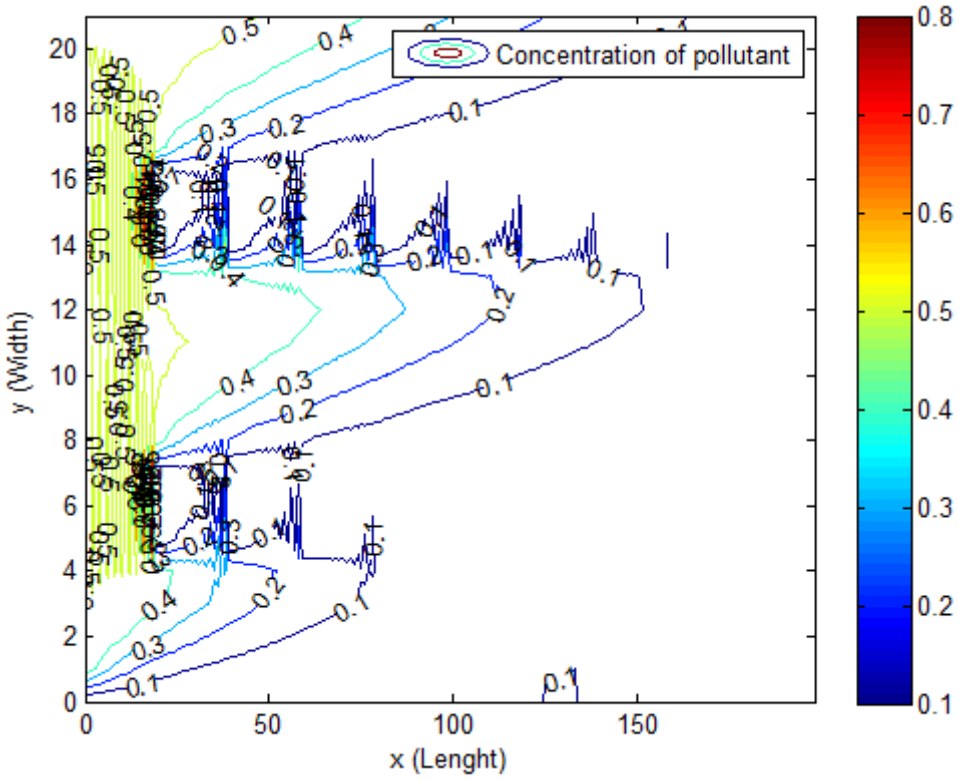

(a)

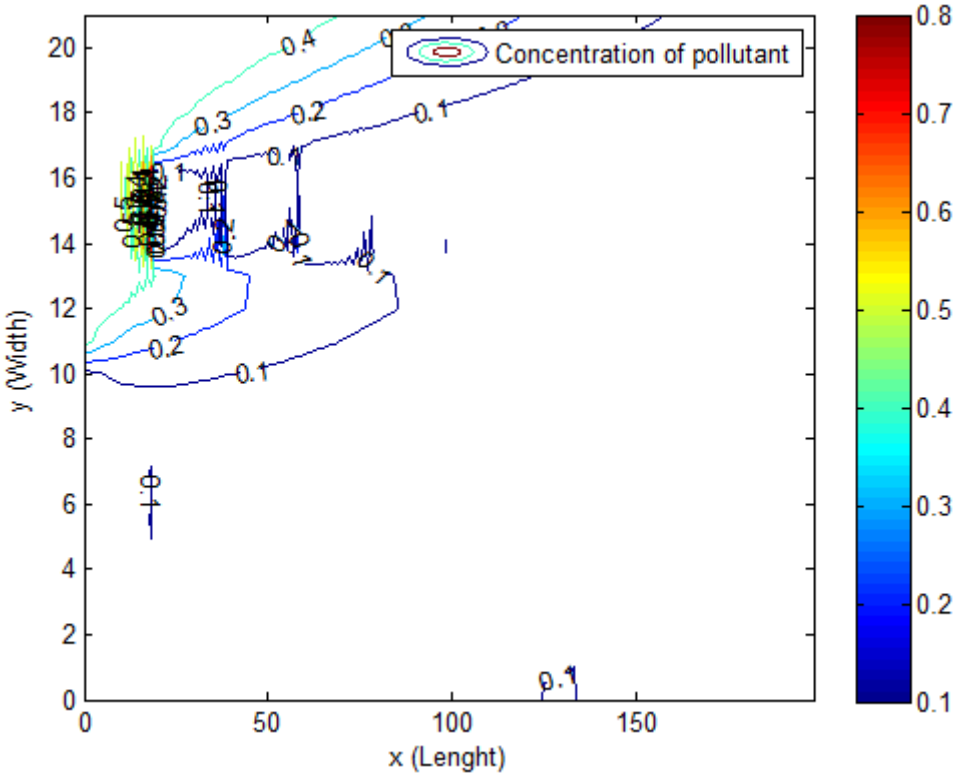
Concentration of pollutant
y (Width)
x (Lenght)
0
50
100
150
0
2
4
6
8
10
12
14
16
18
20
0.8
0.7
0.6
0.5
0.4
0.3
0.2
0.1

(b)

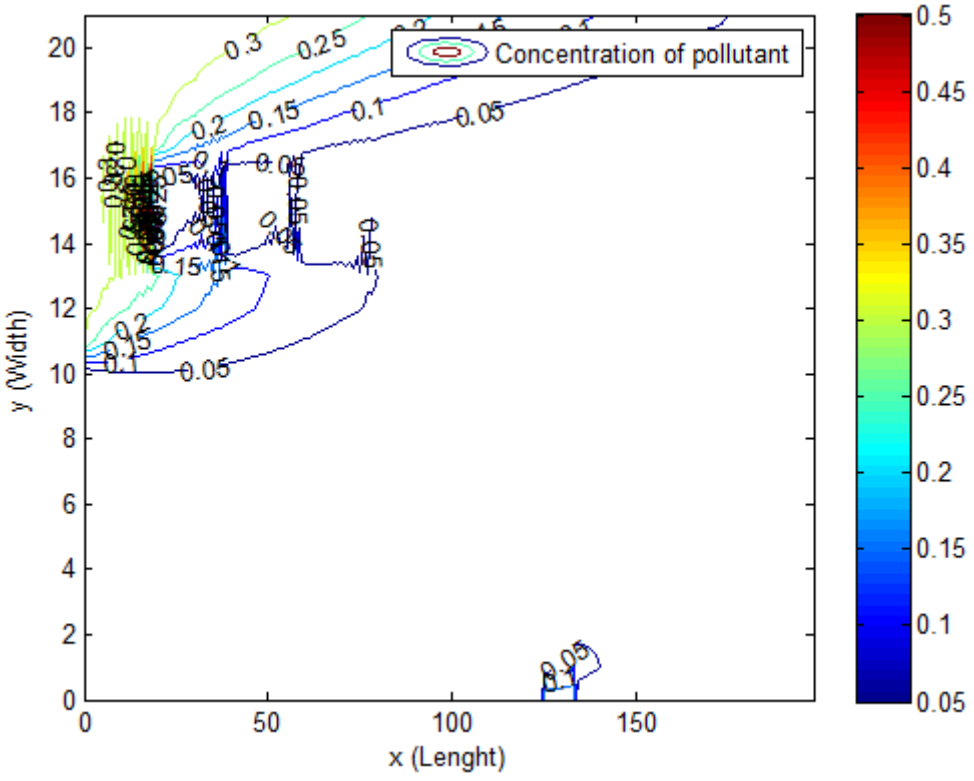
Concentration of pollutant
y (Width)
x (Lenght)
0
50
100
150
0
2
4
6
8
10
12
14
16
18
20
0.5
0.45
0.4
0.35
0.3
0.25
0.2
0.15
0.1
0.05

(c)

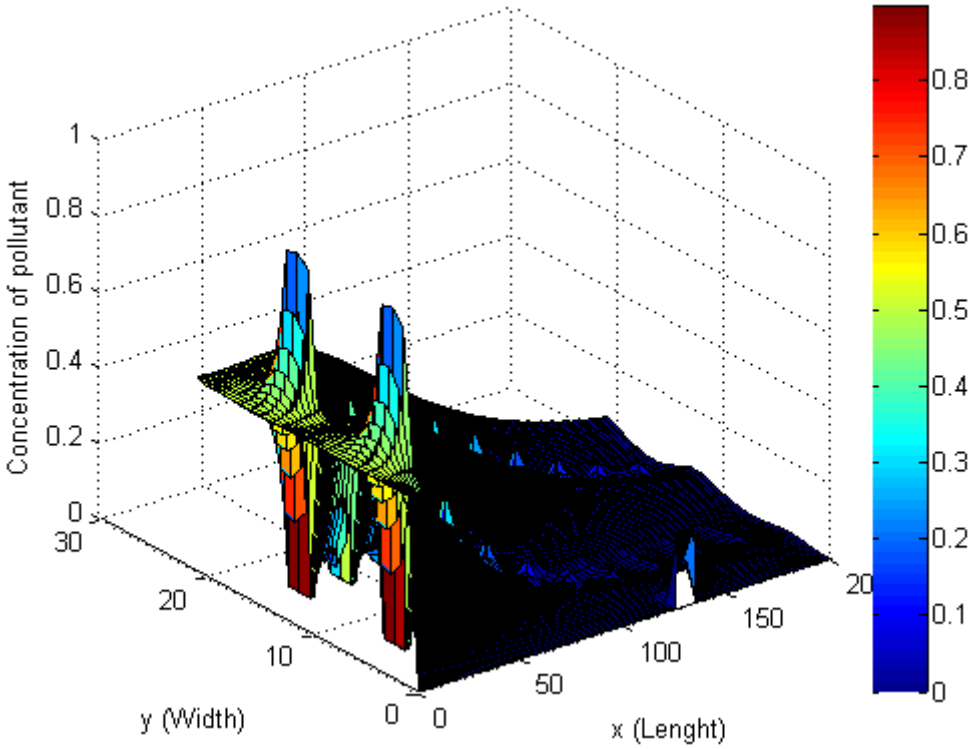
Concentration of pollutant
1
0.8
0.6
0.4
0.2
0
30
20
10
0
y (Width)
0
50
100
150
200
x (Lenght)
0.8
0.7
0.6
0.5
0.4
0.3
0.2
0.1
0

(d)

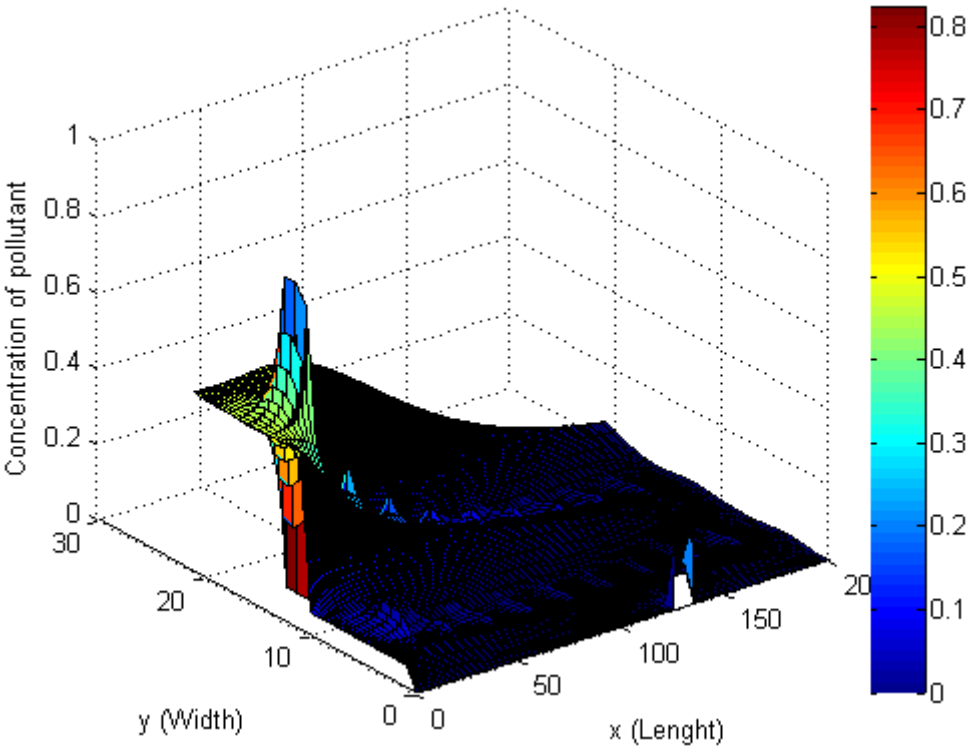
Concentration of pollutant
1
0.8
0.6
0.4
0.2
0
30
20
10
0
y (Width)
0
50
100
150
200
x (Lenght)
0.8
0.7
0.6
0.5
0.4
0.3
0.2
0.1
0

(e)

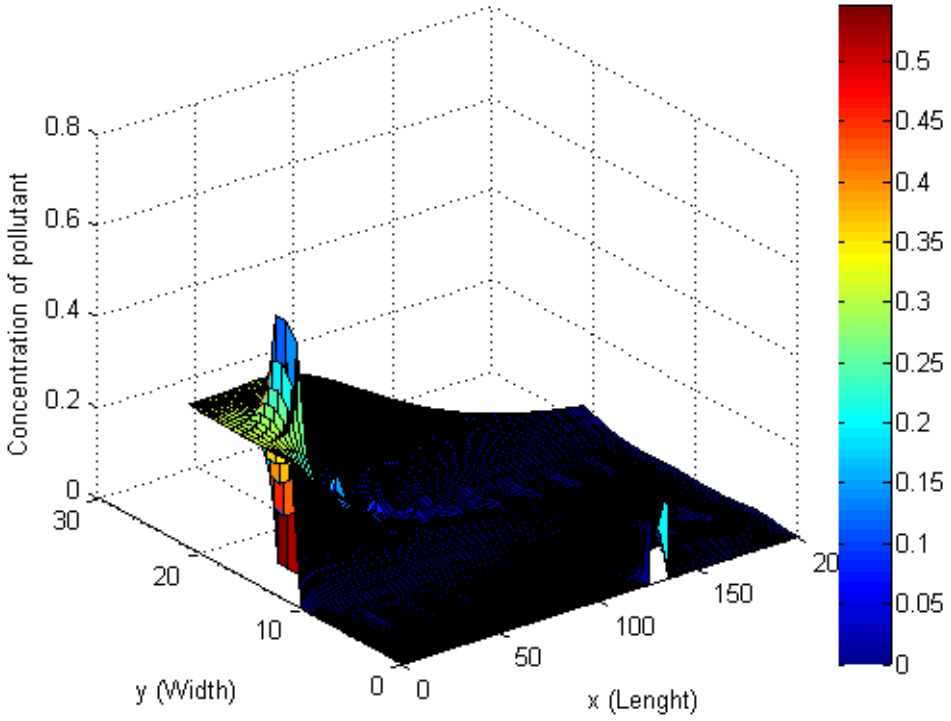

(f)

Figure 4.14 Contour and surface plot of air pollutant concentration levels after the past 2 minutes for the respective streets, tickets, and platform floors (Scenario C)

The air pollutant concentration of Scenario C with the different floors are shown in Figure 4.15.

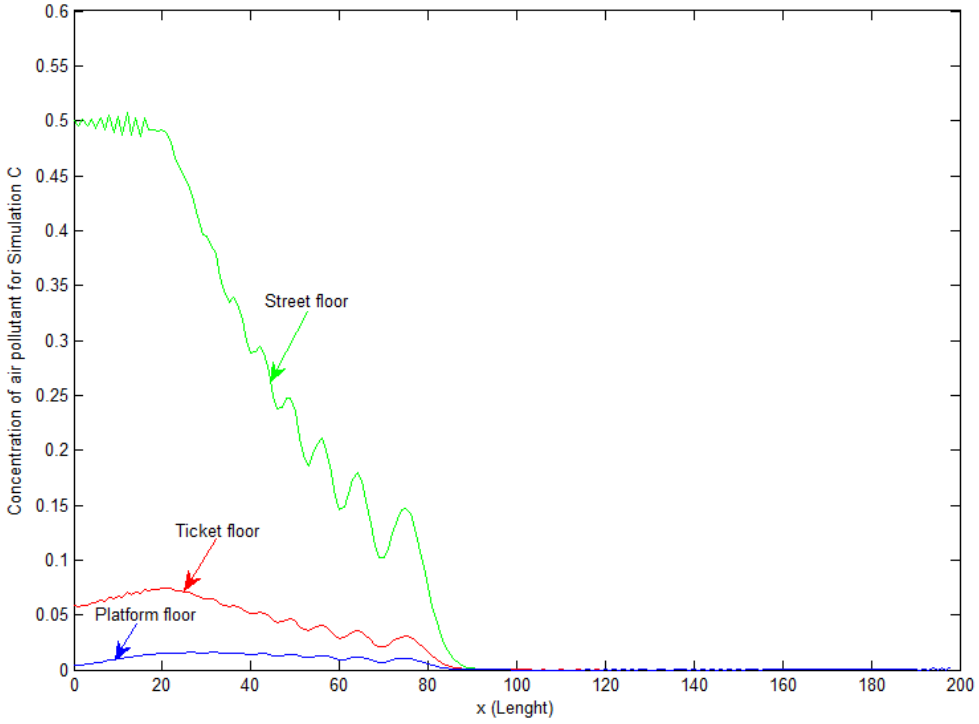

Figure 4.15 The air pollutant concentration with the different floors of Scenario C

Chapter 5
Discussion and Conclusion

5.1 Discussion

In the numerical simulation of a three-dimensional air quality model of an area under a Bangkok skytrain platform using an explicit finite difference scheme, we divided the air pollutant concentration data into three cases. In Cases I and II, we assumed that there was a wind inflow only in the x-direction. Case II was similar to Case I, but we added the boundary conditions of obstacles in the tunnel. For Case III, we assumed that there was wind inflow in the x- and y-directions. In Case I, for a more realistic problem, parallel gaps along the tunnel, between the ceiling and the buildings on both sides, were added in to the domain. It was assumed that the rate of change was decreased at the parallel gaps and the exit gate. If we increased the time into our system, the results of the pollutant concentrations were reduced. In Case II, in reality, there were obstacles in the street tunnel, such as columns. Therefore, we added the boundary conditions of obstacles into the tunnel. It was assumed there was no rate of change at the columns. The results were agreeable, and the concentration of pollutants was decreased away from the source. Moreover, the front of columns had a higher concentration than the back of columns. In Case III, we considered the wind inflow in the x- and y-directions. We added u in the x-direction and v in the y-direction. The results were reasonable, and the concentration of pollutants was decreased away from the entrance gate and the right side wall gap. Moreover, the concentration of pollution in the left side wall was higher than in other areas.

In the numerical simulation of a three-dimensional air pollution measurement model in a heavy traffic area under the Bangkok skytrain platform, there were three simulations of released air pollutant concentration. In Simulation A, we took an increased source rate into our system, and could see that the concentration of air pollutant levels increased. On the other hand, the sink could lower the concentration of air pollutant levels. Therefore, the concentration varied with the source or sinks. In Simulation B, if R was a function of both source and sink, the concentration of air pollutants increased and decreased, respectively. That is, it increased when R was the source; if R was sink, the concentration of air pollutants decreased. In Simulation C, we added a large quantity of sources in at the beginning, and it affected the concentration of pollutants.

In three-dimensional air quality assessment simulations inside the skytrain platform with airflow obstacles on heavy traffic road, we proposed three scenarios for estimating the air pollutant concentration, as follows: In Scenario A, there was no rate of change of air pollutant concentration at the entrance gate of the ticket and platform floors. Based on the results, the air pollution on the platform floor was low because it only emitted pollution at the wall gap on the right side. In Scenario B, the air pollutant concentration at the entrances of the three floors could be described by different decreasing functions depending on the height of the tunnel. As a result, the air pollution continuesds to be released as the function decreased, but gradually decreased. Therefore, the air pollution in this scenario was high when compared to the other scenarios. In Scenario C, the air pollution at the entrance of the next floor was the average of the air pollutant concentration of gaps on the previous floor. The results of this scenario showed that the pollution gradually decreased, because we used the value of the previous floor to the next floor, which significantly reduced air pollution.

5.2 Conclusion

In the numerical simulation of a three-dimensional air quality model in an area under a Bangkok skytrain platform using an explicit finite difference scheme, the proposed model can be used to measure air pollutant concentration in a partly opened street tunnel, especially, an area under a Bangkok skytrain platform. The model is governed by a three-dimensional in space and one-dimensional in time advection-diffusion equation. The results from 3 cases can be summarized as follows: if we increased the time, it could be seen that the concentration of air pollutants decreases even though the distance increased; that is, the concentration varied with the length of distance. The results were satisfactory, because there was no outside air flow. Then, there was wind inflow only in the x-direction from the entrance gate into the tunnel. However, we added obstacles into the tunnel, such as columns along the middle. As a result, the concentration of air pollutants increased; especially, the front of columns had a higher concentration than the back of columns. The higher air pollution came from the columns. Furthermore, there was wind inflow in the x- and y-directions. We assumed that the sources were emitted from the entrance gate and the right side wall gap. This caused the concentration of pollution in the left side wall to be higher than in other areas.

In numerical simulation for a three-dimensional air pollution measurement model in a heavy traffic area under the Bangkok skytrain platform, the released vehicles air pollutants could be assumed by source functions. Source functions were defined by many methods, such as averaged collected data methods or numerical

interpolations. The concentration of air pollutants decreased if we increased sink rate into our system. On the other hand, the concentration of air pollutants increased if we increased source rate. Therefore, the concentration of pollutants varied with the sink or source.

An air pollutant concentration model for three-dimensional air quality assessment simulations inside a skytrain platform with airflow obstacles on a heavy traffic road is presented. The finite difference methods, such as the FTCS and FTBS methods, can be used to estimate the air pollutant concentrations. Additionally, it is appealing that the grid spacing is different, so that the FTCS method has been chosen because, when making comparisons between the FTCS and FTBS methods, in some cases, the solution for the FTBS method is unstable, while the solution for the FTCS method is stable. Therefore, the FTCS method provides a better result than the FTBS method. In a summary of the three scenarios, Scenario A is a simple model that is an economical method to use. It requires little collected data. Scenario B is a realistic numerical simulation. The approximated air pollutant concentration depends on the height, but requires a lot of field data. Scenario C is a fairly good model. The simulation needs to average the pollutant concentration levels. It is used in the case of input air pollutant concentration to the above floor.

All of the simulations, we can summarize that the air pollution problems arose from external and internal vehicles that released air pollution. The pollution in a heavy traffic in the Bangkok skytrain station area was larger than outside due to inside air flow obstacles. Therefore, a heavy traffic, the wind inflow directions, and the obstacles are an important factor of the air pollutant concentration. Moreover, the boundary conditions were not limited only to constant functions, but could be assumed to have several interpolated functions. The proposed an explicit finite difference method gave a good agreement and reasonable results. However, the most suitable model to use depends on the provided field data.

References

[1] Charusombat, U. 1998. "Air Pollution Distribution under an Elevated Train Station (A Case Study of Silom Station in Downtown Bangkok)." The degree of master of science in environmental engineering.

[2] Alvarez-Vazquez, L.J., Garcia-Chan, N., Martinez, A. and Vzquez-Mendez, M.E. 2007. "Numerical Simulation of Air Pollution due to Traffic Flow in Urban Networks." *Journal of Computational and Applied Mathematics*. 326 : 44-61.

[3] Leong, S.T., Muttamara, S. and Laortanakul, P. 2002. "Air Pollution and Traffic Measurements in Bangkok Streets." *Asian J. Energy Environ*. 3 : 185-213.

[4] Dehghan, M. 2004. "Numerical Solution of the Three-Dimensional Advection-Diffusion Equation." *Applied Mathematics and Computation.* 150(1) : 5–19.

[5] Thongmoon, M. 2010. "Numerical Experiment of Air Pollutant Concentration in the Street Tunnel." *International Mathematical Forum*. 10 : 449-465.

[6] Kumar, A. and Jaiswal, D.K. 2010. "Analytical Solutions to One-Dimensional Advection-Diffusion Equation with Variable Coefficients in Semi-in Finite Media." *Journal of Hydrology*. 380 : 330-337.

[7] Kanakiya, R.S., Singh, S.K. and Mehta, P.M. 2015. "Urban Canyon Modelling : a Need for the Design of Future Indian Cities." *International Research Journal of Environment Sciences*. 4(7) : 86-95.

[8] Pochai, N. 2011. "A Finite Element Solution of the Mathematical Model for Smoke Dispersion from Two Sources." *World Academy of Science, Engineering and Technology*. 60 : 1691-1695.

[9] Konglok, S.A. and Pochai, N. 2016. "Numerical Computations of Three-Dimensional Air-Quality Model with Variations on Atmospheric Stability Classes and Wind Velocities using Fractional Step Method." *IAENG International Journal of Applied Mathematics*. 46(1) : 112-120.

[10] Sun, L.K.. Wong, C., Wei, P., Ye, S., Huang, H., Yang, F., Westerdahl, D., Louie, K.K., Luk, W.Y. and Ning, Z. 2016. "Development and Application of a next Generation Air Sensor Network for the Hong Kong Marathon 2015 Air Quality Monitoring." *Lecture Notes in Engineering and Computer Science: Sensors.* 16 : 211.

[11] Suebyat, K. and Pochat, N. 2017. "A Numerical Simulation of a Three-Dimensional Air Quality Model in an Area under a Bangkok Skytrain Platform Using an Explicit Finite Difference Scheme." *IAENG International Journal of Applied Mathematics*. 47 : 471–476.

[12] Wikipedia, the free encyclopedia. 2018. **BTS Skytrain**. [Online]. Available : https://en.wikipedia.org/wiki/BTS_Skytrain.

References (Continue)

[13] BTS Group Holdings Public Company Limited. 2011. **BTS Ridership**. [Online]. Available : http://bts.listedcompany.com/bts_ridership.html.

[14] Prachachat Business. 2018. **10 Stations BTS Riders to the Maximum**. [Online]. Available : https://www.prachachat.net/news_detail.php?newsid=1339485497&grpid=09&catid=no&subcatid=0000.

[15] Waller, R. E., Commins, B. T., and Lawther, P. J. 1961. "Air pollution in road tunnels." *Brit. J. industr. Med*. 18 : 250.

[16] Hindmarsh, A. C., Gresho, P. M., and Griffiths, D. F. 1984. "The Stability of Explicit Euler Time-Integration for Certain Finite Difference Approximations of the Multidimen-Sional Advection-Diffusion Equation." *nt. J. Numer Methods Fluids*. 4 : 853-897.

[17] Sanin, N. and Montero, G. 2007. "A Finite Difference Model for Air Pollution Simulation." *Advances in Engineering Software*. 38 : 358-365.

[18] Kampa, M. and Castanas, E. 2008. "Human Health Effects of Air Pollution." *Environmental Pollution*. 151 : 362-367.

[19] Lambers, J. V. 2008. "An Explicit Stable High–Order Spectral Method for the Wave Equation Based on Block Gaussian Quadrature." *IAENG International Journal of Applied Mathematics*. 38(4) : 233-248.

[20] Siddique, M. 2010. "Numerical Computation of Two-Dimensional Diffusion Equation with Nonlocal Boundary Conditions." *IAENG International Journal of Applied Mathematics*. 40(1) : 26-31.

[21] Pochai, N. 2011. "A Finite Element Solution of the Mathematical Model for Smoke Dispersion from Two Sources." *World Academy of Science, Engineering and Technology*. 60 : 1691-1695.

[22] Savovic, S. and Djordjevich, A. 2012. "Finite Difference Solution of the One-Dimensional Advection-Diffusion Equation with Variable Coefficients in Semi-Infinite Media." *International Journal of Heat and Mass Transfer*. 55 : 4291-4294.

[23] Salim, S. M. and Ong, K. C. 2013. "Performance of RANS, URANS and LES in the Prediction of Airflow and Pollutant Dispersion." *IAENG Transactions on Engineering Technologies: Lecture Notes in Electrical Engineering*. 170 : 263-274.

[24] Kwa, S. M. and Salim, S. M. 2015. "Numerical Simulation of Dispersion in an Urban Street Canyon: Comparison Between Steady and Fluctuating Boundary Conditions." *Engineering Letters*. 23(1) : 55-64.

References (Continue)

[25] Iodice, P. and Senatore, A. 2015. "Environmental Assessment of a Wide Area Under Surveillance with Different Air Pollution Sources." *Engineering Letters*, 23(3) : 156-162.

[26] Suebyat, K. and Pochat, N. 2018. "Numerical Simulation for a Three-Dimensional Air Pollution Measurement Model in a Heavy Traffic Area under the Bangkok Skytrain Platform." *Abstract and Applied Analysis*. 2018. Article ID 9025851. 10 pages. https://doi.org/10.1155/2018/9025851.

[27] Mackenzie, J. 2018. **Air pollution: Everything you need to know**. [Online]. Available : http://www.nrdc.org/health/effects/fasthma.asp.

[28] Suebyat, K. and Pochat, N. 2018. "Three-Dimensional Air Quality Assessment Simulations inside Skytrain Platform with Airflow Obstacles on Heavy Traffic Road." *Italian Journal of Pure and Applied Mathematics*. 40 : 615-632.

Appendices

Appendix A
Research Papers

IAENG International Journal of Applied Mathematics, 47:4, IJAM_47_4_16

A Numerical Simulation of a Three-dimensional Air Quality Model in an Area Under a Bangkok Sky Train Platform Using an Explicit Finite Difference Scheme

Kewalee Suebyat, Nopparat Pochai

***Abstract*—One of the air pollution problems in areas under Bangkok sky train platforms are caused by the pollutant coming from the entrance to the tunnel. It increases the concentration of pollutant. This affects the well-being of humans and the environment. In this research, the governing equation of the air quality model in a considered area is a three-dimensional advection-diffusion equation with time dependence. A finite difference technique is employed to approximate the solution of the governing equation. This model is solved by using an explicit forward difference in time and central difference in space (FTCS). We consider the wind inflow in two cases: there is wind inflow only in x-direction and there are wind inflow in x-direction and y-direction. In addition, we added obstacles such as the columns along the middle into the tunnel. The results of the model are satisfactory. It will be able to be implemented on a problem of air pollution control in a more complicated tunnel.**

***Index Terms*—air quality, advection-diffusion equation, finite difference method, FTCS, Bangkok sky train, tunnel.**

I. Introduction

AIR pollution is a global problem for human life and environment that should be realized. It comes from many sources such as forest fires, industrial factory area, traffic jam and more, especially, an area under Sky Train of the Bangkok Transit System (BTS). It provides an effective route of urban transport for people of Bangkok because BTS facilitates quick and easy transportation. However, it is also causing some of the environmental impacts especially the air pollutant impact to the vicinity area around its platform with heavy traffic and a lot of people. The major source of air pollution under Bangkok sky train platform comes from vehicle exhaust, mobile source and others sources including commercial, smoke from the store, construction and building demolition. The air pollutants emitted from mobile source are Carbon Monoxide (CO) and Nitrogen Oxides (NOx). CO is a product of incomplete combustion of fuel such as natural gas, coal or wood. Vehicular exhaust is a major source of carbon monoxide. In areas of high vehicle traffic, such as in large cities, NOx emitted can be a significant source of air pollution. It raises the earth's temperature and becomes air pollutants. Their concentration levels cause injury to human health and an harmful for survival. The effects of air pollution are alarming. Several people are known to have died due to direct or indirect effect of air pollution. It is known that air pollution contributes to cancer among other threats to the body.

Nowadays, there are heavy traffic and an increase in population. It's the cause of air pollution on the road. Air pollution around the platform in an area under Bangkok sky train platform has increased greatly, so it is interesting to study. However this area should be implemented into the wind inflow direction near the tunnel because it affects the concentration of air pollutant. Then the wind inflow is an important factor of the model.

In 1961, [1] studied the pollution of the air by motor vehicles, measurements were made in two London road tunnels during periods of high traffic density. The concentrations of smoke and polycyclic hydrocarbons found that there were much higher than the average values in Central London, but they were of the same order of magnitude as those occurring during temperature inversions on winter evenings when smoke from coal fires accumulates at a low level. In 2004, [2] defined and calculated the stability conditions for several numerical methods for a three-dimensional advection-diffusion equation and compared the numerical solutions. In 2008, [3] presented the modification of Krylov Subspace Spectral (KSS) methods by using the Lanczos iteration to computed the quadrature rules. KSS methods were second-order accurate and unconditionally stable. For more than one node are shown to possess favorable stability properties as well. In 2010, [4] presented a new Pad numerical scheme for the solution of two-dimensional diffusion equations with nonlocal boundary conditions on four boundaries. The numerical results are shown that these Pad schemes are efficient and provided very accurate results. In 2010, [5] studied a three dimensional advection-diffusion equation of air pollutant is applied to a street tunnel configuration. In 2011, [6] studied a mathematical model of the smoke dispersion from two sources and one source with a structural obstacle was considered. In 2013, [7] studied and compared the performance of 3 different CFD numerical approaches, namely RANS, URANS and LES for evaluation to determine suitability in the prediction of air flow and pollutant dispersion in urban street canyons. The results showed that LES was observed to produce accurate more than RANS and URANS. In 2015, [8] developed the Fluctuating Wind Boundary Conditions (FWBC) and compared to SWBC in order to determine suitability in the investigation of air flow and pollutant dispersion in urban street canyons. 3D numer-

Manuscript received May 02, 2017; revised September 14, 2017.

Kewalee Suebyat and Nopparat Pochai are with Department of Mathematics, Faculty of Science, King Mongkuts Institute of Technology Ladkrabang, Bangkok 10520, Thailand and Centre of Excellence in Mathematics, Commission on Higher Education (CHE), Si Ayutthaya Road, Bangkok 10400, Thailand. Email: kew26_tan@hotmail.com and nop_math@yahoo.com.

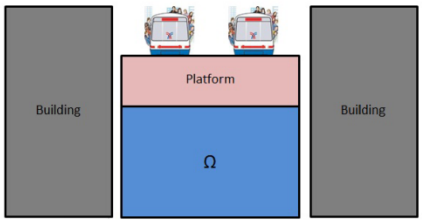

Fig. 1. The steet tunnel configuration.

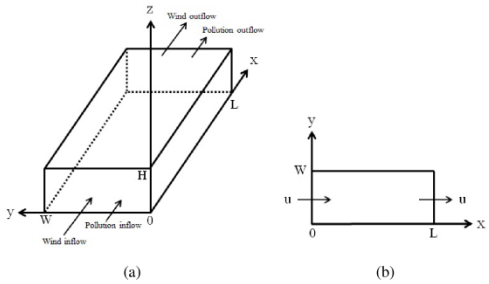

Fig. 2. (a) The domain for street tunnel (Case 1). (b) The wind direction (Case 1).

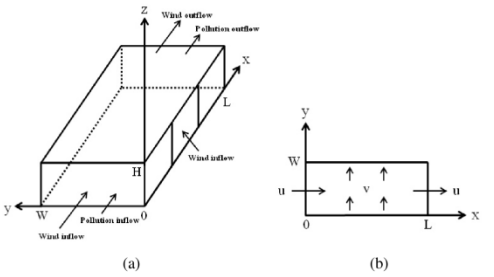

Fig. 3. (a) The domain for street tunnel (Case 2). (b) The wind direction (Case 2).

ical simulations are performed using Large Eddy Simulation (LES). The FWBC has produced more realistic results when compared to the frequently employed SWBC. In 2015, [9] calculated the concentration of air pollutant and to assessed the air quality state all over the Region. The analysis was carried out by using the Gaussian model ISC. This modeling approach can be considered as an important assessment tool for the local environmental authorities in Campania region, Southern Italy. In 2016, [10] studied a mathematical model for describing the dispersion of the air pollutants released from the source into the atmosphere was examined by using the three-dimensional fractional step method. The results obtained indicated that the proposed experimental variations of the atmospheric stability classes and wind velocities did affect the air quality around the industrial areas. In 2016, [11] studied and presented the development of a next generation air sensor system and application in an $ad\ hoc$ air monitoring network, in which the air sensors were placed and operated at the street level to monitor the air along the Marathon route in urban Hong Kong and the near-real time calculation and communication of health-indexed findings of air quality to the public.

The purpose of this paper is to approximate the concentration of air pollutant in two cases: there is wind inflow only in x-direction and there are wind inflow in x- and y-directions by using the finite difference technique.

II. Governing Equation

The tunnel is an underground passageway with is enclosed except for the entrance and exit. In this paper, the configuration of the area street tunnel is shown in Fig. 1. That is, above the street is sky train platform and both sides of the street are section of buildings. The simulation of configuration of street tunnel are divided into two cases: Case 1: we assume that there is wind inflow only in x-direction. The domain for street tunnel in Case 1 is shown in Fig. 2(a) and the wind direction in this case is shown in Fig. 2(b). Case 2: we assume that there are wind inflow in x- and y-directions. The domain for street tunnel in Case 2 is shown in Fig. 3(a) and the wind direction in this case is shown in Fig. 3(b). Then the consider domain becomes: $\Omega = \{(x, y, z);\ 0 \le x \le L,\ 0 \le y \le W,\ 0 \le z \le H\}$, where W is the width (m), L is the length (m) and H is the height (m) of the street tunnel. The air pollutant concentration can be described by the advection-diffusion equation following:

$$\frac{\partial C}{\partial t} + V \cdot \bigtriangledown C = \bigtriangledown \cdot \left(\bar{K} \otimes \bigtriangledown C\right), \tag{1}$$

where $C = C(x, y, z, t)$ is the air pollutant concentration at (x, y, z) and time t (kg/m^3), $\bigtriangledown = \frac{\partial}{\partial x}\vec{i} + \frac{\partial}{\partial y}\vec{j} + \frac{\partial}{\partial z}\vec{k}$, and $\otimes$ is matrix multiplication. The vector V is the wind velocity field (m/sec) and $\bar{K}$ is the eddy-diffusivity or dispersion tensor (m^2/sec).

By the assumption, we assumed that the wind inflow is horizontal direction. We shall consider the three-dimensional advection-diffusion equation in Eq. (1), which can be written as:

$$\frac{\partial C}{\partial t} + u\frac{\partial C}{\partial x} + v\frac{\partial C}{\partial y} = D_h\frac{\partial^2 C}{\partial x^2} + D_h\frac{\partial^2 C}{\partial y^2} + D_v\frac{\partial^2 C}{\partial z^2}, \tag{2}$$

where u is a constant wind velocity in the x-direction (m/sec), v is a constant wind velocity in the y-direction (m/sec), D_h is a constant dispersion coefficient in the horizontal direction (m^2/sec) and D_v is a constant dispersion coefficient in the the z-direction (vertical) (m^2/sec) appropriate initial and boundary conditions. When we consider the components of the tunnel, it is shown in Fig. 4. The initial condition is assumed by the cold start technique that the air pollutant concentration is to be zero in the whole domain. It is obtained that

$$C(x, y, z, 0) = 0, \tag{3}$$

for all $0 \le x \le L$, $0 \le y \le W$, $0 \le z \le H$. For the boundary conditions, we distinguish three different cases in the considered domain as following:

Case I: assuming that there is the wind inflows in x-direction. In Fig. 5, model of the Case I is shown.

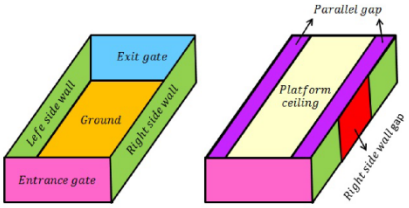

Fig. 4. Components of the tunnel.

Entrance gate : $C(0,y,z,t) = c_1$.
Exit gate : $\frac{\partial C}{\partial x}(L,y,z,t) = c_2$.
Side walls : $\frac{\partial C}{\partial y}(x,0,z,t) = \frac{\partial C}{\partial y}(x,W,z,t) = 0$.
Ground : $\frac{\partial C}{\partial z}(x,y,0,t) = 0$.
Platform ceiling : $\frac{\partial C}{\partial z}(x,y,H,t) = 0, A < y < B$.
Parallel gap : $\frac{\partial C}{\partial z}(x,y,H,t) = c_3$, otherwise,

where c_1 is the inflow air pollutant concentration in x-direction, c_2 is the average rate of change of air pollutant concentration at the exit gate, c_3 is the average rate of change of air pollutant concentration along the both parallel gap, A is the right parallel gap size along the ceiling, and B is the left parallel gap size along the ceiling.

Case II: assuming that there are the obstacles as the platform column. For the model in this case shown in Fig.6.

Entrance gate : $C(0,y,z,t) = c_1$.
Exit gate : $\frac{\partial C}{\partial x}(L,y,z,t) = c_2$.
Side walls : $\frac{\partial C}{\partial y}(x,0,z,t) = \frac{\partial C}{\partial y}(x,W,z,t) = 0$.
Ground : $\frac{\partial C}{\partial z}(x,y,0,t) = 0$.
Platform ceiling : $\frac{\partial C}{\partial z}(x,y,H,t) = 0, A < y < B$.
Parallel gap : $\frac{\partial C}{\partial z}(x,y,H,t) = c_3$, otherwise.
Center column : $C(D_i,E,z,t) = 0, 0 \le z \le H$.
Front and back column : $\frac{\partial C}{\partial x}(D_i - 1,y,z,t) = \frac{\partial C}{\partial x}(D_i + 1,y,z,t) = 0, E-1 \le y \le E+1; t > 0$.
Left and right column : $\frac{\partial C}{\partial y}(x,E-1,z,t) = \frac{\partial C}{\partial y}(x,E+1,z,t) = 0, D_i - 1 \le x \le D_i + 1; t > 0$,

where (D_i, E) is a center point of the platform column in x- and y-directions, for $i = 1,2,...,ncl$, ncl is the number of platform column.

Case III: assuming that there are the wind inflow in x- and y-directions. In Fig. 7, model of the Case III is shown.

Entrance gate : $C(0,y,z,t) = c_1$.
Exit gate : $\frac{\partial C}{\partial x}(L,y,z,t) = c_2$.
Ground : $\frac{\partial C}{\partial z}(x,y,0,t) = 0$.
Platform ceiling : $\frac{\partial C}{\partial z}(x,y,H,t) = 0, A < y < B$.
Parallel gap : $\frac{\partial C}{\partial z}(x,y,H,t) = c_3$, otherwise.
Left side wall : $\frac{\partial C}{\partial y}(x,W,z,t) = 0$.
Right side wall gap : $C(x,0,z,t) = c_4, F \le x \le G, 0 \le z \le H$.
Right side wall : $\frac{\partial C}{\partial y}(x,0,z,t) = 0$, otherwise,

where c_4 is the inflow air pollutant concentration in y-direction and $F-G$ is the side wall gap of the beside consider domain.

III. Numerical Techniques

We use the finite difference method for approximating the solution of the three-dimensional advection-diffusion equation. The solution domain of the problem over a time $0 \le t \le T$ is covered by a mesh of grid-lines: $x_i = i\Delta x, i = 0,1,2,...,M; y_j = j\Delta y, j = 0,1,2,...,N; z_k = k\Delta z, k = 0,1,2,...,O; t_n = n\Delta t, n = 0,1,2,...,R$; parallel to the space and time coordinate axes, respectively. Approximations $C^n_{i,j,k}$ to $C(i\Delta x, j\Delta y, k\Delta z, n\Delta t)$ are calculated at the point of intersection of these lines, namely, $(i\Delta x, j\Delta y, k\Delta z, n\Delta t)$ which is referred to as the (i,j,k,n) grid point. The constant spatial and temporal grid-spacing are $\Delta x = \frac{L}{M}, \Delta y = \frac{W}{N}, \Delta z = \frac{H}{O}, \Delta t = \frac{T}{R}$, respectively.

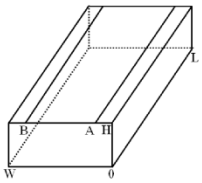

Fig. 5. Model of the Case I.

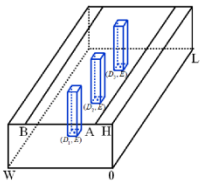

Fig. 6. Model of the Case II.

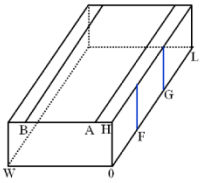

Fig. 7. Model of the Case III.

In this paper, we use an explicit forward-difference approximation for the time-derivative (FT), and central-difference approximations for the space-derivatives (CS). It is called FTCS. The approximate solution of the governing equation uses the finite difference scheme satisfies:

$$\begin{aligned}\frac{C^{n+1}_{i,j,k} - C^n_{i,j,k}}{\Delta t} &+ u\left(\frac{C^n_{i+1,j,k} - C^n_{i-1,j,k}}{2\Delta x}\right) \\ &+ v\left(\frac{C^n_{i,j+1,k} - C^n_{i,j-1,k}}{2\Delta y}\right) \\ = D_h&\left(\frac{C^n_{i+1,j,k} - 2C^n_{i,j,k} + C^n_{i-1,j,k}}{(\Delta x)^2}\right) \\ + D_h&\left(\frac{C^n_{i,j+1,k} - 2C^n_{i,j,k} + C^n_{i,j-1,k}}{(\Delta y)^2}\right) \\ + D_v&\left(\frac{C^n_{i,j,k+1} - 2C^n_{i,j,k} + C^n_{i,j,k-1}}{(\Delta z)^2}\right). \end{aligned} \quad (4)$$

Rearrangement of Eq. (4) gives,

$$C^{n+1}_{i,j,k} = \left(s_x + \frac{r_x}{2}\right) C^n_{i-1,j,k} + \left(s_y + \frac{r_y}{2}\right) C^n_{i,j-1,k}$$

$$+ \quad (s_z)\, C^n_{i,j,k-1} + \left(s_x - \frac{r_x}{2}\right) C^n_{i+1,j,k}$$
$$+ \quad \left(s_y - \frac{r_y}{2}\right) C^n_{i,j+1,k} + (s_z)\, C^n_{i,j,k+1}$$
$$+ \quad (1 - 2s_x - 2s_y - 2s_z)\, C^n_{i,j,k}, \tag{5}$$

in which $r_x = \frac{u\Delta t}{\Delta x}, r_y = \frac{v\Delta t}{\Delta y}, s_x = \frac{D_h \Delta t}{(\Delta x)^2}, s_y = \frac{D_h \Delta t}{(\Delta y)^2}$ and $s_z = \frac{D_v \Delta t}{(\Delta z)^2}$. The stability of this three-dimensional finite difference method may be investigated by using the von Neumann method shows that [2], [12] are stable if both

$$s_x + s_y + s_z \leq \frac{1}{2}, \tag{6}$$

and

$$\frac{r_x^2}{s_x} + \frac{r_y^2}{s_y} \leq 3, \tag{7}$$

are satisfied. The finite difference scheme for the left-hand side $(x = 0)$ and the right-hand side $(x = L)$ as following:

$$\frac{\partial C}{\partial x}(x_0, y_j, z_k) \approx \frac{-3C^n_{0,j,k} + 4C^n_{1,j,k} - C^n_{2,j,k}}{2\Delta x}, \tag{8}$$

$$\frac{\partial C}{\partial x}(x_M, y_j, z_k) \approx \frac{3C^n_{M,j,k} - 4C^n_{M-1,j,k} + C^n_{M-2,j,k}}{2\Delta x}, \tag{9}$$

respectively. In y- and z- directions are obtained in the same way.

IV. Numerical Experiments

In this section, we will show 3 cases as already mentioned in the previous section, i.e. an area under Sky Train of the Bangkok Transit System (BTS). For Case I and Case II, we assume that there is wind inflow only in x-direction. Case II is similar to Case I, but we add the boundary conditions of obstacles in the tunnel. For Case III, we assume that there are wind inflow in x- and y-directions. We consider the length, width and height of tunnel are 192, 26 and 6 meters, respectively. Then, the problem domain is $\Omega = \{(x, y, z); 0 \leq x \leq 192, 0 \leq y \leq 26, 0 \leq z \leq 6\}$.

Case I: for more realistic problem, the parallel gaps along the tunnel between the ceiling and their building of the both sides are added in to the domain. It is assumed that the rate of change are decreased at the parallel gaps and the exit gate. We consider the three-dimensional advection-diffusion equation in Eq. (2) and we assume that $c_1 = 1$, $c_2 = c_3 = -0.01$, $A = 4$, $B = 24$.

The numerical results of Case I are shown in Table I and Figs. 8-11. Fig. 8 and Fig. 9 show the air pollutant concentration levels after passed 30 second in contour plot and surface plot, respectively. Fig. 10 and Fig. 11 show the air pollutant concentration levels after 120 second has passed in contour plot and surface plot, respectively.

Those figures show the numerical solutions in Case I, where $\Delta x = \Delta y = \Delta z = 2$ m; $\Delta t = 0.06$ sec; $D_h = 0.1592$ m^2/sec; $D_v = 0.05$ m^2/sec; $u = 2.7778$m/sec; $v = 0$m/sec; $z = 4$ m. If we take more time into our system, the concentration of pollutant will be reduce as well.

Case II: in reality, there are obstacles such as columns. So, we will add the boundary conditions of obstacles in the tunnel. It is assumed that no rate of change at the columns. We consider the three-dimensional advection-diffusion equation in Eq. (2) and we assume that $c_1 = 1$, $c_2 = c_3 = -0.01$, $A = 4$, $B = 24$, $D_1 = 41$, $D_2 = 101$, $D_3 = 161$, $E = 14$.

The numerical results of Case II are shown in Table II and Figs. 12-15. Fig. 12 and Fig. 13 show the air pollutant concentration levels after passed 30 second in contour plot and surface plot, respectively. Fig. 14 and Fig. 15 show the air pollutant concentration levels after 120 second has passed in contour plot and surface plot, respectively.

Those figures show the numerical solutions in Case II where $\Delta x = \Delta y = \Delta z = 1$ m; $\Delta t = 0.06$ sec; $D_h = 0.1592$ m^2/sec; $D_v = 0.05$ m^2/sec; $u = 2.7778$ m/sec; $v = 0$ m/sec; $z = 4$ m. The results are agreeable, the concentration of pollutant are decreased away from the source.

Case III: in this example, we consider the wind inflow in x- and y-directions. That is, we will add u in x-direction and v in y-direction. We consider the three-dimensional advection-diffusion equation in Eq. (2) and we assume $c_1 = 1$, $c_2 = c_3 = -0.01$, $c_4 = 0.5$, $A = 4, B = 24$, $F = 64$, $G = 129$.

The numerical results of Case III are shown in Table III and Figs. 16-19. Fig. 16 and Fig. 17 show the air pollutant concentration levels after passed 30 second in contour plot and surface plot, respectively. Fig. 18 and Fig. 19 show the air pollutant concentration levels after 120 second has passed in contour plot and surface plot, respectively.

Those figures show the numerical solutions in Case III, where $\Delta x = \Delta y = \Delta z = 2$ m; $\Delta t = 0.06$ sec; $D_h = 0.1592$ m^2/sec; $D_v = 0.05$ m^2/sec; $u = 2.7778$ m/sec; $v = \frac{u}{20}$ m/sec; $z = 4$ m. The results are reasonable, the calculated of pollutant are decreased away from the source.

V. Conclusion

The proposed model can be used to measure air pollutant concentration in a partly opened street tunnel, especially, an area under Bangkok sky train platform. The model is governed by a three-dimensional in space and one-dimensional in time of the advection-diffusion equation. The results from 3 cases can be summarized as follows: if we take a long time, it can be seen that the concentration of air pollutant has decreased even though the distance has increased. That is, the concentration varied with the length of distance. The results are satisfactory because there is no outside air flow. Then, there is the wind inflow only in x-direction from the entrance gate into the tunnel. However, we added obstacles into the tunnel such as the columns along the middle. As results, the concentration of air pollutant has increased, especially the front of columns has a higher concentration than the back of columns. The higher of air pollution comes from the columns. Furthermore, there are the wind inflow in x- and y-directions. We assume that the sources are emitted from the entrance gate and the right side wall gap. It caused the concentration of pollution in the left side wall to be higher than other areas. The boundary conditions are not limited only to constant functions but can be assumed to have several interpolated functions. The proposed explicit finite difference method gives a good agreement and reasonable results. Furthermore, the implicit method that unconditionally stable should be introduced as well.

Acknowledgment

This paper is supported by the Centre of Excellence in Mathematics Program of the Commission on Higher Education (CEM), Thailand. The authors greatly appreciate valuable comments received from the reviewers.

Table. I. The air pollutant concentration for Case I at $z = 4$ m and $T = 30$ sec.

$y(m) \setminus x(m)$	30	60	90	120	150
6	0.8949	0.6173	0.0390	-0.0005	-0.0010
10	0.9278	0.6704	0.0454	-0.0001	-0.0006
14	0.9288	0.6727	0.0460	-0.0000	-0.0004
18	0.9287	0.6724	0.0459	-0.0000	-0.0005
22	0.9229	0.6599	0.0436	-0.0003	-0.0009

Table. II. The air pollutant concentration for Case II at $z = 4$ m and $T = 30$ sec.

$y(m) \setminus x(m)$	30	60	90	120	150
6	0.9435	0.7615	0.0165	-0.0001	-0.0001
10	0.9353	0.6499	0.0131	-0.0000	-0.0000
14	0.8718	0.2665	0.0085	-0.0000	-0.0000
18	0.9432	0.7561	0.0161	-0.0000	-0.0000
22	0.9406	0.7469	0.0152	-0.0003	-0.0003

Table. III. The air pollutant concentration for Case III at $z = 4$ m and $T = 30$ sec.

$y(m) \setminus x(m)$	30	60	90	120	150
6	0.7350	0.3842	0.0936	0.1909	0.2055
10	0.9141	0.6336	0.0417	0.0284	0.0653
14	0.9278	0.6710	0.0451	0.0021	0.0083
18	0.9288	0.6727	0.0460	0.0001	0.0002
22	0.9287	0.6725	0.0458	-0.0001	-0.0006

REFERENCES

[1] R. E. Waller, B. T. Commins and P. J. Lawther, "Air pollution in road tunnels," *Brit. J. industr. Med.*, vol. 18, pp. 250, 1961.

[2] M. Dehghan, "Numerical solution of the three-dimensional advection diffusion equation," *Applied Mathematics and Computation*, vol. 150, pp. 5-19, 2004.

[3] J. V. Lambers, "An explicit, stable, highorder spectral method for the wave equation based on block gaussian quadrature," *IAENG International Journal of Applied Mathematics*, vol. 38, no. 4, pp. 233-248, 2008.

[4] M. Siddique, "Numerical computation of two-dimensional diffusion equation with nonlocal boundary conditions," *IAENG International Journal of Applied Mathematics*, vol. 40, no. 1, pp. 26-31, 2010.

[5] M. Thongmoon, "Numerical experiment of air pollutant concentration in the street tunnel," *International Mathematical Forum*, vol. 10, pp. 449-465, 2010.

[6] N. Pochai, "A finite element solution of the mathematical model for smoke dispersion from two sources," *World Academy of Science, Engineering and Technology*, vol. 60, pp. 1691-1695, 2011.

[7] S. M. Salim and K. C. Ong, "Performance of RANS, URANS and LES in the prediction of airflow and pollutant dispersion," *IAENG Transactions on Engineering Technologies: Lecture Notes in Electrical Engineering*, vol. 170, pp. 263-274, 2013.

[8] S. M. Kwa and S. M. Salim, "Numerical simulation of dispersion in an urban street canyon: comparison between steady and fluctuating boundary conditions," *Engineering Letters*, vol. 23, no.1, pp. 55-64, 2015.

[9] P. Iodice and A. Senatore, "Environmental assessment of a wide area under surveillance with different air pollution sources," *Engineering Letters*, vol. 23, no.3, pp. 156-162, 2015.

[10] S. A. Konglok and N. M. Pochai, "Numerical computations of three-dimensional air-Quality model with variations on atmospheric stability classes and wind velocities using fractional step method," *IAENG International Journal of Applied Mathematics*, vol. 46, no.1, pp. 112-120, 2016.

[11] L. Sun, K. C. Wong, P. Wei, S. Ye, H. Huang, F. Yang, D. Westerdahl, K. K. Louie, W. Y. Luk, and Z. Ning, "Development and application of a next generation air sensor network for the Hong Kong marathon 2015 air quality monitoring," in *Lecture Notes in Engineering and Computer Science: Sensors*, vol. 16, pp. 211, 2016.

[12] A. C. Hindmarsh, P. M. Gresho, and D. F. Griffiths, "The stability of explicit euler time-integration for certain finite difference approximations of the multi-dimensional advection-diffusion equation," in *nt. J. Numer. Methods Fluids*, vol. 4, pp. 853-897, 1984.

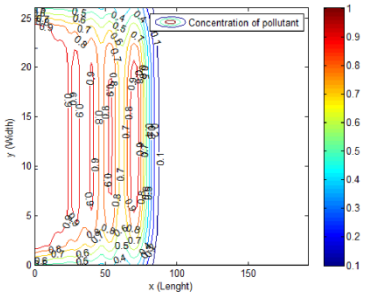

Fig. 8. Contour plot of concentration of air pollutant levels for Case I after passed 30 second.

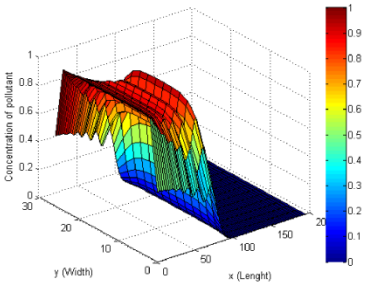

Fig. 9. Surface plot of concentration of air pollutant levels for Case I after passed 30 second.

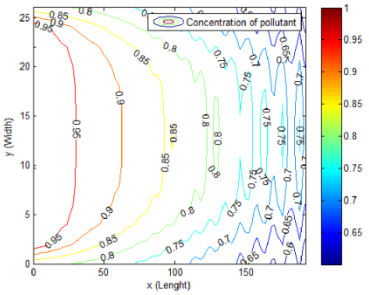

Fig. 10. Contour plot of concentration of air pollutant levels for Case I after passed 120 second.

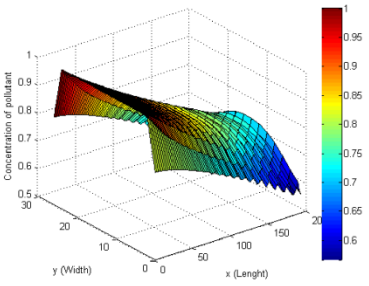

Fig. 11. Surface plot of concentration of air pollutant levels for Case I after passed 120 second.

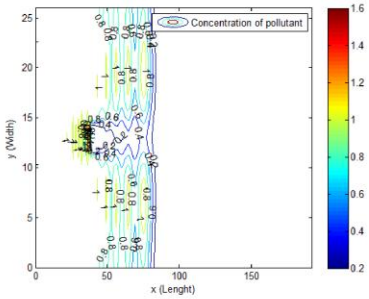

Fig. 12. Contour plot of concentration of air pollutant levels for Case II after passed 30 second.

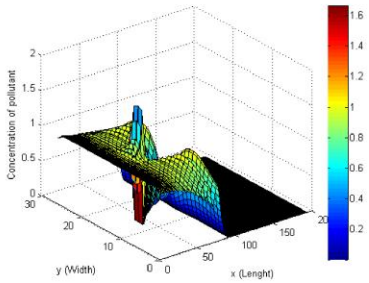

Fig. 13. Surface plot of concentration of air pollutant levels for Case II after passed 30 second.

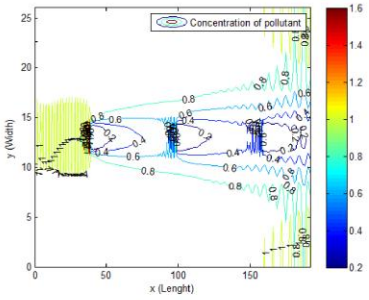

Fig. 14. Contour plot of concentration of air pollutant levels for Case II after passed 120 second.

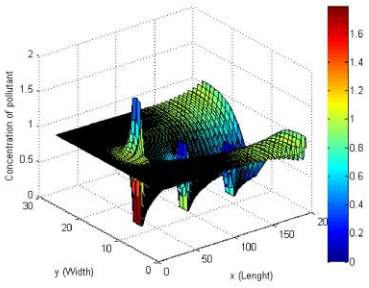

Fig. 15. Surface plot of concentration of air pollutant levels for Case II after passed 120 second.

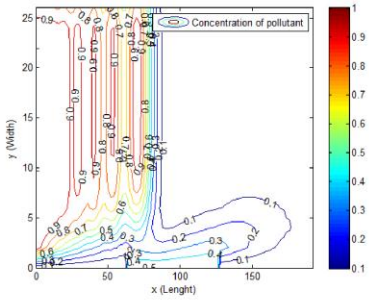

Fig. 16. Contour plot of concentration of air pollutant levels for Case III after passed 30 second.

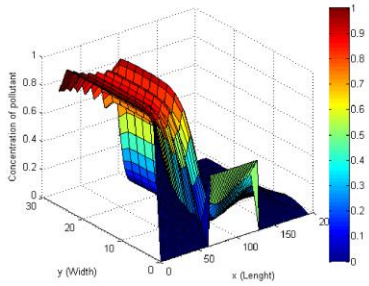

Fig. 17. Surface plot of concentration of air pollutant levels for Case III after passed 30 second.

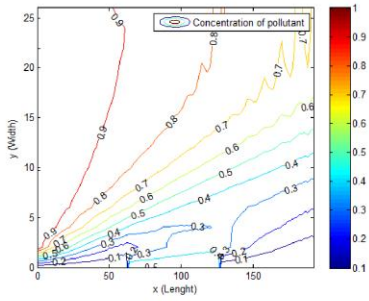

Fig. 18. Contour plot of concentration of air pollutant levels for Case III after passed 120 second.

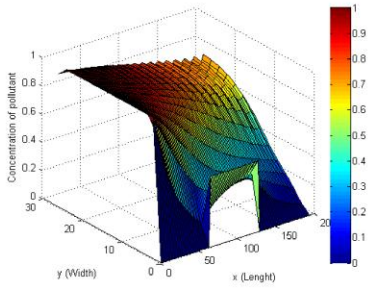

Fig. 19. Surface plot of concentration of air pollutant levels for Case III after passed 120 second.

Hindawi
Abstract and Applied Analysis
Volume 2018, Article ID 9025851, 10 pages
https://doi.org/10.1155/2018/9025851

Research Article

Numerical Simulation for a Three-Dimensional Air Pollution Measurement Model in a Heavy Traffic Area under the Bangkok Sky Train Platform

Kewalee Suebyat[1,2] **and Nopparat Pochai**[1,2]

[1]*Department of Mathematics, Faculty of Science, King Mongkut's Institute of Technology Ladkrabang, Bangkok 10520, Thailand*
[2]*Centre of Excellence in Mathematics, Commission on Higher Education (CHE), Si Ayutthaya Road, Bangkok 10400, Thailand*

Correspondence should be addressed to Nopparat Pochai; nop_math@yahoo.com

Received 10 October 2017; Accepted 1 February 2018; Published 5 March 2018

Academic Editor: Felix Sadyrbaev

Copyright © 2018 Kewalee Suebyat and Nopparat Pochai. This is an open access article distributed under the Creative Commons Attribution License, which permits unrestricted use, distribution, and reproduction in any medium, provided the original work is properly cited.

Air pollutant levels in Bangkok are generally high in street tunnels. They are particularly elevated in almost closed street tunnels such as an area under the Bangkok sky train platform with high traffic volume where dispersion is limited. There are no air quality measurement stations in the vicinity, while the human population is high. In this research, the numerical simulation is used to measure the air pollutant levels. The three-dimensional air pollution measurement model in a heavy traffic area under the Bangkok sky train platform is proposed. The finite difference techniques are employed to approximate the modelled solutions. The vehicle air pollutant emission due to the high traffic volume is mathematically assumed by the pollutant sources term. The simulation is also considered in averaged and moving pollutant sources due to manner vehicle emission. The proposed approximated air pollutant concentration indicators can be replaced by user required gaseous pollutants indices such as NOx, SO2, CO, and PM2.5.

1. Introduction

Nowadays if we are talking about pollution, surely one of the pollution sources that we face and have a big effect on society is "air pollution." Air pollution does not only affect one society but also the problem for human life and environment that everyone all over the world should realize. Air pollution is harmful to human health because it releases pollutants and dirty air which caused asthma, lungs, and cancer. Moreover, it is a major factor which affects environmental resources as well as human-made structures and facilities and contributes to climate change.

Sources of air pollution can be classified into two types which are natural sources and artificial sources. Natural sources of pollution come from natural phenomena such as volcanic eruptions, forest fires, biological decay, pollen grains, marshes, and radioactive materials. On the other hand, artificial sources are those created by human beings such as thermal power plants, vehicular emissions, fossil fuel burning, and agricultural activities. Air pollution can occur in many forms but in general it occurs in the form gas and particulate contaminants which are in our atmosphere. Gaseous pollutants include carbon monoxide (CO), nitrogen oxides (NOx), sulfur dioxide (SO2), ozone (O3), and various gaseous.

Some people might wonder if indoor or outdoor air is more polluted. According to studies of scientists, indoor air pollution is often more harmful than outdoor air pollution, especially because we spend most of the time per day indoor inside our home or office. The air inside our homes and offices can sometimes be much more polluted compared to outdoor air and thus presents a major health threat. In their latest study, the British scientists measured air quality inside and outside three residential buildings with different types of energy use. What they found was that the levels of one of the most common air pollutants, nitrogen dioxide (NO2), in kitchens in the city center apartments with gas cookers were as much as three times higher than the levels measured outdoors and well above clean air quality standards.

In [1], also in October 2016, more than 140 countries reached an agreement to reduce the use of these chemicals which are used in air conditioners and refrigerators and to find greener alternatives over time. David Doniger, director of NRDC's Climate and Clean Air program, wrote, "NRDC estimates that the agreed HFC phase-down will avoid the equivalent of more than 80 billion tons of CO2 over the next 35 years." Moreover, Walke said, "make good choices about transportation. When you can walk, ride a bike, or take public transportation. For driving, choose cars that get better miles per gallon of gas or choose an electric car." The sources of smog and soot are similar. Walke said, "both come from cars and trucks, factories, power plants, incinerators, engines." So, a wise decision is encouraged to make our world green.

In 1961, [2] studied the pollution of the air (smoke, polycyclic hydrocarbons, carbon monoxide, and lead) by motor vehicles in two London road tunnels. It was found that the concentration of air pollution in the tunnels does not appear to be high but the effect of traffic on the concentration of smoke, polycyclic hydrocarbons, carbon monoxide, and lead in the air of city streets deserves continued study. In 2002, [3] studied average air pollutant concentration during weekdays and found it to be higher than during the weekend. The test result showed that the average air pollutant concentrations for the three urban sites are noticeably higher than the suburban site. Our analysis revealed that an obvious way to reduce the build-up of pollutant concentration on Bangkok streets would be to speed up the flow of traffic and prevent long periods of idling in congested streets. In 2004, [4] studied the stability conditions for several different numerical techniques which were developed and compared for solving the three-dimensional advection-diffusion equation with constant coefficient. The results of a numerical experiment were presented, and the accuracy and central processor time needed were discussed and compared. In 2006, [5] studied the numerical methods for solving the advection-diffusion equation. It was solved by using cubic splines to estimate first and second derivatives and also by solving the same problem using two standard finite difference schemes (the FTCS and Crank-Nicolson methods). The numerical results were compared with analytical solutions. It was found that, for the examples studied, the finite difference methods yielded better pointwise solutions than the spline methods. In 2016, [6] studied the three-dimensional air quality model. The considered domain was divided into two zones: a factory zone and a residential zone. The modifications of the atmospheric stability classes and wind velocities from multiple point sources were also analyzed by using the three-dimensional fractional step method. In 2017, [7] studied a three-dimensional advection-diffusion equation by using the explicit forward difference method. The wind inflows are considered in two cases: there is wind inflow only in x-direction and there are wind inflow in x-direction and y-direction. Moreover, we added the obstacles along the middle into the tunnel. The results of the model are satisfactory.

Currently in Bangkok, Thailand, air pollution from car exhaust on the street, which contains particulates, especially from old cars or diesel cars, is harmful to people's health. Scientists are concerned that the particulates carrying toxic chemicals, such as nitrous oxide and carbon monoxide, when deeply in haled, can be harmful to people's health. Bangkok Transit System (BTS) provides an effective route of urban transport for Bangkok people because BTS facilitates speed and convenience for transportation. The major source of air pollution under Bangkok sky train platform comes from vehicle exhaust, mobile source, and others sources including smoke from restaurants, construction, and building demolition. Therefore, it is also causing some of the environmental impacts, especially the air pollutant impact to the vicinity area around its platform with high traffic and large amount of people.

These days, an increasing in population caused heavy traffic and air pollution on the road. Air pollution around the platform in an area under BTS platform has increased dramatically. So, if we know the value of the concentration of pollution that is likely to occur from the existing pollution accumulation or may be from sources of emissions, such as from car smoke, we might be able to control the concentration of air pollution in that area not to exceed the standard. As already mentioned, we recognized the importance of air pollution. Therefore, the purpose of this research is to approximate the concentration of air pollutant in the area under the Bangkok sky train platform with moving air pollutant sources by heavy traffic of vehicles in different time by using the finite difference technique. It can help control the pollutant from the traffic and crowded people in this area. It will be beneficial to human and environment. However, this area should be implemented into the wind inflow directions near the tunnel because it affects the concentration of air pollutant. Then the wind inflow directions are an important factor of the model. So, we distinguish two cases: there is wind inflow only in x-direction and there is wind inflow in x- and y-directions.

2. Governing Equation

A street tunnel is a place for foot or vehicular road traffic, where the street is flanked by buildings on both sides, including the top area that is also closed. The street tunnel configuration is shown in Figure 1. An overhead part of the street is the sky train platform and both sides of the street are composed of sections of building. In this research, the simulation of configuration of street tunnel is divided into two cases.

Case 1. Assume that the wind is flowing only in x-direction. The considered street tunnel is illustrated in Figure 2(a). The wind direction field is shown in Figure 2(b).

Case 2. Assume that the wind is flowing in x- and y-directions. The considered street tunnel is illustrated in Figure 3(a). The wind direction field is shown in Figure 3(b).

The considered domain is restricted by $\Omega = \{(x, y, z);\ 0 \le x \le L,\ 0 \le y \le W,\ 0 \le z \le H\}$, where W is the platform width (m), L is the platform length (m), and H is the platform height (m) over the street tunnel.

Figure 1: The street tunnel configuration.

The air pollutant concentration can be described by a three-dimensional advection-diffusion equation as follows:

$$\frac{\partial C}{\partial t} + V \cdot \nabla C = \nabla \cdot \left(\overline{K} \otimes \nabla C\right) + R\left(x, y, z, t\right), \quad (1)$$

where $C = C(x, y, z, t)$ is the air pollutant concentration at point (x, y, z) in Cartesian coordinates and at time t (kg/m^3). The vector V is the wind velocity field (m/sec); $\overline{K}$ is the eddy-diffusivity or dispersion tensor (m^2/sec). $\nabla = (\partial/\partial x)\vec{i} + (\partial/\partial y)\vec{j} + (\partial/\partial z)\vec{k}$, $\otimes$ is matrix multiplication, and $R(x, y, z, t)$ describes sources or sinks of air pollutants (sec^{-1}).

If the wind velocity and diffusion coefficient of pollutant are constant, the governing equation becomes

$$\frac{\partial C}{\partial t} + u\frac{\partial C}{\partial x} + v\frac{\partial C}{\partial y} + w\frac{\partial C}{\partial z} = k_x\frac{\partial^2 C}{\partial x^2} + k_y\frac{\partial^2 C}{\partial y^2} + k_z\frac{\partial^2 C}{\partial z^2} + R\left(x, y, z, t\right), \quad (2)$$

where u, v, and w are the constant wind velocity (m/sec) in x, y, and z-directions, respectively, and k_x, k_y, and k_z are the constant diffusion coefficient (m^2/sec) in x, y, and z-directions, respectively.

By the assumption, we assumed that the wind inflow is along the horizontal direction and the dispersion is horizontally isotropic. Consequently, the three-dimensional advection-diffusion equation in (2) can be written as

$$\frac{\partial C}{\partial t} + u\frac{\partial C}{\partial x} + v\frac{\partial C}{\partial y} = k_h\frac{\partial^2 C}{\partial x^2} + k_h\frac{\partial^2 C}{\partial y^2} + k_v\frac{\partial^2 C}{\partial z^2} + R\left(x, y, z, t\right), \quad (3)$$

where k_h is a constant dispersion coefficient in the horizontal direction (m^2/sec) and k_v is a constant dispersion coefficient in the z-direction (vertical) (m^2/sec) with the appropriate initial and boundary conditions.

We consider the components of the tunnel in Figure 4 and the model of the problem is divided into three zones as shown in Figure 5. The potential air pollutant concentration can be described by $C(x, y, z, 0) = f(x, y, z)$, for all $(x, y, z) \in \Omega$. The boundary conditions are as follows:

Entrance gate: $C(0, y, z, t) = c_{N_1}$, $0 < y < W$, $0 < z < H$.

Margin of entrance gate: $(\partial C/\partial x)(0, y, z, t) = c_{N_2}$, $y = 0, W, z = 0, H$.

Exit gate: $(\partial C/\partial x)(L, y, z, t) = c_X$.

Both side walls: $(\partial C/\partial y)(x, 0, z, t) = c_{W_1}$, $(\partial C/\partial y)(x, W, z, t) = c_{W_2}$.

Ground: $(\partial C/\partial z)(x, y, 0, t) = c_F$.

Platform ceiling: $(\partial C/\partial z)(x, y, H, t) = c_T$, $A < y < B$.

Ceiling parallel gaps: $(\partial C/\partial z)(x, y, H, t) = c_{G_1}$, $0 \le y \le A$, $(\partial C/\partial z)(x, y, H, t) = c_{G_2}$, $B \le y \le W$,

where c_{N_1} is the inflow air pollutant concentration at the entrance gate. c_{N_2}, c_X, c_{W_1}, c_{W_2}, c_F, c_T, c_{G_1}, c_{G_2} are the average rate of change of air pollutant concentration at the margin of entrance gate, exit gate, both side walls, ground, platform ceiling, and both ceiling parallel gaps, respectively. A is the distance from the right wall to the right-ended platform ceiling; see in Figure 5. B is also the distance from the right wall to the left-ended platform ceiling; see in Figure 5.

3. Numerical Techniques

The finite difference method is used to approximate the solutions to the governing equation. The domain Ω is divided by $x_i = i\Delta x$, $i = 0, 1, 2, \ldots, M$; $y_j = j\Delta y$, $j = 0, 1, 2, \ldots, N$; $z_k = k\Delta z$, $k = 0, 1, 2, \ldots, P$; $t_n = n\Delta t$, $n = 0, 1, 2, \ldots, Q$ over three spaces and time coordinate axes, respectively. The approximated air pollutant concentration at point $(i\Delta x, j\Delta y, k\Delta z, n\Delta t)$ is denoted by $C^n_{i,j,k} = C(i\Delta x, j\Delta y, k\Delta z, n\Delta t)$ at the grid point (i, j, k, n). The constant spatial and temporal grid spacing are $\Delta x = L/M$, $\Delta y = W/N$, $\Delta z = H/P$, $\Delta t = T/Q$, respectively.

In this research, an explicit forward time central space (FTCS) method is employed. Consequently, the finite difference equation to (3) becomes

$$\begin{aligned}
&\frac{C^{n+1}_{i,j,k} - C^n_{i,j,k}}{\Delta t} + u\left(\frac{C^n_{i+1,j,k} - C^n_{i-1,j,k}}{2\Delta x}\right) \\
&\quad + v\left(\frac{C^n_{i,j+1,k} - C^n_{i,j-1,k}}{2\Delta y}\right) \\
&= D_h\left(\frac{C^n_{i+1,j,k} - 2C^n_{i,j,k} + C^n_{i-1,j,k}}{(\Delta x)^2}\right) \\
&\quad + D_h\left(\frac{C^n_{i,j+1,k} - 2C^n_{i,j,k} + C^n_{i,j-1,k}}{(\Delta y)^2}\right) \\
&\quad + D_v\left(\frac{C^n_{i,j,k+1} - 2C^n_{i,j,k} + C^n_{i,j,k-1}}{(\Delta z)^2}\right) + (\Delta t)\, R^n_{i,j,k}.
\end{aligned} \quad (4)$$

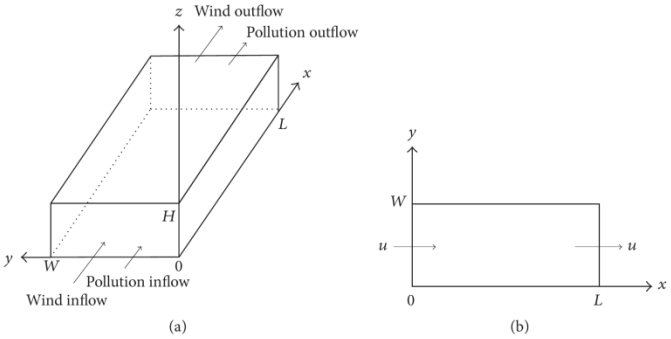

Figure 2: (a) The domain for street tunnel (Case 1). (b) The wind direction (Case 1).

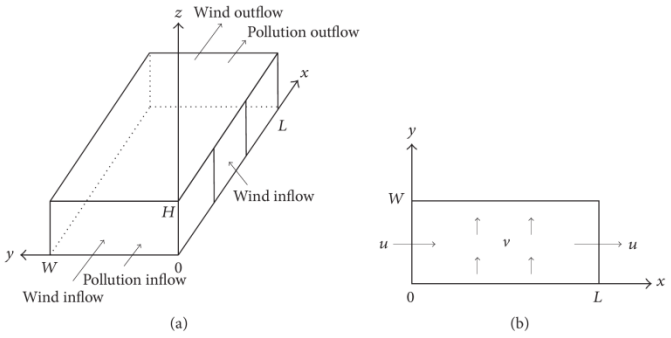

Figure 3: (a) The domain for street tunnel (Case 2). (b) The wind direction (Case 2).

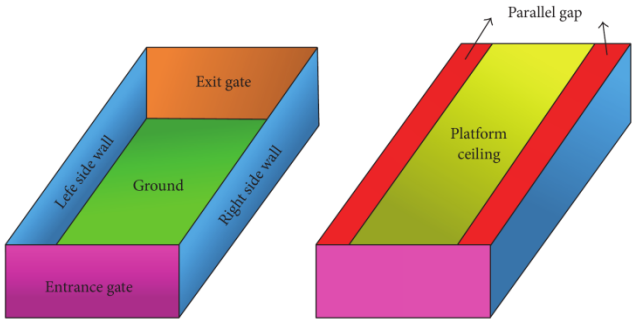

Figure 4: Components of the tunnel.

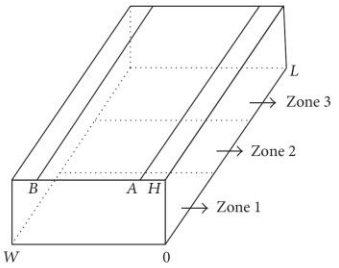

FIGURE 5: Model of the problem.

Rearrangement of (4) gives

$$\begin{aligned} C_{i,j,k}^{n+1} &= \left(s_x + \frac{r_x}{2}\right) C_{i-1,j,k}^{n} + \left(s_y + \frac{r_y}{2}\right) C_{i,j-1,k}^{n} \\ &+ \left(s_z\right) C_{i,j,k-1}^{n} + \left(s_x - \frac{r_x}{2}\right) C_{i+1,j,k}^{n} \\ &+ \left(s_y - \frac{r_y}{2}\right) C_{i,j+1,k}^{n} + \left(s_z\right) C_{i,j,k+1}^{n} \\ &+ \left(1 - 2s_x - 2s_y - 2s_z\right) C_{i,j,k}^{n} + (\Delta t)\, R_{i,j,k}^{n}, \end{aligned} \tag{5}$$

in which $r_x = u\Delta t/\Delta x$, $r_y = v\Delta t/\Delta y$, $s_x = D_h\Delta t/(\Delta x)^2$, $s_y = D_h\Delta t/(\Delta y)^2$, and $s_z = D_v\Delta t/(\Delta z)^2$.

The stability condition of the proposed finite difference scheme, which can be investigated by using the von Neumann method [4, 8], is stable if both

$$\begin{aligned} s_x + s_y + s_z &\le \frac{1}{2} \\ \frac{r_x^2}{s_x} + \frac{r_y^2}{s_y} &\le 3, \end{aligned} \tag{6}$$

are satisfied.

The finite difference scheme for the left end and the right end of the fictitious points is as follows:

$$\begin{aligned} \frac{\partial C}{\partial x}\left(x_0, y_j, z_k, t_n\right) &\approx \frac{-3C_{0,j,k}^{n} + 4C_{1,j,k}^{n} - C_{2,j,k}^{n}}{2\Delta x} = c_{N_2}, \\ \frac{\partial C}{\partial y}\left(x_i, y_0, z_k, t_n\right) &\approx \frac{-3C_{i,0,k}^{n} + 4C_{i,1,k}^{n} - C_{i,2,k}^{n}}{2\Delta y} = c_{W_1}, \\ \frac{\partial C}{\partial z}\left(x_i, y_i, z_0, t_n\right) &\approx \frac{-3C_{i,j,0}^{n} + 4C_{i,j,1}^{n} - C_{i,j,2}^{n}}{2\Delta z} = c_F, \\ \frac{\partial C}{\partial x}\left(x_M, y_j, z_k, t_n\right) &\approx \frac{3C_{M,j,k}^{n} - 4C_{M-1,j,k}^{n} + C_{M-2,j,k}^{n}}{2\Delta x} \\ &= c_X, \\ \frac{\partial C}{\partial y}\left(x_i, y_N, z_k, t_n\right) &\approx \frac{3C_{i,N,k}^{n} - 4C_{i,N-1,k}^{n} + C_{i,N-2,k}^{n}}{2\Delta y} \\ &= c_{W_2}, \\ \frac{\partial C}{\partial z}\left(x_i, y_j, z_P, t_n\right) &\approx \frac{3C_{i,j,P}^{n} - 4C_{i,j,P-1}^{n} + C_{i,j,P-2}^{n}}{2\Delta z} = c_T \\ &= c_{G_2} = c_{G_2}. \end{aligned} \tag{7}$$

4. Numerical Experiments

In this section, there are three simulations of released air pollutant phenomena demonstrated by using the finite difference in (5). In all simulations, the air is flowing along the x-direction from the entrance to the exit gates. There are two parallel gaps along the celling; see Figures 1 and 4. There is no potential ambient air pollution. There are two buildings that were bracing the areas as well; see Figures 1 and 4. All of building walls are nonabsorbing air pollution materials. Since there is no potential air pollution, the initial condition is assumed by $f(x, y, z) = 0$.

For three cases, the experimented area has dimensions such that the length, width, and height are 192, 26, and 6 meters, respectively. Then, the simulated domain is defined by $\Omega = \{(x, y, z);\ 0 \le x \le 192,\ 0 \le y \le 26,\ 0 \le z \le 6\}$. We assume that $c_{N_1} = 1$, $c_{W_1} = c_{W_2} = c_F = c_T = 0$, $c_X = c_{G_1} = c_{G_2} = -0.01$, $A = 4$, and $B = 24$. When we consider the model of problem as shown in Figure 5, $0 \le x < 64$, $64 \le x \le 128$, and $128 < x \le 192$ are zones 1, zones 2, and zones 3, respectively. For the grid spacing, $\Delta x = \Delta y = \Delta z = 2$ m, $z = 4$ m, and $\Delta t = 0.06$ s, and for the time, $T = 30$ s. We choose the diffusion coefficient in x- and z-direction as 0.1592 and 0.05 m^2/sec, respectively, with diffusion coefficient in x- and y-direction being equal. The wind velocity in x- and y-direction is 2.7778 and 0 m/sec, respectively.

Simulation A (source or sink emissions are averaged). In this example, we consider two cases. In the first case, R is the constant of source ($R > 0$), which are 0.001, 0.004, and 0.007 sec^{-1}. In the second case, R is the constant of sink ($R < 0$), which are −0.001, −0.004, and −0.007 sec^{-1}. The results of Simulation A are shown in Figures 6–11 and 22-23.

Simulation B (source or sink emissions are moving). In this example, we consider two cases. In the first case, R is the function of source and sink ($R > 0$, $R < 0$), that is, $0.001\sin(xt)$, $0.003\sin(xt)$, and $0.005\sin(xt)$ sec^{-1}. In the second case, R is the function of source ($R > 0$), which are $0.001|\sin(xt)|$, $0.003|\sin(xt)|$, and $0.005|\sin(xt)|$ sec^{-1}. The results of Simulation B are shown in Figures 12–17 and 24.

Simulation C (source or sink emissions are mixed). In this example, we divided R into 3 zones. That is, R_1, R_2, and R_3 are sources of zone 1, zone 2, and zone 3, respectively. We consider three cases when R is the constant of source. In the first case, R is little and gradually increases, which are $R_1 = 0.01$, $R_2 = 0.03$, and $R_3 = 0.05$ sec^{-1}. In the second case, R is the highest at the middle zone, which is $R_1 = 0.03$, $R_2 = 0.05$, and $R_3 = 0.03$ sec^{-1}. In the last case, R in zone 1 is the highest and gradually decreases, which are $R_1 = 0.05$, $R_2 = 0.03$, and $R_3 = 0.01$ sec^{-1}. The results of Simulation C are shown in Figures 18–21 and 25.

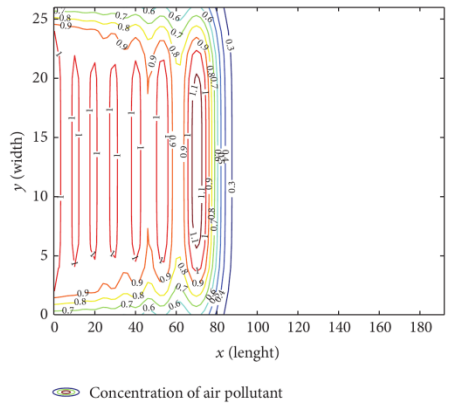

Figure 6: Contour plot of concentration of air pollutant levels for $R = 0.007\ \text{sec}^{-1}$.

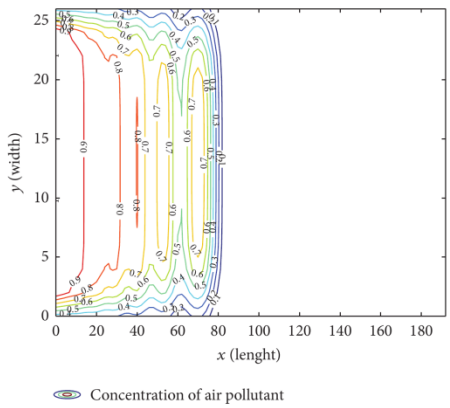

Figure 9: Contour plot of concentration of air pollutant levels for $R = -0.007\ \text{sec}^{-1}$.

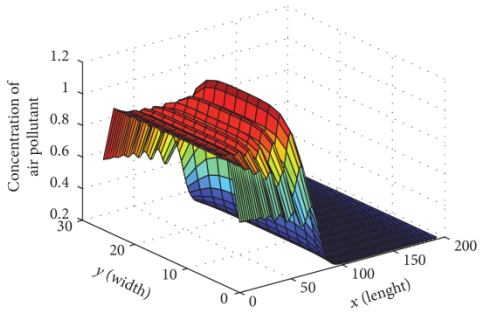

Figure 7: Surface plot of concentration of air pollutant levels for $R = 0.007\ \text{sec}^{-1}$.

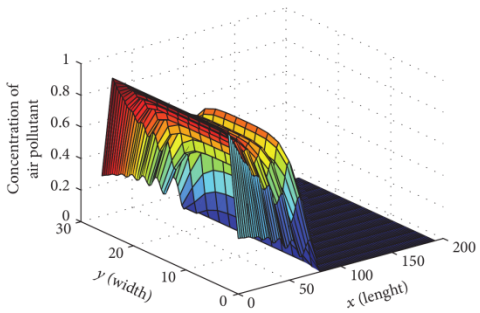

Figure 10: Surface plot of concentration of air pollutant levels for $R = -0.007\ \text{sec}^{-1}$.

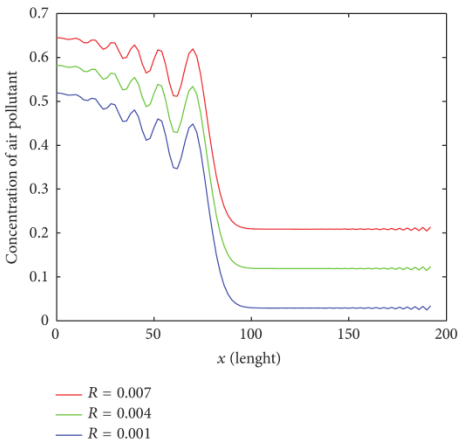

Figure 8: Compare the concentration of air pollutant where $R = 0.001$, $R = 0.004$, and $R = 0.007\ \text{sec}^{-1}$.

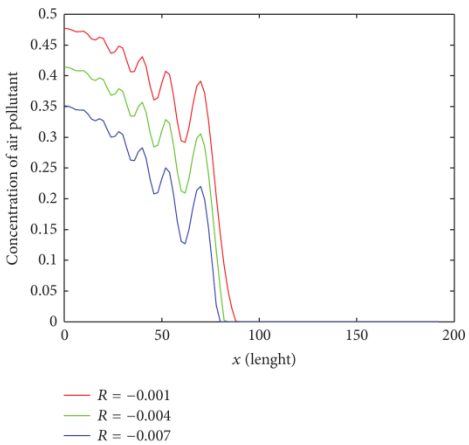

Figure 11: Compare the concentration of air pollutant where $R = -0.001$, $R = -0.004$, and $R = -0.007\ \text{sec}^{-1}$.

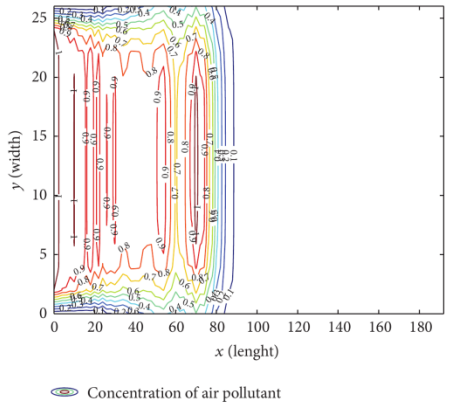

Figure 12: Contour plot of concentration of air pollutant levels for $R = 0.001\sin(xt)$ sec^{-1}.

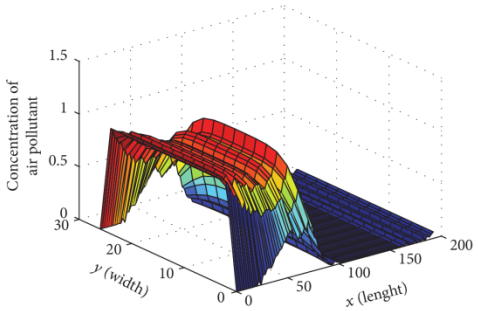

Figure 13: Surface plot of concentration of air pollutant levels for $R = 0.001\sin(xt)$sec^{-1}.

5. Discussion

The air pollutant concentrations are calculated by using a finite difference technique. Whether sources or sinks, it affected the air pollutant concentrations. The comparison of sources or sinks for Simulations A, B, and C are shown in Table 1. Figures 6-7 and 9-10 show the air pollutant concentration levels after passing 30 seconds in contour plot and surface plot between $R = 0.007$ (source) and $R = -0.007$ (sink), respectively. Figures 8 and 11 compare the air pollutant concentration levels where R is the constant in first case and second case of Simulation A, respectively. From the results, if we take more source rate into our system, we can see that the concentration of air pollutant levels has increased (see Figure 8). Therefore, the concentration varied with the sources. Furthermore, the sink can lower the concentration of air pollutant levels (see Figure 11). Furthermore, Figures 12-13 and 15-16 show the air pollutant concentration levels after passing 30 seconds in contour plot and surface plot between

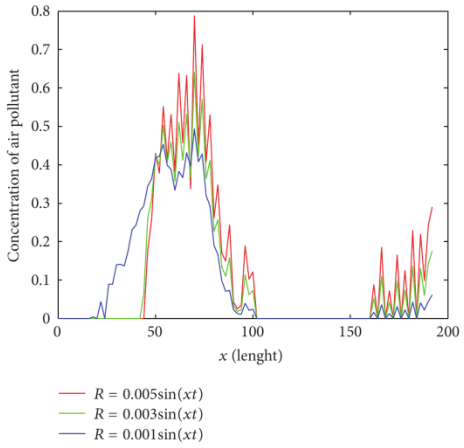

Figure 14: Compare the concentration of air pollutant where $R = 0.001\sin(xt)$, $R = 0.003\sin(xt)$, and $R = 0.005\sin(xt)$ sec^{-1}.

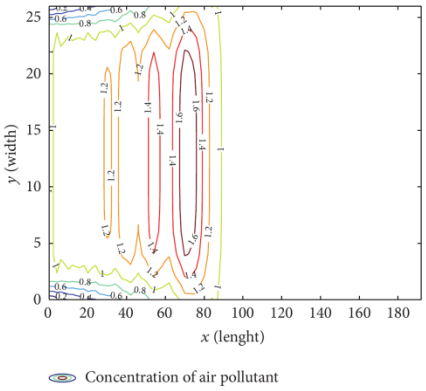

Figure 15: Contour plot of concentration of air pollutant levels for $R = 0.003|\sin(xt)|$ sec^{-1}.

$R = 0.001\sin(xt)$ (source-sink) and $R = 0.003|\sin(xt)|$ (source), respectively. Figures 14 and 17 compare the air pollutant concentration levels where R is the constant in the first case and second case of Simulation B, respectively. As a result, R is a function of both source and sink and the concentration of air pollutant has increased and decreased (see Figure 14). That is, it is increased when R is the source. On the other hand, if R is sink, the concentration of air pollutant has decreased. Moreover, Figures 18–20 show the air pollutant concentration levels after passing 30 seconds in surface plot where R is the constant in first, second, and third cases of Simulation C, respectively. Figure 21

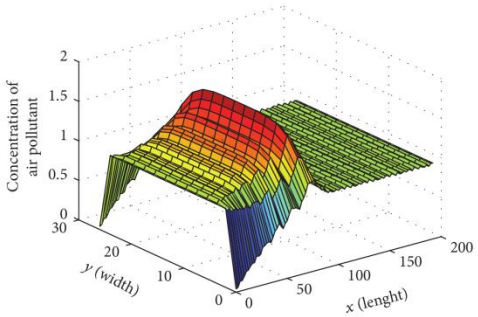

FIGURE 16: Surface plot of concentration of air pollutant levels for $R = 0.003|\sin(xt)|\ \sec^{-1}$.

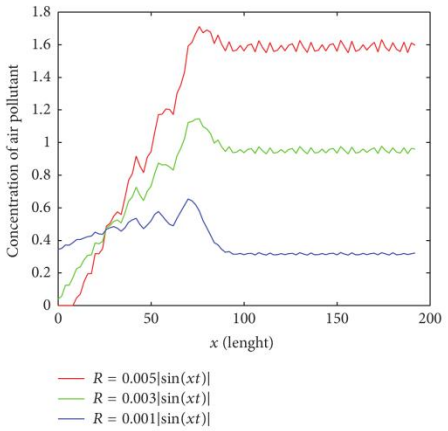

FIGURE 17: Compare the concentration of air pollutant where $R = 0.001|\sin(xt)|$, $R = 0.003|\sin(xt)|$, and $R = 0.005|\sin(xt)|\ \sec^{-1}$.

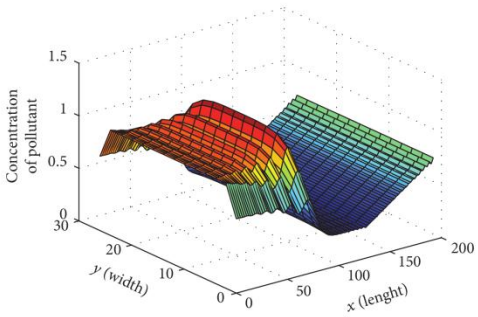

FIGURE 18: Surface plot of concentration of air pollutant levels for $R_1 = 0.01$, $R_2 = 0.03$, and $R_3 = 0.05\ \sec^{-1}$.

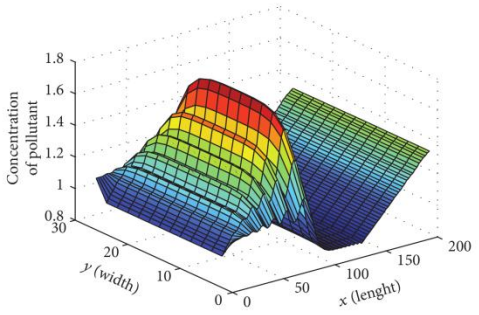

FIGURE 19: Surface plot of concentration of air pollutant levels for $R_1 = 0.03$, $R_2 = 0.05$, and $R_3 = 0.03\ \sec^{-1}$.

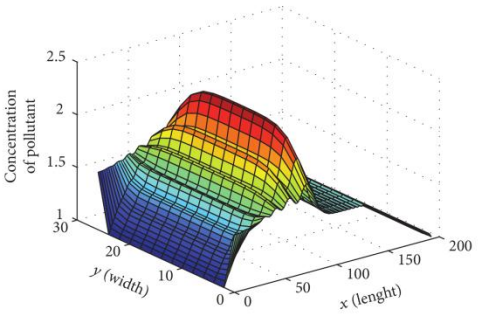

FIGURE 20: Surface plot of concentration of air pollutant levels for $R_1 = 0.05$, $R_2 = 0.03$, and $R_3 = 0.01\ \sec^{-1}$.

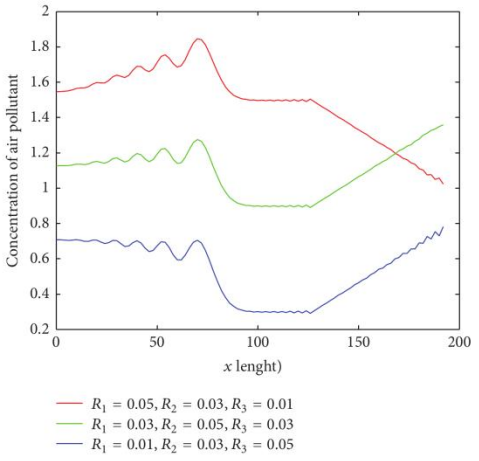

FIGURE 21: Compare the concentration of air pollutant where R_1, R_2, and R_3 are difference of three cases.

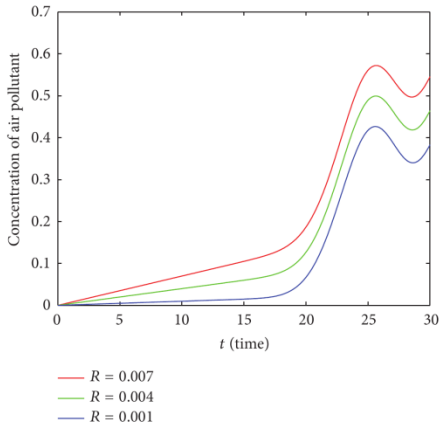

Figure 22: Compare the concentration of air pollutant at $x = 60$ m, $y = 14$ m, $z = 4$ m of sources in different time.

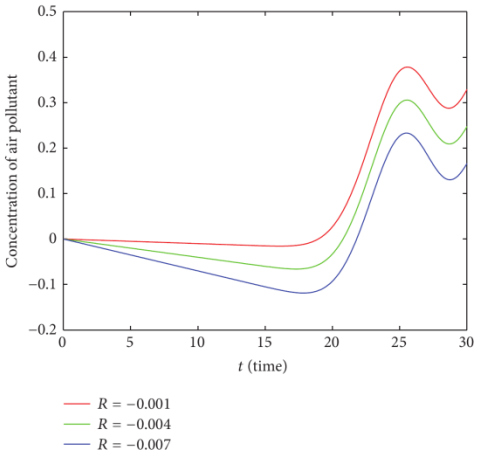

Figure 23: Compare the concentration of air pollutant at $x = 60$ m, $y = 14$ m, $z = 4$ m of sinks in different time.

compares the air pollutant concentration levels of three cases in Simulation C. As a result, it can be concluded that if we add a large quantity of source at the beginning, it affects the concentration of pollutants. Therefore, the source is the cause of high concentration of air pollutant. Moreover, Figures 22–25 compared the concentration of air pollutant at $x = 60$ m, $y = 14$ m, $z = 4$ m in different time of sources, sinks, moving sources (vehicle sources), and 3 averaged zone sources, respectively.

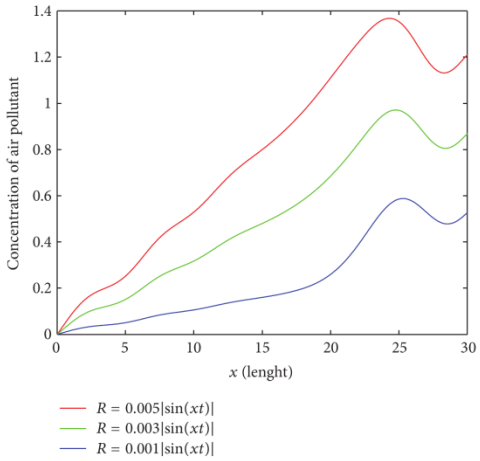

Figure 24: Compare the concentration of air pollutant at $x = 60$ m, $y = 14$ m, $z = 4$ m of moving sources (vehicle sources) in different time.

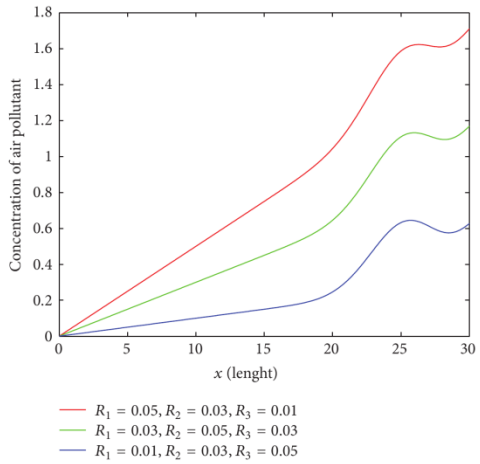

Figure 25: Compare the concentration of air pollutant at $x = 60$ m, $y = 14$ m, $z = 4$ m of 3 averaged zone sources in different time.

6. Conclusion

The released vehicles air pollutant can be assumed by source functions. The source functions are defined by many methods such as averaged collected data methods or numerical interpolations. The simulations show that the air pollution problems arise by external and internal vehicles that released

Table 1: Comparison of sources or sinks for Simulations A, B, and C.

Simulation–Cases	R_1 $0 \le x < 64$	R_2 $64 \le x \le 128$	R_3 $128 < x \le 192$
A-1.1	0.001	0.001	0.001
A-1.2	0.004	0.004	0.004
A-1.3	0.007	0.007	0.007
A-2.1	−0.001	−0.001	−0.001
A-2.2	−0.004	−0.004	−0.004
A-2.3	−0.007	−0.007	−0.007
B-1.1	$0.001\sin(xt)$	$0.001\sin(xt)$	$0.001\sin(xt)$
B-1.2	$0.004\sin(xt)$	$0.004\sin(xt)$	$0.004\sin(xt)$
B-1.3	$0.007\sin(xt)$	$0.007\sin(xt)$	$0.007\sin(xt)$
B-2.1	$0.001\lvert\sin(xt)\rvert$	$0.001\lvert\sin(xt)\rvert$	$0.001\lvert\sin(xt)\rvert$
B-2.2	$0.004\lvert\sin(xt)\rvert$	$0.004\lvert\sin(xt)\rvert$	$0.004\lvert\sin(xt)\rvert$
B-2.3	$0.007\lvert\sin(xt)\rvert$	$0.007\lvert\sin(xt)\rvert$	$0.007\lvert\sin(xt)\rvert$
C-1	0.01	0.03	0.05
C-2	0.03	0.05	0.03
C-3	0.05	0.03	0.01

air pollution. We can see that, under the platform area, air pollutant level is higher than the outside level due to air flow obstacle.

Conflicts of Interest

The authors declare no conflicts of interest.

Acknowledgments

This paper is supported by the Centre of Excellence in Mathematics Program of the Commission on Higher Education (CEM), Thailand.

References

[1] J. Mackenzie, "Air pollution: Everything you need to know," *Natural Resources Defense Council*.

[2] R. E. Waller, B. T. Commins, and P. J. Lawther, "Air pollution in road tunnels," *British Journal of Industrial Medicine*, vol. 18, p. 250, 1961.

[3] S. T. Leong, S. Muttamara, and P. Laortanakul, "Air pollution and traffic measurements in Bangkok streets," *Asian J. Energy Environ*, vol. 3, pp. 185–213, 2002.

[4] M. Dehghan, "Numerical solution of the three-dimensional advection-diffusion equation," *Applied Mathematics and Computation*, vol. 150, no. 1, pp. 5–19, 2004.

[5] M. Thongmoon and R. McKibbin, "A comparison of some numerical methods for the advection-diffusion equation," *Research Letters in the Information and Mathematical Sciences*, vol. 10, pp. 49–62, 2006.

[6] S. A. Konglok and N. Pochai, "Numerical computations of three-dimensional air-quality model with variations on atmospheric stability classes and wind velocities using fractional step method," *IAENG International Journal of Applied Mathematics*, vol. 46, no. 1, pp. 112–120, 2016.

[7] K. Suebyat and N. Pochat, "A numerical simulation of a three-dimensional air quality model in an area under a Bangkok sky train platform using an explicit finite difference scheme," *IAENG International Journal of Applied Mathematics*, vol. 47, pp. 471–476.

[8] A. C. Hindmarsh and P. M. Gresho, "The stability of explicit Euler time-integration for certain finite difference approximations of the multidimensional advection-diffusion equation," *International Journal for Numerical Methods in Fluids*, vol. 4, no. 9, pp. 853–897, 1984.

ITALIAN JOURNAL OF PURE AND APPLIED MATHEMATICS – N. 40–2018 (615–632) 615

THREE-DIMENSIONAL AIR QUALITY ASSESSMENT SIMULATIONS INSIDE SKY TRAIN PLATFORM WITH AIRFLOW OBSTACLES ON HEAVY TRAFFIC ROAD

Kewalee Suebyat

Nopparat Pochai

Department of Mathematics
Faculty of Science
King Mongkut's Institute of Technology Ladkrabang
Bangkok 10520
Thailand
and
Centre of Excellence in Mathematics
Commission on Higher Education (CHE)
Si Ayutthaya Road, Bangkok 10400
Thailand
kew26_tan@hotmail.com
nop_math@yahoo.com

Abstract. Air pollutant levels in Bangkok are generally high in street tunnels. They are particularly elevated in almost closed street tunnels such as an area the Bangkok sky train platform with high traffic volume where dispersion is limited. This area has no air quality measurement stations even though there is a high percentage of people living around this vicinity. We are interested to conduct a research the Bangkok sky train platform due to the traffic density and enormous polluted areas. Therefore, we proposed a numerical modeling of air pollution concentration in sky train platform with airflow obstacles on heavy traffic road as an approximated solution of the three-dimensional advection-diffusion equation by using the finite difference methods. Our research presentation is based on how air pollution model depends on the flow of air pollution and wind directions including the governing equation of the corresponding three-dimensional advection-diffusion equation is presented. This also includes the initial condition and boundary conditions of traffic and polluted areas. In order to illustrate the performance of the model, the numerical experiments are presented. The comparison between the two methods and the simulations of air pollution control are proposed. The three-dimensional advection-diffusion equation is solved by using the Forward Time, Centered Space (FTCS) and Forward Time, Backward Space (FTBS) schemes. The results obtained indicate that the FTCS method provides a better result than FTBS method. Furthermore, the proposed experimental variations of the boundary condition in the entrance gate do affect the air pollutant concentration of each floor.

Keywords: air pollutant concentration, finite difference techniques, air quality, heavy traffic, sky train platform, tunnel.

1. Introduction

Currently, Thailand is facing a rapid growth in both agriculture and industry resulting in Bangkok being the center of prosperity in all aspects with rapid population increase in a blink of an eye, followed by a high demand for travel and transportation. This creates an intensifying traffic congestion and air pollution that derives from the rapid increase of cars and vehicles. Air pollution is one of the main and biggest problems and Bangkok has reached a critical level with hazardous substances in some areas because pollution is created by human beings and natural phenomena damaging the environment and human well-being. Not only is air pollution hazardous locally but it is one of the world's biggest killers and issue because people faced health problems such as asthma, bronchitis, cancer, etc. If people are constantly exposed to high levels of dust, they may suffer from illnesses such as silicosis or asbestosis. So it can be said that air pollution from traffic is tremendously serious especially a Bangkok sky train platform than any other areas. The volume of carbon monoxide and nitrogen oxides in this area is higher than the standard volume. This issue should be realized for the study interest and further research to find solutions to reduce pollution.

In [1], the Kriging method for regression analysis can be used to analytically relate the mass emission rate of carbon monoxide and nitrogen dioxide at the Bangkok Mass Transit System (BTS). The results indicate that the concentration of carbon monoxide exceed the Bangkok standard volume and the concentration of nitrogen dioxide does not exceed the Bangkok standard volume. Undeniably, the air pollutant concentration was related to the traffic flow pattern, traffic characteristic, street geometries, and human activities. The traffic flow is the main pollution source in many urban areas. It causes more ambient air pollutants such as carbon monoxide (CO), sulfur dioxide (SO2), nitrogen dioxide (NO2), nitrogen oxides (NOx), volatile organic compounds (VOCs), ozone (O3), particulate matter (PM10), benzene, heavy metals, and respirable particulate matter (PM2.5 and PM10) [2, 3, 4]. Therefore, 1D Lighthill-Whitham-Richards traffic model and advection-diffusion-reaction pollution model for estimating the pollution emission rate due to traffic flow in big cities are proposed in [3]. The modeling of oxidation and hydrolysis of sulfur and nitrogen oxide used the convection-diffusion-reactions equation for higher order accurate solutions. The technique of Lax and Wendroff is introduced in [5]. A three-dimensional advection-diffusion equation of air pollutant is applied to a street tunnel configuration by using the FTCS finite difference method with air flow in x and y directions in [6]. In [7], a one-dimensional advection-diffusion equation with variable coefficients in semi-infinite media [8] is solved using explicit finite difference method for three dispersion problems: (i) solute dispersion along the

steady flow, (ii) temporarily dependent solute dispersion along the uniform flow, and (iii) solute dispersion is temporarily dependent on the steady flow through inhomogeneous medium to find solutions. A study of vehicle exhaust dispersion within different street canyons models in urban ventilated by cross-wind by using the advanced computational and mathematical models. The pollutant concentrations are estimated for the street canyon models, which may include simplified photochemistry and particle deposition-suspension algorithms. After application of Box model to the street canyon. [9] can be calculated for CO, NOx, SPM, and PM10 by this box model. In [10], the effects of the variations of atmospheric stability classes and wind velocities on the three-dimensional air-quality models are observed. The fractional step method is used to solve the dispersion model for advection-diffusion equation.

In this research, we are interested in traffic density of the area the Bangkok sky train platform. We proposed the numerical modeling of air pollutant concentration in sky train platform with airflow obstacles on heavy traffic road. The estimated three-dimensional advection-diffusion equation is used by the finite difference method. In our research, we indicate that the air pollution modeling depends on air pollution flows and wind directions. In the second section, the governing equation corresponding to the model is the three-dimensional advection-diffusion equation including the initial condition and boundary conditions. The third section is numerical techniques. The finite difference technique introduced two methods for calculating the air pollutant concentration. The three-dimensional advection-diffusion equation is solved by using the Forward Time, Centered Space (FTCS) and Forward Time, Backward Space (FTBS) schemes. In order to illustrate the performance of the model, in section 4 the numerical experiments are presented. This is the comparisons between the two methods and the simulations of the proposed air pollution control. Finally, the discussion and conclusion are presented in section 5.

2. Governing equation

The street tunnel configuration is shown in Figure 1. That is, the street is flanked by buildings on both sides, including the top area is also closed. The bottom floor is the street floor, next up is the ticket floor and the top floor is the platform floor. For both sides of the street are the section of buildings. In this research, we assume that there are wind inflow in x- and y-directions and there are the obstacles as columns. The columns are on both sides of the street tunnel. The air pollutant concentrations are emitted from the entrance gate and the right side gap as Figure 2(a). We consider the wind inflow along x- and y-directions as Figure 2(b). Then the consider domain becomes : $\Omega = \{(x, y, z); 0 \leq x \leq L, 0 \leq y \leq W, 0 \leq z \leq H\}$, where W is the width (m), L is the length (m) and H is the height (m) of the street tunnel.

Figure 1: The street tunnel configuration.

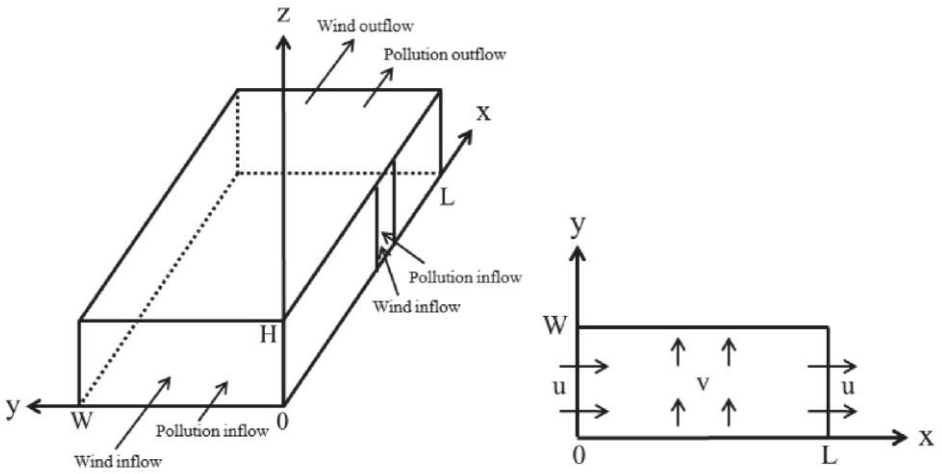

Figure 2: (a) The direction of pollution and wind flows. (b) The wind directions for street tunnel.

The air pollutant concentrations can be described by the three-dimensional advection-diffusion equation as follows:

$$\frac{\partial C}{\partial t} + V \cdot \nabla C = \nabla \cdot \left(\bar{K} \otimes \nabla C \right), \tag{1}$$

where $C = C(x, y, z, t)$ is the air pollutant concentration at point (x, y, z) in Cartesion coordinates at time t (kg/m^3), $\nabla = \frac{\partial}{\partial x}\vec{i} + \frac{\partial}{\partial y}\vec{j} + \frac{\partial}{\partial z}\vec{k}$, and $\otimes$ is matrix multiplication. The vector V is the wind velocity field (m/sec), $\bar{K}$ is the eddy-diffusivity or dispersion tensor (m^2/sec).

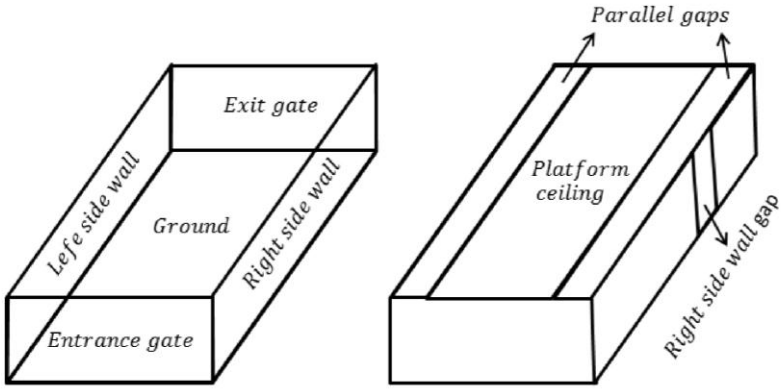

Figure 3: The components of the street tunnel.

The three-dimensional advection-diffusion equation in Eq. (1), can be written as

$$\frac{\partial C}{\partial t} + u\frac{\partial C}{\partial x} + v\frac{\partial C}{\partial y} + w\frac{\partial C}{\partial z} = k_x\frac{\partial^2 C}{\partial x^2} + k_y\frac{\partial^2 C}{\partial y^2} + k_z\frac{\partial^2 C}{\partial z^2}, \tag{2}$$

where u, v, and w are the constant wind velocity (m/sec) in x, y, and z-directions, respectively, k_x, k_y, and k_z are the constant diffusion coefficient (m^2/sec) in x, y, and z-directions, respectively.

The assumptions of Eq. (2) are defined that the wind inflow in x- and y-directions are the horizontal direction and in z-direction is the vertical direction. Consequently, the three-dimensional advection-diffusion equation in Eq. (2), can be written as:

$$\frac{\partial C}{\partial t} + u\frac{\partial C}{\partial x} + v\frac{\partial C}{\partial y} = k_h\frac{\partial^2 C}{\partial x^2} + k_h\frac{\partial^2 C}{\partial y^2} + k_v\frac{\partial^2 C}{\partial z^2}, \tag{3}$$

where k_h is the constant dispersion coefficient in the horizontal direction (m^2/sec) and k_v is the constant dispersion coefficient in the vertical direction (m^2/sec).

We consider the components of the street tunnel shown in Figure 3. Figure 4 shows the model of the problem with A is the right parallel gap size along the ceiling, B is the left parallel gap size along the ceiling and $G - F$ is the right side wall gap of the beside consider domain. (D_{cn}, E_{rn}) is a center point of the columns for $cn = 1, 2, ..., ncl$ and $rn = 1, 2$, where ncl is the number of the columns. The initial condition, there is no initial pollutant $C(x, y, z, 0) = 0$, for all $(x, y, z) \in \Omega$. For the boundary conditions are assumed that

Entrance gate : $C(0, y, z, t) = c_1$.
Margin of entrance gate : $\frac{\partial C}{\partial x}(0, y, z, t) = c_2, y = 0, W, z = 0, H$.
Exit gate : $\frac{\partial C}{\partial x}(L, y, z, t) = c_3$.
Left side wall : $\frac{\partial C}{\partial y}(x, W, z, t) = c_4$.
Right side wall gap : $C(x, 0, z, t) = c_5, F \leq x \leq G$.

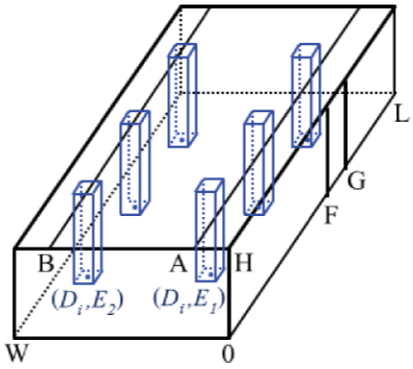

Figure 4: Model of the problem.

Right side wall : $\frac{\partial C}{\partial y}(x,0,z,t) = c_6$, otherwise.

Ground : $\frac{\partial C}{\partial z}(x,y,0,t) = c_7$.

Platform ceiling : $\frac{\partial C}{\partial z}(x,y,H,t) = c_8, A < y < B$.

Parallel gaps : $\frac{\partial C}{\partial z}(x,y,H,t) = c_9$, otherwise.

Center columns : $C(D_{cn}, E_{rn}, z, t) = 0, 0 \leq z \leq H$.

Front and back columns : $\frac{\partial C}{\partial x}(D_{cn} - 1, y, z, t) = \frac{\partial C}{\partial x}(D_{cn} + 1, y, z, t) = c_1 0, E_{rn} - 1 \leq y \leq E_{rn} + 1$, for all $t > 0$.

Left and right columns: $\frac{\partial C}{\partial y}(x, E_{rn} - 1, z, t) = \frac{\partial C}{\partial y}(x, E_{rn} + 1, z, t) = c_1 1, D_{cn} - 1 \leq x \leq D_{cn} + 1$, for all $t > 0$.
Where c_1 and c_5 are the air pollutant concentration inflow in $x-$ and $y-$ directions, respectively, $c_2, c_3, c_4, c_6, c_7, c_8, c_9, c_{10}$, and c_{11} are the rate of change of air pollutant concentration in each the boundary conditions.

3. Numerical techniques

We use the finite difference methods to compute a numerical approximation to the solutions of a three-dimensional advection-diffusion equation. The solution domain of the problem over time $0 \leq t \leq T$ is covered by a mesh of grid spacing: $x_i = i\Delta x, i = 0, 1, 2, ..., M; y_j = j\Delta y, j = 0, 1, 2, ..., N; z_k = k\Delta z, k = 0, 1, 2, ..., P; t_n = n\Delta t, n = 0, 1, 2, ..., Q$; parallel to the space and time coordinate axes, respectively. Approximation the solution of the air pollutant concentration $C^n_{i,j,k}$ to $C(i\Delta x, j\Delta y, k\Delta z, n\Delta t)$ are calculated at the point of intersection of these lines, namely, $(i\Delta x, j\Delta y, k\Delta z, n\Delta t)$ which is referred to as the (i, j, k, n) grid point. The constant spatial and temporal grid-spacing are $\Delta x = \frac{L}{M}, \Delta y = \frac{W}{N}, \Delta z = \frac{H}{P}, \Delta t = \frac{T}{Q}$, respectively. In this research, we distinguish two difference methods as following:

3.1 Forward time central space scheme

The first method, we use an explicit forward difference estimate for the time derivative (FT), and central difference approximations for the space derivative (CS), so the acronym FTCS. Consequently, the three-dimensional advection-diffusion equation in Eq. (3) becomes

$$\frac{C_{i,j,k}^{n+1}-C_{i,j,k}^{n}}{\Delta t}+u\left(\frac{C_{i+1,j,k}^{n}-C_{i-1,j,k}^{n}}{2\Delta x}\right)+v\left(\frac{C_{i,j+1,k}^{n}-C_{i,j-1,k}^{n}}{2\Delta y}\right)$$

$$=D_h\left(\frac{C_{i+1,j,k}^{n}-2C_{i,j,k}^{n}+C_{i-1,j,k}^{n}}{(\Delta x)^2}\right)+D_h\left(\frac{C_{i,j+1,k}^{n}-2C_{i,j,k}^{n}+C_{i,j-1,k}^{n}}{(\Delta y)^2}\right)$$

$$+D_v\left(\frac{C_{i,j,k+1}^{n}-2C_{i,j,k}^{n}+C_{i,j,k-1}^{n}}{(\Delta z)^2}\right). \tag{4}$$

Rearrangement and simplification of Eq. (4),

$$\begin{aligned} C_{i,j,k}^{n+1} &= \left(s_x+\frac{r_x}{2}\right)C_{i-1,j,k}^{n}+\left(s_y+\frac{r_y}{2}\right)C_{i,j-1,k}^{n}+(s_z)\,C_{i,j,k-1}^{n} \\ &+ \left(s_x-\frac{r_x}{2}\right)C_{i+1,j,k}^{n}+\left(s_y-\frac{r_y}{2}\right)C_{i,j+1,k}^{n}+(s_z)\,C_{i,j,k+1}^{n} \\ &+ (1-2s_x-2s_y-2s_z)\,C_{i,j,k}^{n}, \end{aligned} \tag{5}$$

in which $r_x=\frac{u\Delta t}{\Delta x}, r_y=\frac{v\Delta t}{\Delta y}, s_x=\frac{D_h\Delta t}{(\Delta x)^2}, s_y=\frac{D_h\Delta t}{(\Delta y)^2}$ and $s_z=\frac{D_v\Delta t}{(\Delta z)^2}$.

The finite difference scheme for the left end and the right end of the fictitious points are following:

$$C_{-1,j,k}^{n}=\frac{4C_{0,j,k}^{n}-C_{1,j,k}^{n}-2c_2\Delta x}{3}, \tag{6}$$

$$C_{i,-1,k}^{n}=\frac{4C_{i,0,k}^{n}-C_{i,1,k}^{n}-2c_6\Delta y}{3}, \tag{7}$$

$$C_{i,j,-1}^{n}=\frac{4C_{i,j,0}^{n}-C_{i,j,1}^{n}-2c_7\Delta z}{3}, \tag{8}$$

$$C_{M+1,j,k}^{n}=\frac{4C_{M,j,k}^{n}-C_{M-1,j,k}^{n}+2c_3\Delta x}{3}, \tag{9}$$

$$C_{i,N+1,k}^{n}=\frac{4C_{i,N,k}^{n}-C_{i,N-1,k}^{n}+2c_4\Delta y}{3}, \tag{10}$$

$$C_{i,j,P+1}^{n}=\frac{4C_{i,j,P}^{n}-C_{i,j,P-1}^{n}+2c_8\Delta z}{3}. \tag{11}$$

3.2 Forward time backward space scheme

The second method, we calculated by using an explicit forward difference estimate for the time derivative (FT), and backward difference approximations for the space derivative (BS), so the acronym FTBS. The approximate solution of a

three-dimensional advection-diffusion equation in Eq. (3) use the FTCS scheme satisfies

$$\frac{C_{i,j,k}^{n+1}-C_{i,j,k}^{n}}{\Delta t}+u\left(\frac{C_{i,j,k}^{n}-C_{i-1,j,k}^{n}}{2\Delta x}\right)+v\left(\frac{C_{i,j,k}^{n}-C_{i,j-1,k}^{n}}{2\Delta y}\right)$$

$$=D_h\left(\frac{C_{i,j,k}^{n}-2C_{i-1,j,k}^{n}+C_{i-2,j,k}^{n}}{(\Delta x)^2}\right)+D_h\left(\frac{C_{i,j,k}^{n}-2C_{i,j-1,k}^{n}+C_{i,j-2,k}^{n}}{(\Delta y)^2}\right)$$

$$+D_v\left(\frac{C_{i,j,k}^{n}-2C_{i,j,k-1}^{n}+C_{i,j,k-2}^{n}}{(\Delta z)^2}\right). \tag{12}$$

Rearrangement and simplification of Eq. (12),

$$\begin{aligned} C_{i,j,k}^{n+1} &= (s_x)\,C_{i-2,j,k}^{n}+(s_y)\,C_{i,j-2,k}^{n}+(s_z)\,C_{i,j,k-2}^{n} \\ &+ (r_x-2s_x)\,C_{i-1,j,k}^{n}+(r_y-2s_y)\,C_{i,j-1,k}^{n}-(2s_z)\,C_{i,j,k-1}^{n} \\ &+ (1+s_x+s_y+s_z-r_x-r_y)\,C_{i,j,k}^{n}. \end{aligned} \tag{13}$$

The finite difference scheme for the left end of the fictitious points are following:

$$C_{-1,j,k}^{n}=\frac{4C_{0,j,k}^{n}-C_{1,j,k}^{n}-2c_2\Delta x}{3}, \tag{14}$$

$$C_{-2,j,k}^{n}=\frac{13C_{0,j,k}^{n}-4C_{1,j,k}^{n}-14c_2\Delta x}{9}, \tag{15}$$

$$C_{i,-1,k}^{n}=\frac{4C_{i,0,k}^{n}-C_{i,1,k}^{n}-2c_6\Delta y}{3}, \tag{16}$$

$$C_{i,-2,k}^{n}=\frac{13C_{i,0,k}^{n}-4C_{i,1,k}^{n}-14c_6\Delta y}{9}, \tag{17}$$

$$C_{i,j,-1}^{n}=\frac{4C_{i,j,0}^{n}-C_{i,j,1}^{n}-2c_7\Delta z}{3}, \tag{18}$$

$$C_{i,j,-2}^{n}=\frac{13C_{i,j,0}^{n}-4C_{i,j,1}^{n}-14c_7\Delta z}{9}. \tag{19}$$

4. Numerical experiments

4.1 Comparison between FTCS and FTBS solutions in sky train platform on a single

In this section, we describe about a comparision of some numerical methods for solving the three-dimensional advection-diffusion equation. There are two methods. These are forward time central space (FTCS) and forward time backward space (FTBS). We consider the domain as a single layer as shown in Figure 4 that the length(L), width(W) and height(H) of tunnel are 198, 21 and 28 meters, respectively. Then, the problem domain is $\Omega=\{(x,y,z);0\le x\le 198,0\le y\le 21,0\le z\le 28\}$. We assume that $\Delta x=\Delta y=\Delta z=2$ m, $\Delta t=0.06$ sec,

$T = 2$ min, $u = 0.5$ m/sec, $v = 0$ m/sec, $D_h = D_v = 0.001$ m^2/sec, $c_1 = 0.5$, $c_3 = c_9 = -0.01$, $c_2 = c_4 = c_5 = c_6 = c_7 = c_8 = c_{10} = c_{11} = 0$, $A = 4$, $B = 17$, and $ncl = 9$. Figures 6 and 7 are solved by various methods. These are FTCS and FTBS methods, respectively. The solutions of air pollutant concentration by using the FTCS method in Eq. (5) are shown in Figure 6. This figure show about contour and surface plots of air pollutant concentration levels after 2 minutes passed. You can be seen that the maximum value of air pollutant concentration is 0.6 kg/m^3. Furthermore, the contour and surface plots of air pollutant concentration levels after 2 minutes passed for solutions of air pollutant concentration by using the FTBS method in Eq. (13) are shown in Figure 7. The maximum value of air pollutant concentration in Figure 7 is 0.5 kg/m^3.

The approximations of air pollutant concentration for FTCS and FTBS methods are compared in Figure 11. We choose $\Delta x = \Delta y = \Delta z = 2$ m, $\Delta t = 0.06$ sec, $T = 30$ sec, $u = 0.1$ m/sec, $v = 0$ m/sec, $D_h = D_v = 0.001$ m^2/sec, $c_1 = 0.5$, $c_3 = c_9 = -0.01$, $c_2 = c_4 = c_5 = c_6 = c_7 = c_8 = c_{10} = c_{11} = 0$, $A = 4$, $B = 17$ and $ncl = 9$. It can be seen that the trend of results from both methods in the same way. How do you know which one is better? The idea is to find out the method whether we will change the grid-spacing, the solution is stable. Table. 1 shows the stable of FTCS and FTBS approximate solutions. You can be seen that if we choose $\lambda = \gamma = 0.03$, and $\lambda = 0.06$ then the solution of the FTBS method are unstable but the FTCS method is stable. Consequently, the FTCS method gives better than the FTBS method.

4.2 Numerical simulations of air pollutant assessment in sky train platform on triple layers

In this section, explicit forward time and central space (FTCS) scheme have been presented. We distinguish three scenarios of released air pollutant phenomenons demonstrated by using the finite difference in Eq. (5). In all scenarios, the air pollutant concentration is flowing along the x and y-directions, these are constants or functions. In addition, there are two parallel gaps along the ceiling, the rate of change are decreased at the parallel gaps. Moreover, both sides were flanked by buildings. All of the building walls are non-absorbing air pollution materials, there is no rate of change.

For three scenarios, we consider the length, width and height of tunnel are 198, 21 and 28 meters, respectively. Then, the problem domain is $\Omega = \{(x, y, z); 0 \leq x \leq 198, 0 \leq y \leq 21, 0 \leq z \leq 28\}$, when $0 \leq z < 9, 9 \leq z < 22, 22 \leq z \leq 28$ are street floor, ticket floor and platform floor, respectively, see in Figure 5. We consider c_1 in the boundary condition in the entrance gate of each floor, we distinguish 3 scenarios in the consider domain as follows:

4.2.1 Scenario A : Air pollutant flowing into the street floor

If we consider BTS station area, we will see that the street floor has a lot of cars. This causes heavy traffic, as a result air pollution is higher than other

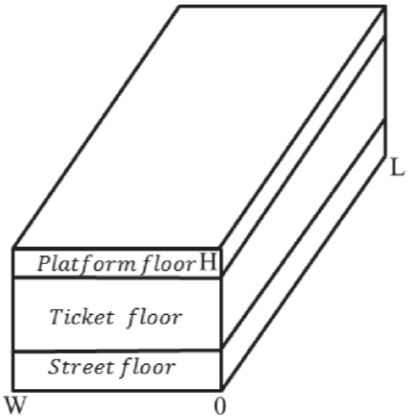

Figure 5: The problem domain.

floors. Therefore, we assumed the air pollutant concentration at the entrance gate of the street floor is constant. However, ticket floor and platform floor are assumed that the pollution cannot be reached. So, we assumed that there is no rate of change of air pollutant concentration at the entrance gate of the ticket and platform floors. Therefore, c_1 in the boundary condition of all 3 floors as follows:

Street floor : $c_1 = 0.5$.
Ticket floor : $c_1 = \frac{\partial C}{\partial x} = 0$.
Platform floor : $c_1 = \frac{\partial C}{\partial x} = 0$.

The problem domain is $\Omega = \{(x, y, z); 0 \leq x \leq 198, 0 \leq y \leq 21, 0 \leq z < 9\}$. The grid spacing: $\Delta x = \Delta y = \Delta z = 1$ m, $\Delta t = 0.06$ sec and for the time $T = 2$ min. We assume: $c_3 = c_9 = -0.01$, $c_5 = 0.2$, $c_2 = c_4 = c_6 = c_7 = c_8 = c_{10} = c_{11} = 0$, $A = 4$, $B = 17$, $F = 125$, $G = 135$ and $ncl = 9$. The wind velocity and diffusion coefficient are taken to be $u = 2.7778, v = u/20$ m/sec and $D_h = 0.1592, D_v = 0.05$ m^2/sec. Therefore, the results of ScenarioA for three different floors are shown in Figure 8. That is, in Figures 8(a), 8(c) and 8(e) show the contour plot of the air pollutant concentration levels for street, ticket and platform floors, respectively. Meanwhile, the surface plot of the air pollutant concentration levels for street, ticket and platform floors are shown in Figures 8(b), 8(d) and 8(f), respectively. It can be seen from Figure 8 that the air pollutant concentration in the platform floor is very low. It comes from only the pollution on the right side wall gap. So, the air pollution on platform floor is less than 0.2 kg/m^3. The air pollutant concentration of Scenario A with the different floors are shown in Figure 12(a).

4.2.2 Scenario B : Air pollutant flowing into every floors

In reality, we noticed that the air pollutant concentration depends on the height of the tunnel, so if the height increases, the air pollutant concentration will be

less. Thus, the air pollutant concentration at the entrance gate for the street floor, ticket floor and platform floor can be described as different decreasing functions varied with the height of the tunnel. Therefore, c_1 in the boundary condition of all 3 floors as follows:

Street floor : $c_1 = 0.5 - 0.02z$.

Ticket floor : $c_1 = 0.32 - 0.015z$.

Platform floor : $c_1 = 0.01 - 0.005z$.

The problem domain is $\Omega = \{(x, y, z); 0 \leq x \leq 198, 0 \leq y \leq 21, 9 \leq z < 22\}$. The grid spacing: $\Delta x = \Delta y = \Delta z = 1$ m, $\Delta t = 0.06$ sec and for the time $T = 2$ min. We assume: $c_3 = c_9 = -0.01$, $c_5 = 0.2$, $c_2 = c_4 = c_6 = c_7 = c_8 = c_{10} = c_{11} = 0$, $A = 4$, $B = 17$, $F = 125$, $G = 135$ and $ncl = 9$. We choose $u = 2.7778, v = u/20$ m/sec, $D_h = 0.1592, D_v = 0.05$ m^2/sec. So, the results of Scenario B for three different floors are shown in Figure 9. That is, in Figures 9(a), 9(c) and 9(e) show the contour plot of the air pollutant concentration levels for street, ticket and platform floors, respectively. Meanwhile, the surface plot of the air pollutant concentration levels for street, ticket and platform floors are shown in Figures 9(b), 9(d) and 9(f), respectively. As the results, the air pollution continues to be released as the decreasing functions but gradually decreases. Therefore, the air pollution in three floors of this scenario is higher especially, the air pollutant concentration on the street floor is as high as 0.7 kg/m^3. The air pollutant concentration of Scenario B with the different floors are shown in Figure 12(b).

4.2.3 Scenario C : Air pollutant flowing through the street floor and their gaps

The air pollutant concentration on the street floor is assumed to be a constant. Furthermore, for more realism, we can see that the air pollutant concentration from the previous floor impact on the next floor. So we will define the pollution of the next floor by applying the principle of average. That is the air pollutant concentration at the entrance of the next floor is the average of air pollutant concentration of gaps on the previous floor. Therefore, c_1 in the boundary condition of all 3 floors as follows:

Street floor : $c_1 = 0.5$.

Ticket floor : $c_1 = c_{avS}$.

Platform floor : $c_1 = c_{avT}$,

where c_{avS} and c_{avT} are the average of air pollutant concentration of gaps on the street floor and ticket floor, respectively.

The problem domain is $\Omega = \{(x, y, z); 0 \leq x \leq 198, 0 \leq y \leq 21, 22 \leq z \leq 28\}$. The grid spacing: $\Delta x = \Delta y = \Delta z = 1$ m, $\Delta t = 0.06$ sec and for the time $T = 2$ min. We assume: $c_3 = c_9 = -0.01$, $c_5 = 0.2$, $c_2 = c_4 = c_6 = c_7 = c_8 = c_{10} = c_{11} = 0$, $A = 4$, $B = 17$, $F = 125$, $G = 135$ and $ncl = 9$. We choose $u = 2.7778, v = u/20$ m/sec, $D_h = 0.1592, D_v = 0.05$ m^2/sec. So, the results of Scenario C for three different floors are shown in Figure 10. That is, in Figures

10(a), 10(c) and 10(e) show the contour plot of the air pollutant concentration levels for street, ticket and platform floors, respectively. Meanwhile, the surface plot of the air pollutant concentration levels for street, ticket and platform floors are shown in Figures 10(b), 10(d) and 10(f), respectively. It can also be obtained by Figure 13 that the air pollutant concentration gradually decreases because we bring the value of the previous floor to the next floor. So, the pollution on the platform floor is least the pollution than other floors as 0.5 kg/m^3. The air pollutant concentration of Scenario C with the different floors are shown in Figure 12(c).

5. Discussion and conclusion

In this research, the air pollutant concentration model is presented. The finite difference methods such as FTCS and FTBS methods can be used to estimate the air pollutant concentration. Also, it is appealing that the grid spacing is different so FTCS method has been chosen because when making comparisons between FTCS and FTBS methods in some cases, the solution for FTBS method is unstable while the solution for FTCS method is stable. Hence, FTCS method provides a better result than FTBS method.

Furthermore, we proposed three scenarios for estimating the air pollutant concentration as follows; Scenario A: there is no rate of change of air pollutant concentration at the entrance gate of the ticket and platform floors. Based on the results, the air pollution in the platform floor is low because it only emits pollution at the wall gap at the right side. Scenario B: the air pollutant concentration at the entrance of three floors can be described by different decreasing functions depended on the height of the tunnel. As the results, the air pollution continues to be released as the decreasing functions but gradually decreases. Therefore, the air pollution in this scenario is high when compared to other scenarios. Scenario C: the air pollution at the entrance of the next floor is the average of air pollutant concentration of gaps on the previous floor. The results of this scenario show that the pollution gradually decreases because we used the value of the previous floor to the next floor which significantly reduces air pollution.

Summary of the three scenarios: Scenario A is a simple model that is an economical method to use. It requires a few of collected data. Scenario B is a realistic numerical simulation. The approximated air pollutant concentration depends on the height but requires a lot of field data. Scenario C is a fairly good model. The simulation needs to average the pollutant concentration level. It is used as the input air pollutant concentration to the above floor. However, the suitable model depends on the provided field data.

Table 1: The stable of FTCS and FTBS approximate solutions.

$\lambda = \frac{\Delta t}{\Delta x}$	$\gamma = \frac{\Delta t}{(\Delta x^2)}$	Δx	Δy	Δz	Δt	$FTCS$	$FTBS$
0.02	0.0067	3.0	3.0	3.0	0.06	stable	stable
	0.0267	1.5	1.5	1.5	0.03	stable	stable
0.03	0.015	2.0	2.0	2.0	0.06	stable	stable
	0.03	1.0	1.0	1.0	0.03	stable	unstable
0.06	0.06	1.0	1.0	1.0	0.06	stable	unstable
	0.12	0.5	0.5	0.5	0.03	stable	unstable

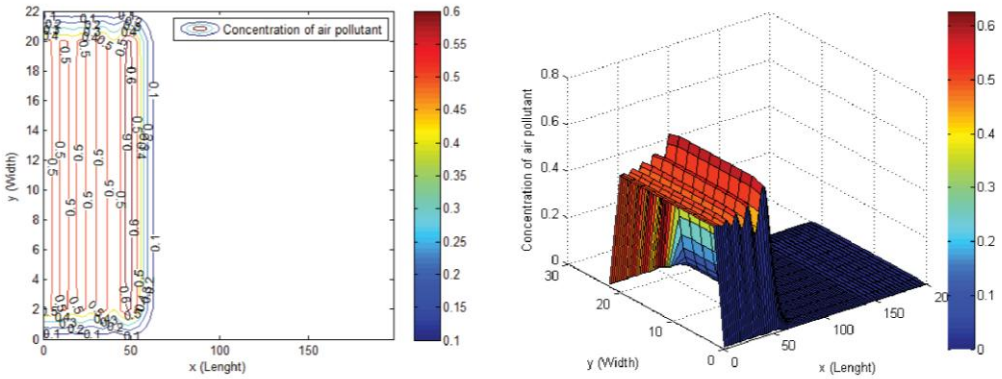

(a) (b)

Figure 6: Contour and surface plot of air pollutant concentration levels after the past 2 minutes computed by FTCS method.

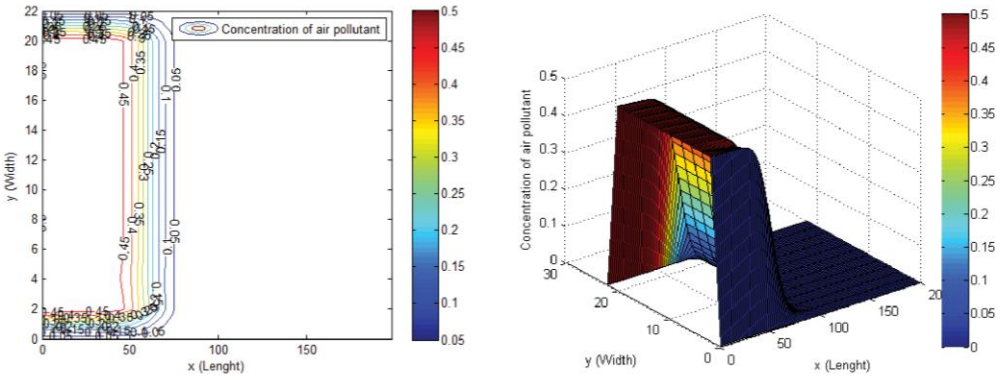

(a) (b)

Figure 7: Contour and surface plot of air pollutant concentration levels after the past 2 minutes computed by FTBS method.

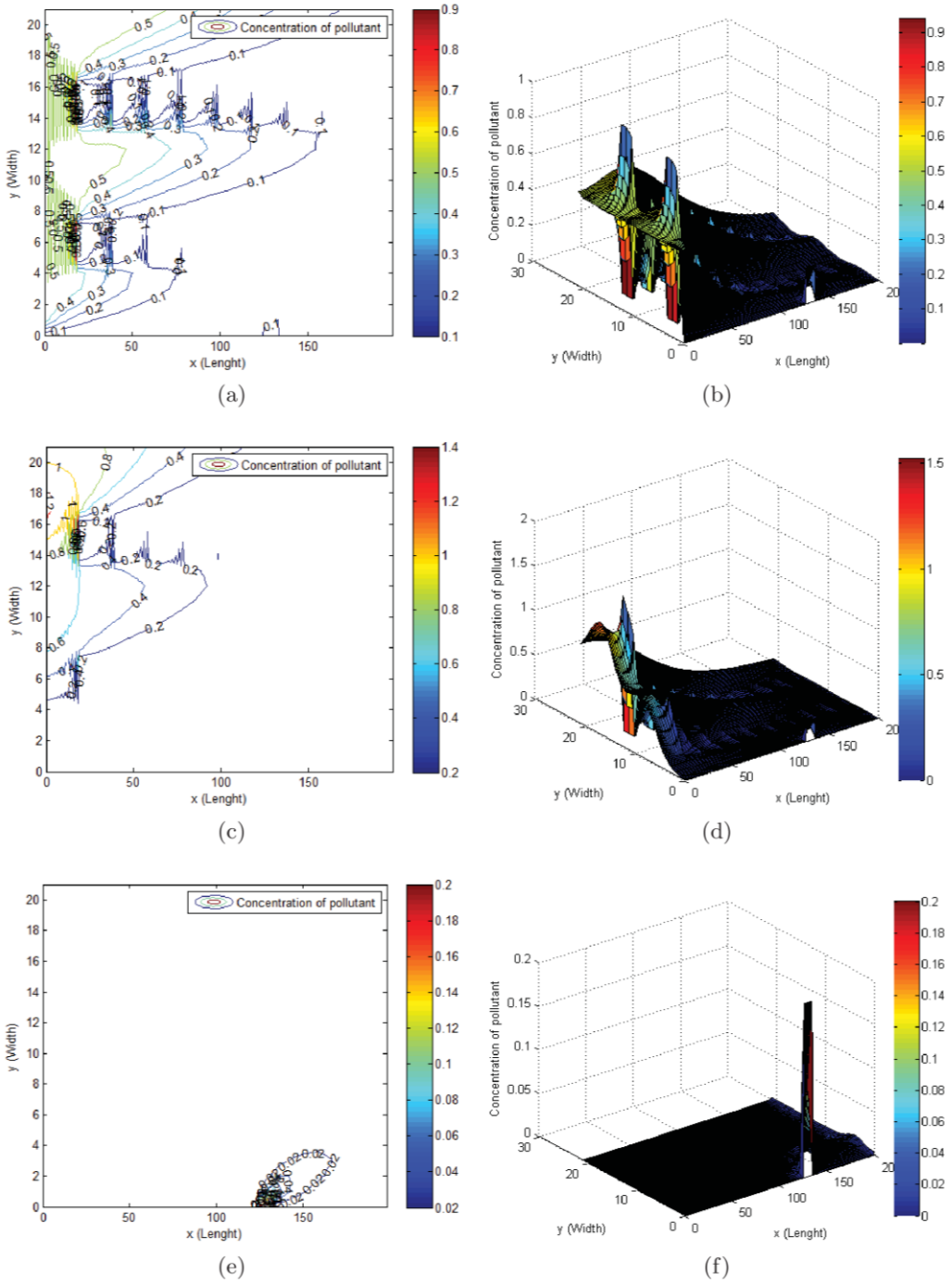

Figure 8: Contour and surface plot of air pollutant concentration levels after the past 2 minutes for the respective streets, tickets and platform floors. (Scenario A)

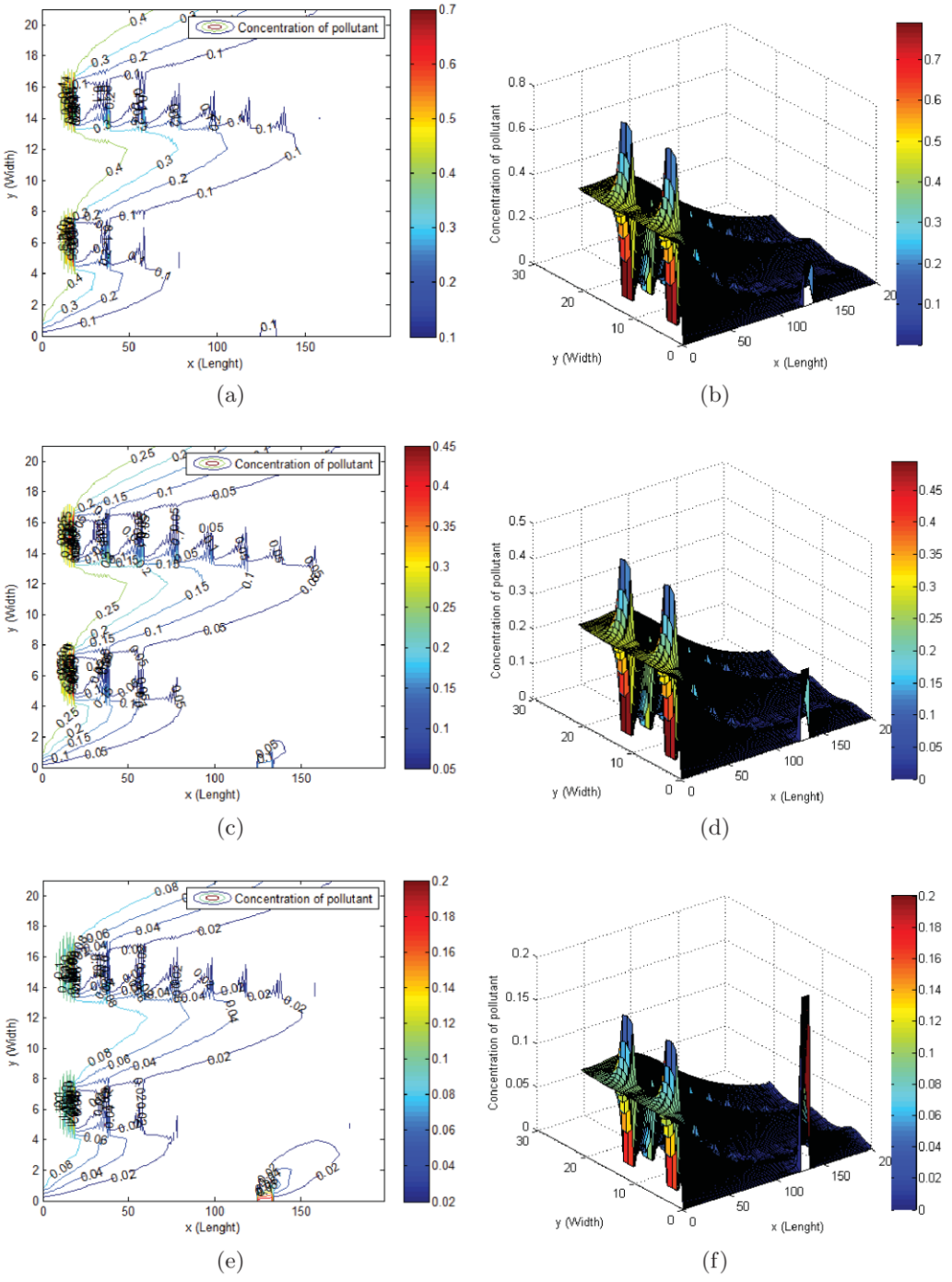

Figure 9: Contour and surface plot of air pollutant concentration levels after the past 2 minutes for the respective streets, tickets and platform floors. (Scenario B)

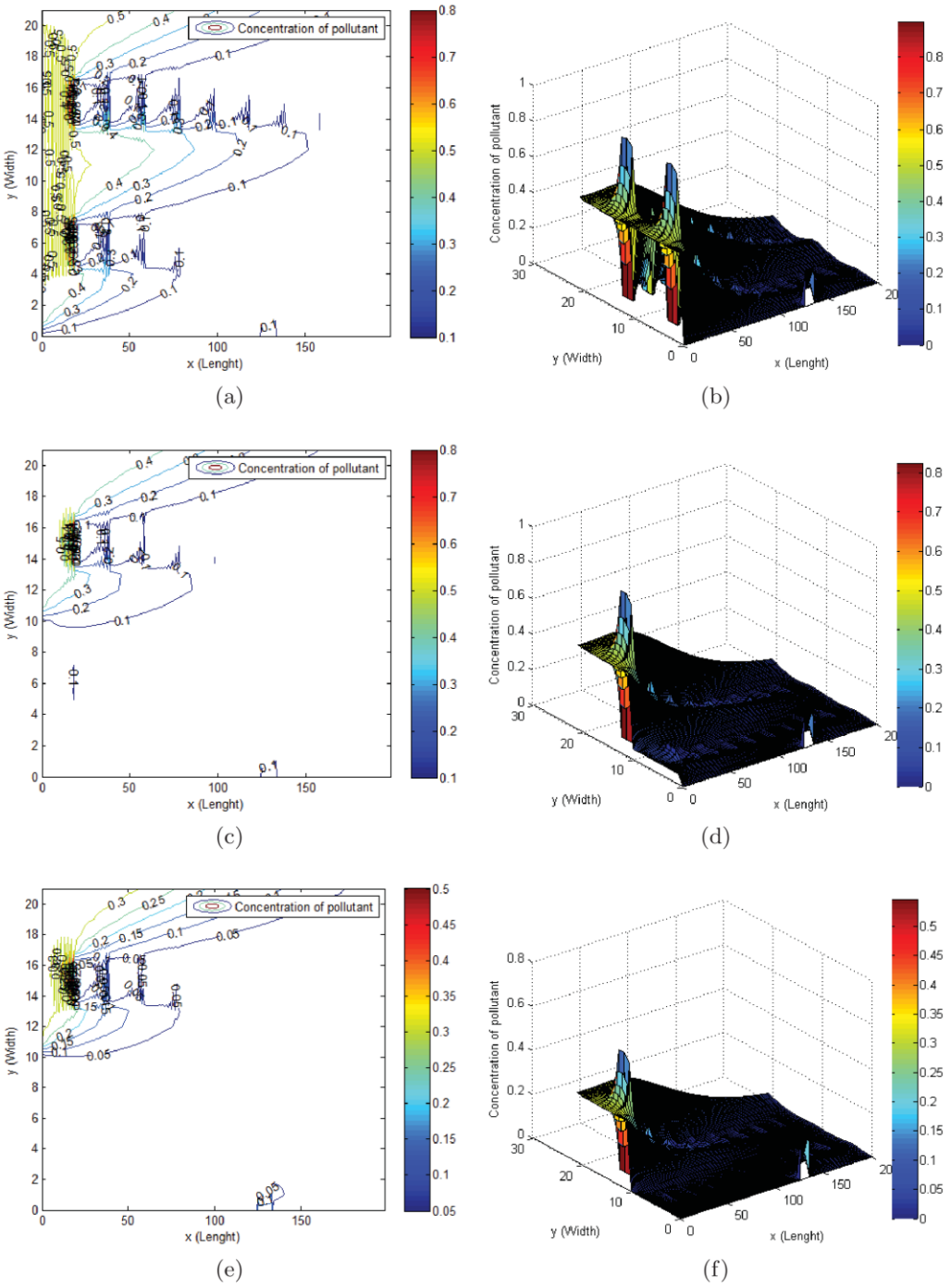

Figure 10: Contour and surface plot of air pollutant concentration levels after the past 2 minutes for the respective streets, tickets and platform floors. (Scenario C)

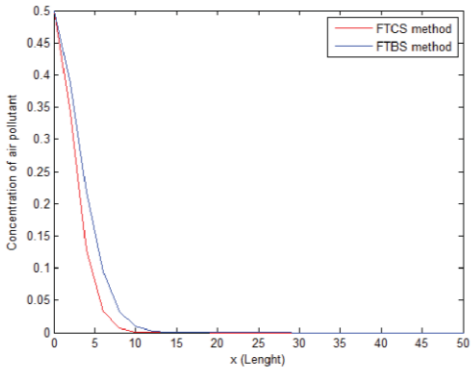

Figure 11: Comparison of air pollutant concentration between FTCS and FTBS methods after the past 30 seconds.

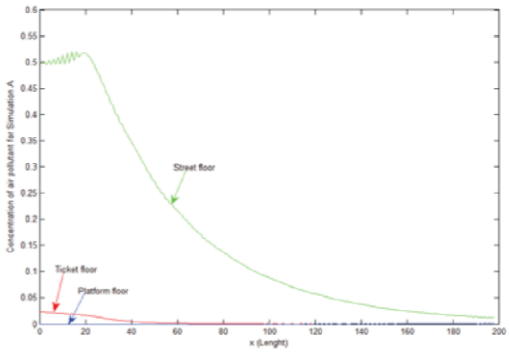

(a)

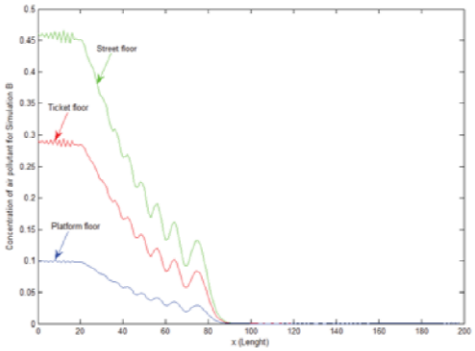

(b)

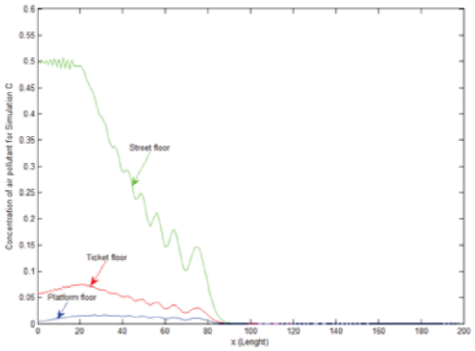

(c)

Figure 12: The air pollutant concentration with the different floors of (a) Scenario A. (b) Scenario B. (c) Scenario C.

Acknowledgements

This research is supported by the Centre of Excellence in Mathematics, the Commission on Higher Education, Thailand. The authors greatly appreciate valuable comments received from the reviewers.

References

[1] U. Charusombat, *Air pollution distribution under an elevated train station (A case study of Silom station in downtown Bangkok)*, Faculty of Virginia Polytechnic Institute and State University, Blacksburg, Virginia, 1994.

[2] S.T. Leong, S. Muttamara and P. Laortanakul, *Air pollution and traffic measurements in Bangkok streets*, Asian J. Energy Environ., 3 (2002), 185-213.

[3] L.J. Alvarez-Vazquez, N. Garcia-Chan, A. Martinez and M.E. Vzquez-Mendez, *Numerical simulation of air pollution due to traffic flow in urban networks*, Journal of Computational and Applied Mathematics, 326 (2007), 44-61.

[4] M. Kampa and E. Castanas, *Human health effects of air pollution*, Environmental Pollution, 151 (2008), 362-367.

[5] N. Sanin and G. Montero, *A finite difference model for air pollution simulation*, Advances in Engineering Software, 38 (2007), 358-365.

[6] M. Thongmoon, *Numerical experiment of air pollutant concentration in the street tunnel*, International Mathematical Forum, 10 (2010), 449-465.

[7] A. Kumar, D. K. Jaiswal, and A. Kumar, *Analytical solutions to one-dimensional advection-diffusion equation with variable coefficients in semi-infinite media*, Journal of Hydrology, 380 (2010), 330-337.

[8] S. Savovic and A. Djordjevich, *Finite difference solution of the one-dimensional advection-diffusion equation with variable coefficients in semi-infinite media*, International Journal of Heat and Mass Transfer, 55 (2012), 4291-4294.

[9] R. S. Kanakiya, S. K. Singh, and P. M. Mehta, *Urban canyon modelling: a need for the design of future Indian cities*, International Research Journal of Environment Sciences, 4(7) (2015), 86-95.

[10] S. A. Konglok and N. M. Pochai, *Numerical computations of three-dimensional air-Quality model with variations on atmospheric stability classes and wind velocities using fractional step method*, IAENG International Journal of Applied Mathematics, 46(1) (2016), 112-120.

[11] L. Sun, K. C. Wong, P. Wei, S. Ye, H. Huang, F. Yang, D. Westerdahl, K. K. Louie, W. Y. Luk, and Z. Ning, *Development and application of a next generation air sensor network for the Hong Kong marathon 2015 air quality monitoring*, Lecture Notes in Engineering and Computer Science: Sensors, 16 (2016), 211.

Accepted: 26.03.2018

Author Biography

Name Miss Kewalee Suebyat

Date of Birth 26th June 1991

Address 46/6 Moo 5, Nongkakha Sub-district, Phanthong District, Chonburi Province, 20160, Thailand

Education

2012. Bachelor of Science in Applied Mathematics. GPA 3.46
King Mongkut's Institute of Technology Ladkrabang
2014. Master of Science in Applied Mathematics. GPA 4.00
King Mongkut's Institute of Technology Ladkrabang
2018. Doctor of Philosophy in Applied Mathematics. GPA 4.00
King Mongkut's Institute of Technology Ladkrabang

Scholarship

2015-2017. Ph.D.Science student scholarship, Faculty of science
King Mongkut's Institute of Technology Ladkrabang

Academic Publications

1. Suebyat, K. and Pochat, N. "A numerical simulation of a three-dimensional air quality model in an area under a Bangkok skytrain platform using an explicit finite difference scheme," *IAENG International Journal of Applied Mathematics*, vol. 47, no. 4, pp. 471-476, 2017.
2. Suebyat, K. and Pochat, N. "Numerical simulation for a three-dimensional air pollution measurement model in a heavy traffic area under the Bangkok skytrain platform," *Abstract and Applied Analysis*, vol. 2018, Article ID 9025851, 10 pages, 2018. https://doi.org/10.1155/2018/9025851.
3. Suebyat, K. and Pochat, N. "Three-dimensional air quality assessment simulations inside skytrain platform with airflow obstacles on heavy traffic road," *Italian Journal of Pure and Applied Mathematics* no. 40-2018, pp. 615-632, 2018.